



**HAL**  
open science

# Transport and spectral properties of low-dimensional superconductors in the presence of spin-dependent fields

Julie Baumard

► **To cite this version:**

Julie Baumard. Transport and spectral properties of low-dimensional superconductors in the presence of spin-dependent fields. Superconductivity [cond-mat.supr-con]. Université de Bordeaux; Universidad del País Vasco. Facultad de ciencias, 2019. English. NNT : 2019BORD0357 . tel-02869589

**HAL Id: tel-02869589**

**<https://theses.hal.science/tel-02869589>**

Submitted on 16 Jun 2020

**HAL** is a multi-disciplinary open access archive for the deposit and dissemination of scientific research documents, whether they are published or not. The documents may come from teaching and research institutions in France or abroad, or from public or private research centers.

L'archive ouverte pluridisciplinaire **HAL**, est destinée au dépôt et à la diffusion de documents scientifiques de niveau recherche, publiés ou non, émanant des établissements d'enseignement et de recherche français ou étrangers, des laboratoires publics ou privés.



THÈSE EN COTUTELLE PRÉSENTÉE  
POUR OBTENIR LE GRADE DE

DOCTEUR DE

L'UNIVERSITÉ DE BORDEAUX

ET DE L'UNIVERSIDAD DEL PAÍS VASCO

ECOLE DOCTORALE SCIENCES PHYSIQUES ET DE L'INGÉNIEUR - UBX  
ESCUELA DE MÁSTER Y DOCTORADO - UPV/EHU

Spécialité: LASERS, MATIÈRE, NANOSCIENCES

par **Julie BAUMARD**

## Transport and spectral properties of low-dimensional superconductors in the presence of spin-dependent fields

Sous la direction de **F. Sebastián BERGERET** et **Alexandre BUZDIN**  
Co-directeur: **Jérôme CAYSSOL**

Soutenue le: 19 Décembre 2019

Membres du jury:

<b>M. Philippe Tamarat,</b>	Professeur	Université de Bordeaux	Président
<b>M. Andrés Arnau Pino,</b>	Professeur	Universidad del País Vasco	Examinateur
<b>Mme. Hélène Bouchiat,</b>	Directrice de recherche	Université Paris Sud	Examinatrice
<b>M. Manuel Houzet,</b>	Chercheur CEA	CEA Grenoble	Rapporteur
<b>M. Pascal Simon,</b>	Professeur	Université Paris Sud	Rapporteur

---

---

## Transport and spectral properties of low-dimensional superconductors in the presence of spin-dependent fields

The interplay between superconductivity and spin-dependent fields is known to lead to striking phenomena, like critical field enhancement, magnetoelectric effects and the appearance of Yu-Shiba-Rusinov bound states at magnetic impurities. In this thesis, we investigate these effects in low dimensional systems.

We first demonstrate that the combination of both spin-orbit and Zeeman fields in superconducting one-dimensional systems leads to the appearance of an inhomogeneous phase at low magnetic field and high critical temperature. We show that the ground state corresponds to a zero-current state where the current stemming from spin-orbit coupling, called anomalous charge current, is exactly compensated by the current coming from the wave-vector of the superconducting order parameter. We also discuss how it is possible to predict the appearance of the anomalous current from symmetry arguments based on the  $SU(2)$ -covariant formalism.

In a second part, we consider a type-II superconducting thin film in contact with a Néel skyrmion. The skyrmion induces spontaneous currents in the superconducting layer, which under the right condition generate a superconducting vortex in the absence of external magnetic fields. We compute the magnetic field and current distributions in the superconducting layer in the presence of the Néel skyrmion.

In the last part of this thesis, we focus on the appearance of Yu-Shiba-Rusinov states in the superconducting crystal  $\beta$ - $Bi_2Pd$ . We propose effective models in order to explain recent experimental results showing a double spatial oscillation of the local density of states at Shiba energy. We demonstrate that the minimal condition to reproduce this double oscillation is the presence of two superconducting channels connected via a hopping term or via a magnetic impurity. These effective models can be easily generalized to describe the spectrum of multiband superconductors with magnetic impurities.

**Keywords :** superconductivity, spin-dependent fields, superconducting inhomogeneous phase, anomalous current, Néel skyrmion, Yu-Shiba-Rusinov states.

## Propriétés spectrales et de transport de supraconducteurs à basse dimension en présence de champs dépendant du spin

Lorsqu'un supraconducteur est soumis à des champs dépendant du spin, on observe l'émergence de nouveaux phénomènes comme l'augmentation du champ magnétique critique, des effets magnétoélectriques ou encore l'apparition d'états de bord de Yu-Shiba-Rusinov autour d'impuretés magnétiques. Dans cette thèse, on s'intéresse à ces effets dans des systèmes de basse dimension.

Tout d'abord, on démontre que la combinaison d'un champ Zeeman avec un couplage spin-orbite dans des systèmes supraconducteurs unidimensionnels induit une phase inhomogène à faible champ magnétique et haute température critiques. On montre que l'état fondamental correspond à un état de courant nul, où le courant induit par le couplage spin-orbite, nommé courant de charges anomal, est exactement compensé par le courant venant du vecteur d'onde du paramètre d'ordre supraconducteur. On discute également la possibilité de prédire l'apparition du courant anomal à partir d'arguments de symétrie basés sur le formalisme covariant  $SU(2)$ .

Dans un second temps, on considère une couche mince supraconductrice de type II en contact avec un skyrmion de Néel. Ce dernier induit des courants spontanés dans la couche supraconductrice, pouvant conduire à l'émergence d'un vortex supraconducteur en l'absence de champ magnétique extérieur. Les distributions de champ magnétique et de courant sont calculées dans le supraconducteur en présence du skyrmion de Néel.

La dernière partie de cette thèse est consacrée à l'étude de l'apparition d'états de Yu-Shiba-Rusinov dans le cristal  $\beta$ - $Bi_2Pd$ . On propose des modèles effectifs pour expliquer les récents résultats expérimentaux montrant une double oscillation spatiale de la densité d'états locale à l'énergie de Shiba. On démontre que la condition minimale pour reproduire cette double oscillation correspond à la présence de deux canaux supraconducteurs connectés via un terme de saut ou via une impureté magnétique. Ces modèles effectifs peuvent facilement être généralisés pour décrire le spectre de supraconducteurs multi-bandes en présence d'impuretés magnétiques.

**Mots-clés :** Supraconductivité, champs dépendant du spin, phase supraconductrice inhomogène, courant anomal, skyrmion de Néel, états de Yu-Shiba-Rusinov.

---

Laboratoire Ondes et Matière d'Aquitaine (LOMA) - UMR 5798

Université de Bordeaux, 33405 Talence, France

Donostia International Physics Center (DIPC)

Manuel de Lardizabal 5, 20018 San Sebastián, Spain

Centro de Física de Materiales (CFM-MPC)

Centro Mixto CSIC-UPV/EHU, Manuel de Lardizabal 4, 20018 San Sebastián, Spain

---

# Résumé en Français

La supraconductivité en présence de champs dépendant du spin a été étudiée de façon approfondie dans des systèmes de basse dimension, comme des nanofils semi-conducteurs, dans le contexte des états liés de Majorana, en raison de leur potentiel application en tant que qubits topologiques. L'interaction entre supraconductivité et champs de spin est également à l'origine de phénomènes physiques impressionnants, comme l'augmentation du champ critique, les effets magnétoélectriques ou encore l'apparition d'états liés de Yu-Shiba-Rusinov en présence d'impuretés magnétiques. Dans cette thèse, on se propose d'étudier chacun des trois effets cités, dans différents systèmes. Tout d'abord, on s'intéresse à la phase supraconductrice hélicale et aux courants anomaux provenant de l'interaction entre le champ Zeeman et le couplage spin-orbite dans deux systèmes supraconducteurs quasi-unidimensionnels distincts. Ensuite, on étudie la formation d'un vortex supraconducteur liée aux effets magnétoélectriques induits par la présence d'un skyrmion de Néel couplé par effet de proximité à un film supraconducteur fin. Finalement, la dernière partie de ce manuscrit est dédiée à la construction de modèles effectifs permettant de comprendre de façon qualitative le couplage entre des impuretés magnétiques et la supraconductivité dans des supraconducteurs non-conventionnels comme le cristal  $\beta$ -Bi<sub>2</sub>Pd.

## Phase hélicale et effets magnétoélectriques dans des fils supraconducteurs

La première partie de cette thèse est consacrée à la description de supraconducteurs quasi-unidimensionnels en présence d'un champ Zeeman et d'une interaction spin-orbite de type Rashba. En particulier, on étudie deux systèmes. Le premier correspond à un fil supraconducteur dans lequel le champ coexiste avec le couplage spin-orbite, tandis que le second est un système à deux fils, dans lequel l'appariement supraconducteur et les champs dépendant du spin sont respectivement présents dans deux fils distincts. En principe, ces systèmes pourraient être réalisés expérimentalement, par exemple en utilisant un supraconducteur organique pour le système à un fil.

Dans un premier temps, on s'intéresse à l'apparition de courants de charges induits par le couplage spin-orbite, appelés courants anomaux. Pour cela, on introduit le formalisme covariant SU(2), dans lequel les champs Zeeman et spin-orbite sont décrits respectivement par les potentiels scalaire et vecteur des champs magnétoélectriques SU(2). Par le biais de cette formulation, on construit une expression générale du courant au premier ordre des champs Zeeman et spin-orbite pour des systèmes 1D, que l'on applique ensuite aux deux systèmes décrits dans ce chapitre. Dans le cas du système à un fil, on prédit que le courant anomal peut apparaître uniquement si le champ Zeeman possède deux composantes, l'une parallèle et l'autre perpendiculaire au champ de spin-orbite. Dans le cas du système à deux fils, la composante du champ Zeeman parallèle au champ de spin-orbite est suffisante pour induire le courant anomal.

---

Ces prédictions sont ensuite confirmées par des calculs explicites utilisant le formalisme de fonctions de Green de Gor'kov. Pour cela, on déduit l'expression des fonctions de Green qui décrivent le système à partir du Hamiltonien écrit dans la base de Nambu spin, pour les deux systèmes, dans la limite de faible couplage spin-orbite  $\alpha p_F \ll T_c$ , où  $\alpha$  est la constante de couplage spin-orbite,  $p_F$  est l'impulsion de Fermi et  $T_c$  est la température critique. Cela nous permet de calculer explicitement l'expression du courant, ainsi que le paramètre d'ordre supraconducteur auto-cohérent. On démontre ainsi que l'état fondamental est en fait un état sans courant, dans lequel le courant anomal est compensé par le courant provenant du vecteur d'onde  $q$  du paramètre d'ordre supraconducteur. Il est intéressant de remarquer que dans le cas du système à deux fils, l'état de courant nul correspond en fait à deux courants circulant dans des directions opposées dans chacun des fils. Enfin, si l'on impose  $q = 0$ , le courant de charge est fini et correspond au résultat prédit grâce au formalisme covariant SU(2).

Dans cette partie, on s'intéresse également à l'émergence de la phase supraconductrice inhomogène induite par la présence du couplage spin-orbite, et appelée phase hélicale. En développant la relation d'auto-cohérence en séries de  $q$ , on s'aperçoit que la combinaison du champ Zeeman avec l'interaction spin-orbite conduit à l'apparition de cette phase hélicale à faible champ magnétique et pour toute température  $T < T_{c0}$ . On peut aussi remarquer que de façon analogue au courant anomal, dans le système à un fil, la phase hélicale n'est présente que si les deux composantes du champ Zeeman, parallèle et perpendiculaire au champ de spin-orbite, sont non-nulles. De même, dans le cas du système à deux fils, la composante parallèle du champ Zeeman est suffisante à l'émergence de la phase hélicale.

Afin de tracer le diagramme de phase du système à un fil, représentant l'évolution de la température en fonction de l'amplitude du champ Zeeman appliqué, nous avons étudié ce système dans la limite d'un fort couplage spin-orbite  $\alpha p_F \gg T_c$ . Dans ce cas-là, l'approche la plus simple consiste à diagonaliser le Hamiltonien, et donc à travailler dans la base hélicale. On démontre ainsi que lorsque le ratio  $\alpha p_F/h$  augmente,  $h$  étant l'amplitude du champ Zeeman, l'appariement supraconducteur est modifié, passant d'un couplage inter-bandes à un couplage intra-bandes. Dans la limite  $\alpha p_F \gg h$ , on peut donc négliger le couplage inter-bandes et calculer l'expression des fonctions de Green séparément pour chaque bande électronique. Le diagramme de phase est ensuite obtenu en résolvant numériquement l'équation d'auto-cohérence, et représenté pour diverses orientations du champ Zeeman et plusieurs valeurs de la constante de couplage spin-orbite  $\alpha$ . On montre notamment que la présence de l'interaction spin-orbite augmente la valeur du champ magnétique critique. Lorsque le champ Zeeman est purement parallèle au champ de spin-orbite, on retrouve exactement le diagramme de phase FFLO, ce qui peut être expliqué par le fait que le couplage spin-orbite peut être éliminé du Hamiltonien par changement de jauge.

Une possible application de ces systèmes consisterait à les utiliser en tant que liaison faible entre deux supraconducteurs identiques pour créer une jonction Josephson anormale, ou jonction  $\varphi_0$ . Le vecteur d'onde supraconducteur  $q$  jouerait ainsi le rôle de la différence de phase requise pour générer un courant dans la jonction, élargissant les possibilités d'application de ces jonctions  $\varphi_0$  dans les dispositifs de stockage d'information.

---

## Génération de vortex supraconducteurs par le biais de skyrmions de Néel

La deuxième partie de ce manuscrit est consacrée à un autre effet lié à l'interaction entre la supraconductivité et les champs dépendant du spin : la possibilité de créer des vortex d'Abrikosov en l'absence d'un champ magnétique extérieur.

Pour cela, on considère un film supraconducteur de type II, d'épaisseur  $d_S$ , caractérisé par sa longueur de cohérence  $\xi$  et par la longueur de pénétration de London  $\lambda \gg d_S$ . Ce supraconducteur est en contact avec une couche ferromagnétique d'épaisseur  $d_F$ , dans laquelle un skyrmion de Néel de rayon  $R$  est présent. On suppose également que la couche ferromagnétique présente une interaction spin-orbite bidimensionnelle.

En principe, dans un tel système, il est possible de générer un vortex dans la couche supraconductrice de deux façons différentes : soit par couplage électromagnétique direct entre le skyrmion et le supraconducteur, soit par effet de proximité. Pour une couche ferromagnétique uniforme en contact avec un supraconducteur, si l'aimantation est très inférieure au premier champ critique,  $\mu_0 M \ll H_{c1}$ , l'interaction électromagnétique standard ne peut pas générer de vortex. Et même dans le cas où  $M$  serait supérieure à  $H_{c1}$ , il est possible d'éviter la formation de vortex en concevant les couches supraconductrice et ferromagnétique de manière à ce que  $\mu_0 M \ll H_{c1} d_S/d_F$ , ce qui peut être facilement obtenu en utilisant une couche ferromagnétique beaucoup plus fine que la couche supraconductrice. Dans cette étude, on va donc négliger l'interaction électromagnétique directe et s'intéresser uniquement à l'effet de proximité en supposant que le champ d'échange et l'interaction spin-orbite pénètrent dans le supraconducteur sur une distance correspondant à l'épaisseur atomique  $a$ , où  $a \ll d_S$ . Cela induit une polarisation de spins dans le supraconducteur qui donne naissance à des courants à l'interface entre les deux couches, et crée un champ magnétique. Si ce dernier est suffisamment fort, il peut à son tour générer un vortex sous le skyrmion, en l'absence de champ magnétique extérieur.

Afin d'obtenir la condition d'émergence du vortex supraconducteur, on s'intéresse à l'énergie libre du système dans l'approche de London, en considérant que la supraconductivité est bien développée, c'est-à-dire que  $T \ll T_c$ . Dans le formalisme de Ginzburg-Landau, le couplage entre le supraconducteur et l'ordre magnétique induit par le skyrmion est décrit par un invariant de Lifshitz. La première étape de cette étude consiste donc à construire cet invariant dans le formalisme de London.

La condition d'apparition du vortex supraconducteur est ensuite obtenue en minimisant l'énergie libre, plus exactement en comparant cette énergie avec et sans vortex. On démontre ainsi que la création du vortex est favorisée par un fort couplage spin-orbite, et par l'augmentation du rayon du skyrmion. De plus, on montre qu'il est également possible de générer un vortex multiquanta, c'est-à-dire un vortex portant plus d'un quantum de flux  $\Phi_0$ , en augmentant encore la constante de couplage spin-orbite et/ou le rayon du skyrmion.

Pour finir, on considère que l'interaction spin-orbite est suffisamment importante pour créer un vortex portant un unique quantum de flux, et on calcule la distribution de champ magnétique et de courant dans la couche supraconductrice. On observe alors que chacune de ces distributions peut s'écrire comme la somme de deux composantes, l'une provenant du skyrmion, et la seconde du vortex lui-même. On met en évidence la compétition entre ces deux contributions, qui induit par exemple plusieurs changements dans le sens de rotation du courant dans la couche supraconductrice.

Cette étude nous ouvre plusieurs perspectives. Tout d'abord, même si la condition d'émergence du vortex n'est pas atteinte, il est toujours possible de créer des vortex en appliquant au système un champ magnétique extérieur supérieur à  $H_{c1}$ . Dans ce

---

cas-là, nos calculs d'énergie libre démontrent une interaction attractive qui va piéger les vortex au skyrmion pour une orientation donnée du champ magnétique. Pour l'orientation opposée, les vortex devraient être repoussés par le skyrmion. Cet effet d'attraction/répulsion entre le skyrmion et les vortex pourrait en principe être détecté expérimentalement. L'effet inverse à celui étudié dans cette thèse, c'est-à-dire la génération d'un skyrmion dans la couche ferromagnétique par effet de proximité avec un vortex supraconducteur, est aussi suggéré par nos résultats, et devrait pouvoir être observé expérimentalement par microscopie à force magnétique ou par effet Hall topologique dans des systèmes comme Nb/Co/Pt. Remarquons finalement que de récents travaux montrent la possible existence d'états liés de Majorana dans des paires skyrmion/vortex, ouvrant ainsi de nouvelles perspectives de contrôle spatial de ces états.

### Supraconductivité multibande en présence d'impuretés magnétiques

La dernière partie de ce manuscrit est consacrée à l'étude de la dépendance spatiale des états liés de Yu-Shiba-Rusinov induits par des impuretés paramagnétiques dans des supraconducteurs non-conventionnels.

Ce travail a été motivé par des résultats expérimentaux obtenus récemment par le groupe de José Ignacio Pascual (CIC nanoGUNE, San Sebastián, Espagne) sur le cristal supraconducteur  $\beta$ -Bi<sub>2</sub>Pd en présence d'impuretés formées par des atomes de Vanadium. De façon surprenante, la densité d'états locale (LDOS) de Shiba de ce matériau est caractérisée par une double oscillation spatiale. Pour expliquer ce résultat, nous avons construit des modèles effectifs permettant d'identifier les mécanismes à l'origine de la double oscillation.

Afin de modéliser les bandes électroniques du matériau, une approche possible consiste à utiliser des simulations basées sur le modèle tight-binding (modèle des liaisons fortes). Bien que le supraconducteur  $\beta$ -Bi<sub>2</sub>Pd soit caractérisé par des bandes électroniques de surface (et même des bandes 3D), nous avons choisi de réduire le problème à un système 1D. Un tel modèle n'est évidemment pas adapté pour décrire les expériences citées ci-dessus, mais peut nous fournir une première compréhension des mécanismes fondamentaux à l'origine de la dépendance spatiale des états de Yu-Shiba-Rusinov. Plus particulièrement, nos modèles 1D permettent de répondre à deux questions simples : est-ce qu'une impureté magnétique couplée à une bande électronique hélicale (c'est-à-dire caractérisée par une dispersion linéaire en impulsion  $p$ ) permet d'obtenir des oscillations spatiales de la LDOS de Shiba? Et quelle est la condition minimale pour observer une double oscillation de cette LDOS? Dans ce but, le groupe d'Alfredo Levy Yeyati, de l'Universidad Autónoma de Madrid, a considéré un modèle tight-binding 1D, qui peut être représenté par des fils à la limite continue. Afin de guider leurs simulations, nous avons développé deux modèles analytiques en 1D.

Le premier modèle correspond à un fil supraconducteur présentant une dispersion hélicale. En présence d'une impureté magnétique, on démontre que des états de Yu-Shiba-Rusinov apparaissent dans le gap supraconducteur, mais qu'ils sont caractérisés par une absence d'oscillations spatiales de la LDOS non polarisée. La dépendance spatiale des états de Shiba observée dans le supraconducteur  $\beta$ -Bi<sub>2</sub>Pd ne peut donc pas être expliquée par des bandes électroniques purement hélicales. On peut cependant remarquer dans ce modèle que la LDOS polarisée présente une oscillation spatiale, qui pourrait en principe être détectée expérimentalement par un microscope à effet tunnel muni d'une pointe magnétique.

---

Nous avons ensuite construit un modèle à deux fils supraconducteurs présentant une dispersion quadratique, connectés par un terme de saut. Une impureté magnétique est couplée au fil supérieur. Comme on peut s'y attendre, des états de Yu-Shiba-Rusinov sont localisés dans ce fil, et leur énergie n'est pas affectée par la présence du second fil. On montre également que la LDOS (polarisée et non-polarisée) présente une double oscillation spatiale, dont les fréquences correspondent respectivement à la somme et à la différence des impulsions de Fermi de chaque fil.

La condition minimale pour obtenir une double oscillation spatiale de la densité d'états locale de Shiba semble donc être la présence de deux bandes électroniques, participant toutes deux à la supraconductivité. De plus, une dispersion hélicale d'au moins l'une des deux bandes supprimerait cette double oscillation. Il est donc nécessaire de considérer d'autres types de dispersions, par exemple quadratiques ou non-purement hélicale.

Cependant, cette étude est toujours en cours, et pour une compréhension complète des résultats expérimentaux, ces modèles effectifs vont à terme être accompagnés de simulations numériques basées sur des modèles tight-binding prenant en compte la structure de bande réelle de  $\beta$ -Bi<sub>2</sub>Pd. Ces simulations sont actuellement en cours de réalisation par M. Alvarado Herrero et A. Levy Yeyati.

Pour finir, on peut noter que les modèles effectifs construits dans ce manuscrit pourraient être facilement généralisés pour décrire le spectre de supraconducteurs multibandes en présence d'impuretés magnétiques.



# Resumen en Español

Debido a su potencial aplicación en la creación de *qubits* topológicos, la interacción entre la superconductividad y los campos dependientes del espín en sistemas de baja dimensionalidad ha sido ampliamente estudiada en el contexto de los estados localizados de Majorana en hilos semiconductores. Es sabido que dicha interacción conduce a resultados sorprendentes, tales como la mejora del campo magnético crítico, efectos magnetoeléctricos y la aparición de los estados localizados Yu-Shiba-Rusinov en presencia de impurezas magnéticas. En esta tesis investigamos cada uno de estos tres efectos en diferentes sistemas. En una primera parte, estudiamos la fase helicoidal y las corrientes anómalas que surgen de acción conjunta de las interacciones de Zeeman y de espín-órbita en dos superconductores cuasi-unidimensionales distintos. A continuación, investigamos la formación de un vórtice superconductor en relación con los efectos magnetoeléctricos originados por un *skyrmion* de Néel que está acoplado por proximidad a una lámina superconductora. Por último, la parte final de la tesis se centra en la construcción de modelos efectivos que nos permitan entender cualitativamente el acoplamiento entre las impurezas magnéticas y la superconductividad en superconductores no convencionales, como el  $\beta$ -Bi<sub>2</sub>Pd.

## Estados helicoidales y efectos magnetoeléctricos en hilos superconductores

La primera parte de esta tesis describe superconductores cuasi-unidimensionales en presencia de interacciones Zeeman y espín-órbita (SO por sus siglas en inglés) del tipo Rashba. En particular, estudiamos dos tipos de sistemas. El primero consiste en un hilo superconductor en el cual ambas interacciones existen simultáneamente, mientras que el segundo es un sistema compuesto por dos hilos en el cual el emparejamiento superconductor y los campos dependientes del espín se encuentran separados espacialmente. En principio, dichos sistemas pueden ser realizados experimentalmente, por ejemplo utilizando superconductores orgánicos para el sistema de un solo hilo.

Comenzamos discutiendo la aparición de corrientes debidas a la interacción espín-órbita, denominadas corrientes anómalas, usando el formalismo de covarianza SU(2), por el cual los campos de Zeeman y de espín-órbita se escriben como el potencial escalar y vector, respectivamente, de un campo SU(2) electromagnético. En el marco de esta formulación, obtenemos una expresión general de la corriente para sistemas unidimensionales a primer orden en el campo Zeeman y de espín-órbita y la aplicamos en la descripción de ambos sistemas descritos en este capítulo. En el caso de un único hilo, predecimos que solamente cuando el campo Zeeman tiene una componente paralela y otra ortogonal al campo de espín-órbita aparece una corriente anómala finita. En el caso del sistema compuesto por dos hilos, demostramos que un campo Zeeman paralelo al campo de espín-órbita es condición suficiente para inducir una corriente anómala.

Estas predicciones son corroboradas por cálculos detallados utilizando funciones de Green en el formalismo de Gor'kov. Partiendo del Hamiltoniano de ambas confi-

---

guraciones derivamos las funciones de Green que describen el sistema en el límite de acoplamiento SO débil,  $\alpha p_F \ll T_c$ , donde  $\alpha$  es la constante de espín-órbita,  $p_F$  es el momento de Fermi y  $T_c$  es la temperatura crítica. En este límite podemos obtener explícitamente la expresión de la corriente, junto con la del parámetro de orden autoconsistente. Descubrimos que el estado fundamental del sistema es, de hecho, un estado de corriente total nula en el cual la corriente anómala es compensada por la corriente derivada del vector de onda  $q$  del parámetro de orden superconductor. Resulta interesante comprobar que en el caso del sistema compuesto por dos hilos el estado de corriente nula corresponde a dos corrientes opuestas fluyendo a través de cada uno de los hilos. Finalmente, al imponer  $q = 0$ , la corriente de carga anómala es finita y obtenemos los resultados predichos por el formalismo de covarianza SU(2).

Asimismo, investigamos la aparición de una fase superconductor inhomogénea, llamada fase helicoidal, debida a la presencia de interacción espín-órbita. Al considerar la relación de autoconsistencia en valores de  $q$  no nulos, descubrimos que la coexistencia de interacciones Zeeman y espín-órbita resultan en la aparición de dicha fase helicoidal para campos magnéticos débiles y cualquier temperatura menor a la temperatura crítica,  $T < T_{c0}$ . Nótese que, de manera similar a la corriente anómala, la fase inhomogénea aparece únicamente si tanto las componentes paralelas y perpendiculares del campo Zeeman con respecto al de espín-órbita son finitas en el sistema de un único hilo, mientras que en el sistema de dos hilos tan solo hace falta que la componente paralela sea no nula.

Para representar el diagrama de fase campo magnético-temperatura del sistema de un único hilo estudiamos la relación de autoconsistencia para campos de espín-órbita grandes  $\alpha p_F \gg T_c$ . Para ello, es conveniente trabajar en una base diagonal, también llamada base helicoidal. Demostramos que a medida que la proporción  $\alpha p_F/h$  aumenta, donde  $h$  es el campo de Zeeman, las correlaciones superconductoras pasan de suceder entre bandas (interbanda) a suceder dentro de cada una de las bandas (intrabanda). Por lo tanto, en el límite donde  $\alpha p_F \gg h$ , podemos desprejir el emparejamiento interbanda y derivar las funciones de Green para cada una de las bandas por separado. Resolver numéricamente la relación de autoconsistencia de este modo, obtenemos el diagrama de fases para varios orientaciones del campo de Zeeman y diversos valores de la constante de espín-órbita,  $\alpha$ . Mostramos que la presencia de interacción SO de manera global incrementa el campo magnético crítico. Cuando los campos de espín-órbita y Zeeman son paralelos, podemos obviar el acoplamiento espín-órbita por medio de una transformación *gauge*, de modo que recuperamos un diagrama de fases FFLO.

Estos sistemas podrían ser usados como un enlace débil entre dos superconductores idénticos para crear uniones  $\varphi_0$ -Josephson anómalas. En dichos sistemas, el vector de onda superconductor jugaría el papel de la diferencia de fase necesaria para generar una corriente a través de la unión, pudiendo abrir nuevas aplicaciones a este tipo de uniones  $\varphi_0$  en dispositivos de memoria.

## Generación de vórtices superconductores a través de skyrmions de Néel

En una segunda parte, vamos a estudiar otro de los efectos procedentes de la interacción entre superconductividad y campos dependientes del espín : la posible aparición de vórtices de Abrikosov en ausencia de campos magnéticos externos.

Para ello, consideramos una lámina fina superconductor de tipo II con un grosor  $d_S$ , caracterizada por su longitud de coherencia  $\xi$  y su longitud de penetración de London  $\lambda \gg d_S$ . El superconductor está en contacto con un material ferromagnético

---

de grosor  $d_F$  que alberga un skyrmion de Néel de radio  $R$ . Además, asumimos que la capa ferromagnética presenta interacción de espín-órbita bidimensional.

En principio, tanto el acoplamiento electromagnético directo entre el skyrmion y el superconductor, y el efecto de proximidad magnético pueden resultar en la nucleación de un vórtice. Para una capa ferromagnética uniforme en contacto con un superconductor, si la magnetización es menor que el primer campo crítico,  $\mu_0 M \ll H_{c1}$ , la interacción electromagnética estándar no puede nuclear un vórtice. Incluso en el caso en que  $M$  supera el valor de  $H_{c1}$ , es posible evitar la formación del vórtice diseñando las capas ferromagnética y superconductora de tal manera que  $\mu_0 M \ll H_{c1} d_S/d_F$ , lo cual se puede conseguir fácilmente si el ferromagneto es mucho más fino que el superconductor. Pues en este trabajo, vamos a dejar de lado este efecto y nos centramos solamente en el efecto de proximidad asumiendo que el campo de canje y la interacción de espín-órbita tienen en el superconductor una longitud de penetración atómica  $a$ , con  $a \ll d_S$ . Esto induce una polarización de espín en el superconductor, que da lugar a una supercorriente en la superficie de contacto entre este y la capa ferromagnética, creando un campo magnético. Si el campo magnético es suficientemente grande, el vórtice se genera debajo del skyrmion sin necesidad de un campo magnético externo.

Para obtener la condición necesaria para que el vórtice superconductor aparezca, derivamos la energía libre del sistema en la aproximación de London, considerando que la superconductividad está perfectamente establecida, *i.e.*,  $T \ll T_c$ . En términos de la energía libre de Ginzburg-Landau, el acoplo entre el superconductor y el orden magnético inducido por el skyrmion se puede describir a través de una invarianza de Lifshitz. Por consiguiente, comenzamos el estudio de este sistema construyendo tal invariante en la aproximación de London.

Con ello, minimizando la energía libre, concretamente comparando el valor de la energía con y sin vórtice, obtenemos la condición que ha de cumplirse para generar un vórtice en la capa superconductora. En este trabajo, mostramos que un acoplo de espín-órbita grande y/o un skyrmion de gran radio favorecen la aparición del vórtice. Además, demostramos que también es posible generar un vórtice multicuántico, *i.e.*, un vórtice que tiene más de un cuanto de flujo  $\Phi_0$ , incrementando de nuevo la constante de acoplo de espín-órbita y/o el radio del skyrmion.

Finalmente, consideramos una interacción de espín-órbita suficientemente grande como para generar un vórtice de un cuanto de flujo, y calculamos la distribución del campo magnético y de la corriente en la capa superconductora. Mostramos cómo ambas distribuciones han de escribirse como la suma de dos componentes, una proveniente del skyrmion y la segunda generada por el vórtice en sí. Destacamos además la competición entre ambas distribuciones, que lleva por ejemplo a varios cambios en la dirección de rotación de la corriente en la lámina superconductora.

Incluso si la condición para la emergencia del vórtice no se cumple, es posible nuclear los vórtices en la capa superconductora aplicando simplemente un campo magnético externo mayor que  $H_{c1}$ . En este caso, nuestros cálculos de la energía libre demuestran un acoplo atractivo que unirá los vórtices al skyrmion en una de las orientaciones del campo magnético. En la orientación opuesta, los vórtices serán eliminados por el skyrmion. Esta atracción o repulsión del skyrmion por los vórtices puede ser, en principio, detectada experimentalmente. Nuestros resultados también sugieren el efecto inverso, es decir, la nucleación de un skyrmion debido a la proximidad de un vórtice superconductor, y podría en principio ser observado experimentalmente gracias a la microscopía de fuerza magnética o al efecto Hall topológico en sistemas como Nb/Co/Pt. Es importante recalcar que recientemente se ha demostrado que este tipo de pares skyrmion/vórtice

---

han de conllevar estados ligados de Majorana, abriendo nuevas perspectivas para el control espacial de Majorana.

## Superconductividad en multibandas en presencia de impurezas magnéticas

Finalmente, la última parte de la tesis está dedicada al estudio de la dependencia espacial de los estados Yu-Shiba-Rusinov (YSR o Shiba) inducidos por impurezas paramagnéticas en superconductores no convencionales.

Este trabajo está motivado por resultados experimentales recientemente obtenidos por el grupo de José Ignacio Pascual (CIC nanoGUNE, San Sebastián, Spain) basados en el cristal superconductor  $\beta$ -Bi<sub>2</sub>Pd en presencia de impurezas de Vanadio. De forma sorprendente, se ha encontrado una oscilación espacial de doble periodo de la densidad local de estados (LDOS) de Shiba en este material. Con el fin de explicar este resultado, nos centraremos en desarrollar modelos efectivos que sirvan para identificar los mecanismos en el origen de esta doble oscilación.

Una posible aproximación para modelar la estructura de bandas del electrón es usar simulaciones basadas en el modelo de enlace fuerte (usualmente conocido como modelo de "tight-binding"). A pesar de que hay observaciones que indican bandas de superficie en 2D (e incluso algunas bandas de volumen) que participan en la dispersión de electrones del  $\beta$ -Bi<sub>2</sub>Pd, elegiremos simplificar este problema a un sistema unidimensional. Por supuesto, este modelo no es aplicable para describir los experimentos; sin embargo, puede proporcionarnos un entendimiento fundamental acerca de los mecanismos en el origen de la dependencia espacial de los estados de Shiba. Específicamente, nuestros modelos unidimensionales nos permiten entender dos cuestiones básicas, a saber, cuándo una impureza magnética acoplada a una banda helicoidal da lugar a oscilaciones espaciales de Shiba y cuál es la mínima condición para observar una oscilación espacial doble de los estados YSR. Para abordar estas cuestiones, el grupo de Alfredo Levy Yeyati de la Universidad Autónoma de Madrid, usó un modelo unidimensional de tight-binding que en el límite continuo se puede representar mediante hilos. Con el fin de guiar sus simulaciones, debemos por tanto desarrollar dos modelos analíticos efectivos unidimensionales.

El primer modelo consiste en un solo hilo superconductor con dispersión helicoidal. Demostramos que, en presencia de una impureza magnética, estados de Shiba aparecen en el gap superconductor, aunque estos se caracterizan por la ausencia de oscilaciones espaciales de los LDOS no polarizados. Por tanto, la dependencia espacial de los estados YSR no puede explicarse basándonos en bandas puramente quirales. Nótese que los LDOS con polarización de espín del hilo helicoidal muestran una oscilación espacial, que en principio podría ser detectados de forma experimental gracias a un STM con puntas magnéticas en materiales reales.

Después hemos desarrollado un modelo para dos hilos : dos hilos superconductores con una dispersión cuadrática se conectan a través de un término de efecto túnel. Una impureza magnética se acopla al hilo superior. Como cabía esperar, los estados de Shiba están localizados en dicho hilo superior, y su energía no se ve afectada por la presencia del segundo hilo. Puede verse cómo ambos LDOS, polarizados y no polarizados, muestran una oscilación espacial doble con frecuencias que corresponden a la suma y la diferencia de los momentos de Fermi de cada hilo.

Por tanto, la condición mínima para obtener una oscilación espacial de doble periodo de los estados de Shiba parece estar presente en dos bandas electrónicas, siendo sendas participes en la superconductividad. Además, una dispersión helicoidal de al menos

---

una de las bandas eliminaría la oscilación doble de la LDOS. Es por tanto necesario considerar otro tipo de dispersiones como, por ejemplo, cuadrática o al menos una dispersión que no sea perfectamente helicoidal.

Sin embargo, este trabajo está aún en progreso y, para un entendimiento completo del experimento, estos cálculos del modelo efectivo serán acompañados por simulaciones numéricas basadas en modelos de enlace fuerte, teniendo en cuenta la estructura de bandas real de  $\beta$ -Bi<sub>2</sub>Pd. Estas simulaciones están siendo actualmente realizadas por M. Alvarado Herrero y A. Levy Yeyati.

Finalmente, destacamos que estos modelos efectivos podrían ser fácilmente generalizables para describir el espectro de los superconductores de multibanda en presencia de impurezas magnéticas.



# Remerciements

Ce travail de thèse s'est déroulé en cotutelle entre l'Université de Bordeaux et la Universidad del País Vasco à San Sebastián (Espagne). Dans ce cadre, j'ai effectué la première partie de mon doctorat au sein du Laboratoire Ondes et Matière d'Aquitaine (LOMA) de l'Université de Bordeaux. Je remercie les deux directeurs successifs, Jean-Pierre Delville et Fabio Pistolesi, ainsi que tous les membres du laboratoire, de m'avoir accueillie chaleureusement. La seconde partie de ma thèse s'est déroulée au sein du Donostia International Physics Center (DIPC) et du Centro de Física de Materiales (CFM) à San Sebastián, dirigés respectivement par Ricardo Diez Muiño et Daniel Sánchez Portal. Merci aux membres de ces deux laboratoires, qui m'ont également accueillie à bras ouverts, et m'ont beaucoup aidée pour les différentes démarches administratives.

Je remercie Pascal Simon et Manuel Houzet d'avoir accepté d'être rapporteurs de mon manuscrit, malgré les grèves de transport ayant empêché M. Simon d'être physiquement présent à ma soutenance; les questions soulevées, aussi bien dans les rapports que lors de ma soutenance, m'ont permis d'aller plus loin dans ma réflexion, notamment sur la mise en pratique expérimentale des systèmes physiques proposés dans ce manuscrit. Merci à Philippe Tamarat d'avoir présidé ce jury, ainsi qu'à Andrés Arnau et Hélène Bouchiat pour leur participation active et leurs remarques et questions pertinentes sur mon travail.

Bien évidemment, je tiens à remercier chaleureusement mes trois directeurs de thèse, Alexandre Buzdin et Jérôme Cayssol pour Bordeaux, et F. Sebastian Bergeret pour San Sebastián. J'ai beaucoup appris de leurs façons de travailler respectives, ce qui m'a poussée à m'intéresser aux différents aspects de la supraconductivité présentés dans ce manuscrit. Mes remerciements vont tout particulièrement à Sebastian : merci pour ta disponibilité et ton écoute, merci de m'avoir laissé m'entêter et faire des erreurs, merci d'avoir toujours écouté mes questions et tenté de m'expliquer ce que je ne comprenais pas. Grâce à tes conseils attentifs, j'ai pu entre autres comprendre d'où venait cette incohérence que nous trouvions entre la méthode des fonctions de Green et le formalisme  $SU(2)$  dans le problème à un fil, ce qui m'a permis de développer une méthodologie pour décrire des supraconducteurs 1D soumis au couplage spin-orbite. Le jour où j'ai enfin compris comment faire a été le plus beau de ces trois ans de thèse!

Sebastian me l'a souvent fait remarquer (non sans raison) durant les 18 mois que j'ai passés au CFM, j'ai toujours tendance à privilégier l'aspect mathématique par rapport au sens physique de mon travail. Et il faut dire que j'ai été à bonne école pour cela! Monsieur Bruno Mendiboure, maître de conférence à l'Université de Pau et des Pays de l'Adour, a été mon enseignant durant mes trois ans de Licence; il m'a fait découvrir les mathématiques cachés derrière la physique, et la beauté de la mécanique quantique. Merci pour ces cours, qui ont été ma principale motivation à continuer jusqu'au doctorat!

---

Je me dois également de remercier deux autres enseignants, dont l'appui a été déterminant pour moi : Nathalie Guihéry, professeure à l'Université Paul Sabatier de Toulouse et Nicolas Suaud, maître de conférence. C'est au cours de mon stage de Master 1 au Laboratoire de Chimie et Physique Quantiques (LCPQ) de Toulouse, effectué sous leur direction conjointe, que j'ai réellement découvert le monde de la recherche.

Malgré les nombreuses difficultés d'ordres scientifique, administratif (et autres) rencontrées au cours de ces trois ans de thèse, j'ai pu compter sur le soutien de nombreuses personnes, aussi bien au LOMA qu'au CFM. Je tiens en particulier à remercier mes amis LOMiens, qui ont égayé mes pauses déjeuners : Paul, Marion, Alexandre et Houssein, dont les parties de babyfoot ont rythmé les après-repas, Alizée et ses talents pour les origamis, Goce et ses métaphores quelques peu insolites. Evidemment je remercie aussi Quentin, qui était comme moi en cotutelle entre le LOMA et le DIPC, même si je sais que s'il lit un jour ces lignes, il détestera ça ! Je voudrais également remercier les permanents du LOMA, et notamment Joseph, Rémi et Ludo, avec lesquels j'ai eu de nombreuses discussions très enrichissantes.

Je voudrais aussi remercier les membres de l'équipe Matière Condensée du DIPC et CFM, qui m'ont accueillie avec beaucoup de gentillesse à mon arrivée : Alba, Cristina, Mikel, Tineke, Xian-Peng, Dario et Vitaly. Au cours de ces 18 mois passés à San Sebastián, j'ai eu l'occasion de découvrir de nombreuses coutumes locales, et notamment les fameux Pizza Pote du mardi, et Pintxo Pote du jeudi ! Merci à Miguel, Martín, Carlos, Auguste et Sophie pour ces soirées, qui ont bien souvent fini sur la plage !

Finalement, je terminerai cette longue liste de remerciements par ma famille. Mes parents m'ont soutenue moralement durant ces trois ans de thèse, et ont vaillamment tenu bon durant toute ma soutenance, même si le mélange de Physique, de Mathématiques et d'Anglais n'était pas forcément très digeste ! Mes petites sœurs Lou et Prunille ont également contribué à leur façon à adoucir cette période, notamment avec des parties de jeux de société interminables alors que j'avais du travail ! Et bien sûr Éva, avec qui je me suis évadée de ma thèse en 4L jusqu'au Maroc il y a maintenant presque un an, pour participer au célèbre raid humanitaire 4L Trophy (auquel on a fini 4<sup>èmes</sup>/1000, et 2<sup>ndes</sup> au classement féminin !) ! Merci à ma grand-mère Françoise, et à Titisse et Papi pour leur soutien indéfectible et les longues conversations que nous avons eues. Et je n'oublierai pas ma cousine Astrid, dont la présence à ma soutenance m'a fait chaud au cœur. Et enfin, merci à Maxime, qui a supporté pendant plus de trois ans mes absences, les week-ends passés à bosser, mon humeur parfois déclinante, et qui a tenté de me changer les idées à sa manière, en m'apprenant l'art des machines à traire et de l'élevage des chèvres.

# Acknowledgments

This thesis work was realized in cotutela between the University of Bordeaux and the Basque country University in San Sebastián (Spain). Thus I spent the first part of my PhD in the Laboratoire Ondes et Matière d'Aquitaine (LOMA) of the University of Bordeaux. I thank the successive directors, Jean-Pierre Delville and Fabio Pistolesi, as well as all the members of the LOMA, who welcomed me warmly. The second part of my thesis was done in the Donostia International Physics Center (DIPC) and in the Centro de Física de Materiales (CFM) in San Sebastián, which are directed by Ricardo Diez Muiño and Daniel Sánchez Portal respectively. I would like to thank all the members of both centers, who also welcomed me very nicely and helped me a lot concerning administrative procedures.

I thank Pascal Simon and Manuel Houzet for accepting to refer my manuscript, even though Pascal Simon could not be physically present in my defense due to some strikes in France; They rose questions both in their reports and during the defense which allowed me to go deeper into my thinking, specially concerning the experimental realizations of the physical setups described in this manuscript. Thanks to Philippe Tamarat for heading the committee, and to Andrés Arnau and H el ene Bouchiat for their active participation and for their relevant questions and remarks about my work.

Of course, I would like to thank warmly my three supervisors, Alexandre Buzdin and J er ome Cayssol for Bordeaux, and F. Sebastian Bergeret for Donostia. I learned a lot from their respective ways of working, which made me interest in the different aspects of superconductivity presented in this manuscript. My acknowledgements are in particular addressed to Sebastian : thank you for your availability and your attention, thank you for letting me be stubborn and make mistakes, thank you for having always listened my questions and tried to explain me what I did not understand. Thanks to your attentive advice, I finally understood where this inconsistency between the Green's function method and the  $SU(2)$  formalism came from in the one-wire system, which allowed me to develop a methodology to describe 1D superconductors in the presence of spin-orbit interaction. This day when at least I understood how to do this was the most beautiful one of those three years of PhD!

During the 18 months that I spent in Donostia, Sebastian often pointed out (with some reason) that I tend to favour mathematics with respect to the physical meaning of my work. And it has to be said that I learned mathematics from the best! Mr. Bruno Mendiboure, who is a researcher in the University of Pau, was my teacher during my first three years at university; He made me discover the mathematics hidden under physics, and the beauty of quantum mechanics. Thank you for these lectures, which were my main motivation to continue until PhD!

I also have to thank two other teachers, whose support was decisive for me : Nathalie Guih ery, professor in the University Paul Sabatier in Toulouse, and Nicolas Suaud,

---

researcher. I made my Master 1 internship under their joint supervision in the Laboratoire de Chimie et Physique Quantiques (LCPQ) in Toulouse, and it really made me discover research.

Even though I encountered lots of difficulties during these three years, I know that I was supported by many persons, in the LOMA as well as in the CFM. I would like in particular to thank my friends from LOMA, who brightened up my lunch breaks : Paul, Marion, Alexandre and Houssein, whose babyfoot matches were very important events of the after-lunch, Alizée and her origami talent, Goce and his surprising metaphors. Of course I also thank Quentin, who was in cotutela between the LOMA and DIPC as me, even if I know that he will hate this if he reads it one day. And I would like to thank the researchers from the LOMA, in particular Joseph, Rémi and Ludo, whose discussions were very rewarding.

I also thank the members of the Condensed Matter team in DIPC and CFM, who welcomed me very nicely when I arrived in Spain : Alba, Cristina, Mikel, Tineke, Xian-Peng, Dario and Vitaly. During these 18 months spent in Donostia, I discovered several local customs, and especially the Tuesday Pizza Pote and Thursday Pintxo Pote ! Many thanks to Miguel, Martín, Carlos, Auguste and Sophie for these evenings which ended very often in the beach !

Finally, I will finish this acknowledgement list by my family. My parents supported me morally during these three years of PhD, and held up valiantly during the defense, even if the mix of Physics, Mathematics and English was not so digest ! My little sisters Lou and Prunille also helped me in their way, in particular with endless board games whereas I had to work ! And of course Éva, with who I escaped my thesis in 4L until Morocco about one year ago now, to participate in the famous humanitarian raid 4L Trophy (in which we arrived 4<sup>th</sup>/1000, and 2<sup>nd</sup> in the female ranking ! ) ! I thank my grandma Françoise, and Titisse and papi for their unfailing support and the long discussions that we had. I will not forget my cousin Astrid, whose presence at my defense was very important for me. And to finish, I would like to thank Maxime, who endured my absences during more than three years, the working week-ends, my mood sometimes decreasing, and who tried to make me think to something else in his way, by teaching me the art of milking machines and goat rearing.

# Contents

Résumé en Français	v
Resumen en Español	xi
Remerciements	xvii
Acknowledgments	xix
Contents	xxi
<b>1 General introduction</b>	<b>1</b>
<b>2 Brief survey of theories of superconductivity</b>	<b>5</b>
2.1 Ginzburg-Landau approach	6
2.1.1 The Ginzburg-Landau free energy	6
2.1.2 The Ginzburg-Landau equations	7
2.1.3 Two characteristic lengths : Penetration length and coherence length	8
2.1.4 Two types of superconductors	9
2.2 Gor'kov formalism for the BCS theory	10
2.2.1 Gor'kov equations	11
2.2.2 The self-consistency relation	12
2.3 Conclusion	14
<b>3 Introduction to inhomogeneous superconductivity</b>	<b>15</b>
3.1 First prediction of inhomogeneous superconductivity : The FFLO state	16
3.1.1 Two pair-breaking mechanisms	16
3.1.2 Qualitative arguments for the appearance of the FFLO state	17
3.1.3 Characteristics of the FFLO phase of a quasi-1D superconductor	19
3.1.4 Experimental evidence of the existence of the FFLO state	22
3.2 Another type of inhomogeneous superconductivity : The helical state	23
3.3 Conclusion	25
<b>4 Helical state and magnetoelectric effects in superconducting wires</b>	<b>27</b>
4.1 Spin-galvanic effects in superconducting wires	28
4.1.1 Brief introduction to the SU(2)-covariant formalism	28
4.1.2 One dimensional systems	29
4.1.3 The double wire setup : A quasi-2D system	30
4.2 Self-consistent order parameter for weak spin-orbit coupling	31
4.2.1 Single wire system	31
4.2.2 Double wire system	34

4.3	Superconducting wire with a strong spin-orbit coupling . . . . .	37
4.3.1	Normal state Green's functions in the helical basis . . . . .	38
4.3.2	Emergence of the modulated phase . . . . .	39
4.3.3	Field-temperature phase diagrams . . . . .	41
4.4	Conclusion . . . . .	44
<b>5</b>	<b>Generation of a superconducting vortex via Néel skyrmions</b>	<b>45</b>
5.1	Two types of vortices : Magnetic skyrmions and Abrikosov superconducting vortices . . . . .	46
5.1.1	Néel skyrmion in a ferromagnetic layer . . . . .	46
5.1.2	Superconducting vortices in a thin film . . . . .	46
5.2	Superconducting layer in contact with a Néel skyrmion : Free energy . . . . .	50
5.3	Creation of a superconducting vortex . . . . .	54
5.3.1	Magnetic field induced by the skyrmion . . . . .	54
5.3.2	Superconducting vortex generation . . . . .	54
5.3.3	Multiquanta vortices . . . . .	55
5.4	Magnetic field and current distributions . . . . .	56
5.4.1	Magnetic field distribution . . . . .	56
5.4.2	Current distribution . . . . .	57
5.5	Conclusion . . . . .	58
<b>6</b>	<b>Multiband superconductivity in the presence of magnetic impurities</b>	<b>59</b>
6.1	Introduction to Yu-Shiba-Rusinov bound states . . . . .	60
6.1.1	Energy of the Shiba states . . . . .	60
6.1.2	Local density of states . . . . .	63
6.2	Superconducting crystal $\beta$ -Bi <sub>2</sub> Pd in the presence of Vanadium impurities . . . . .	65
6.3	First model : Single superconducting band with helical dispersion . . . . .	68
6.3.1	Model . . . . .	68
6.3.2	Shiba energy . . . . .	69
6.3.3	Local density of states . . . . .	69
6.4	Second model : Two superconducting wires coupled via a hopping term . . . . .	71
6.4.1	Model . . . . .	71
6.4.2	Shiba energy . . . . .	72
6.4.3	Local density of states . . . . .	72
6.5	Conclusion . . . . .	74
<b>7</b>	<b>General conclusion</b>	<b>77</b>
<b>A</b>	<b>One wire system : Linear-in-<math>q</math> term of the self-consistency equation</b>	<b>79</b>
A.1	Self-consistency equation . . . . .	79
A.2	Expansion in $h_x$ and $h_z$ . . . . .	80
A.3	Linear term in $q$ . . . . .	80
A.4	Expansion in $\alpha$ . . . . .	82
A.5	Integration over $p$ . . . . .	82
<b>B</b>	<b>Two wire system : Linear-in-<math>q</math> term of the self-consistency equation</b>	<b>83</b>
B.1	Self-consistency equation . . . . .	83
B.2	Expansion in $t$ . . . . .	84
B.3	Expansion in $h_z$ . . . . .	84
B.4	Linear term in $q$ . . . . .	85

B.5	Expansion in $\alpha$ . . . . .	85
B.6	Integration over $p$ . . . . .	85
<b>C</b>	<b>Free energy of the S/F bilayer in the presence of a Néel skyrmion</b>	<b>87</b>
C.1	Derivation of the magnetoelectric energy $\mathbf{F}_L$ . . . . .	87
C.2	Final expression of the free energy $\mathbf{F}$ . . . . .	88
	<b>Bibliography</b>	<b>91</b>



# Chapter 1

## General introduction

**T**HE PRESENCE OF A MAGNETIC FIELD in a s-wave superconductor is detrimental in two distinct ways. First, if the magnetic field interacts with the motion of the superconducting electrons, it induces opposite Lorentz forces on each electron of the Cooper pairs, which spreads the pairs and can even break them for fields larger than the critical magnetic field. This is the orbital effect. On the other hand, if the field interacts with the spin of the electrons, it induces a spin polarization which tends to align the opposite spins of the Cooper pair electrons in the same direction, thus breaking the pairs. This is the Pauli paramagnetic effect, due to the Zeeman effect on conduction electrons. Usually, the critical field is determined by both orbital and paramagnetic effects. We will go back on these mechanisms in Chapter 3.

In some materials like heavy fermion superconductors or thin superconducting films (like Al films) with an in-plane magnetic field, the paramagnetic effect becomes predominant. Peter Fulde, Richard Ferrell, Anatoly Larkin and Yurii Ovchinnikov predicted in 1964 the existence of a new superconducting state emerging in the presence of a Zeeman field, the so-called FFLO state [1, 2]. This state appears at low temperatures  $T < 0.56 T_{c0}$  and magnetic field  $h > 1.07 T_{c0}$ , where  $T_{c0}$  is the critical temperature in the absence of magnetic field, and is characterized by a spatially dependent order parameter, as we show in Chapter 3, leading to enhance the critical field at low temperatures. Despite its prediction more than 50 years ago, the FFLO state has only been experimentally evidenced very recently [3], mainly because of the difficulty to stabilize this phase, which is very sensitive to impurities and orbital effect.

If the superconductor in a Zeeman field also displays spin-orbit interaction, new phenomena emerge due to the interplay between both spin fields. Among them, we can cite the critical field enhancement related to the existence of a helical phase, another type of inhomogeneous superconducting phase which appears at high temperatures and low magnetic fields, briefly described in Chapter 3. Contrary to the FFLO case, such a superconducting helical state is expected to exist even in the presence of impurities, which has motivated numerous investigations in two and three-dimensional systems [4, 5, 6, 7, 8, 9]. In addition to this non-uniform phase, magnetoelectric effects stemming from the coupling between spin and charge degrees of freedom, namely anomalous charge currents, may appear in superconductors with both Zeeman and spin-orbit interactions [10, 11, 12, 13]. In infinite systems, the ground state corresponds to a zero current state in which these anomalous currents are compensated by the currents coming from the spatial modulation of the superconducting order parameter [6]. In realistic setups, such (finite) systems could be used for example in the realization of  $\varphi_0$ -Josephson junctions [14]. The appearance of such anomalous currents

in superconducting wires in the presence of both Rashba spin-orbit and Zeeman fields, together with the helical superconducting state is the topic of Chapter 4.

Another interesting phenomenon resulting from the interplay between superconductivity and spin-dependent fields is the possible emergence of a vortex in a superconducting layer proximity coupled to a ferromagnet hosting a Néel skyrmion with spin-orbit interaction, in the absence of external magnetic field [15]. The nucleation of vortices in type-II superconductors in the presence of a magnetic field  $H_{c1} < H < H_{c2}$ , where  $H_{c1}$  and  $H_{c2}$  are respectively the lower and upper critical fields characterizing type-II superconductors, was predicted by Alexei Abrikosov in 1957 [16]. Due to the negative surface energy of such superconductors, the magnetic flux can penetrate the material in a regular array of tubes, the so-called Abrikosov vortices, each carrying a quantum of flux  $\Phi_0 = h/2e$ . This coexistence of superconducting and normal states was anticipated by Ginzburg and Landau with their classification of two types of superconductors. However, it has been demonstrated that it is also possible to nucleate a vortex even in the absence of an external magnetic field. Indeed, in the system described at the beginning of the present paragraph, the coupling between Zeeman and spin-orbit interactions in the skyrmion (which can basically be seen as a vortex of spins) leads to the appearance of anomalous currents, which induce a spin polarization at the interface with the superconductor due to the proximity effect. Then, if this current is sufficiently strong, the associated magnetic field can nucleate a vortex in the superconducting layer, which surprisingly can even carry more than one quantum of flux  $\Phi_0$ . We emphasize that such skyrmion/vortex pair is expected to host Majorana zero modes [17], which are one of the most promising candidates for the realization of qubits [18, 19, 20, 21, 22, 23, 24, 25, 26]. Chapter 5 is devoted to the study of the vortex emergence in a superconducting layer proximity coupled to a Néel skyrmion.

Up to now, we have presented examples in which the entire superconducting system was subjected to the action of spin-dependent fields. However, it is also possible to induce a localized exchange field acting like a Zeeman field in a superconductor, via magnetic impurities. The effect of such impurities on s-wave superconductors was investigated by Luh Yu, Hiroyuki Shiba and A. I. Rusinov in the 1960's, who found the appearance of localized bound states in the superconducting gap, the so-called Yu-Shiba-Rusinov states [27, 28, 29, 30]. The underlying mechanism is once again the paramagnetic effect, which locally breaks Cooper pairs : the impurity couples to one of the electron of the pair, whereas the remaining one forms a spin polarized bound state. Yu-Shiba-Rusinov states are characterized by a spatially oscillating and decaying local density of states (LDOS), which allowed them to be detected experimentally for the first time in 1997, thanks to the development of Scanning Tunneling Microscopy (STM) [31]. This field is still very much under investigation, mainly because of two potential applications : First, it has been demonstrated that chains of magnetic impurities on top of superconductors lead to the appearance of Majorana zero modes. Then, Yu-Shiba-Rusinov states in low-dimensional superconductors were proposed as a probe to determine the nature of superconducting correlations, namely singlet or triplet pairing [32]. This last idea was one of the motivations of recent experiments by the group of José Ignacio Pascual in CIC nanoGUNE (San Sebastián, Spain) on the superconductor  $\beta$ -Bi<sub>2</sub>Pd in the presence of Vanadium impurities. They obtained a rather surprising result : the LDOS of Yu-Shiba-Rusinov states displays a double period spatial oscillation. In Chapter 6, we focus on building effective models to explain this result.

In this thesis, we study the three effects previously mentioned stemming from the

interaction between superconductivity and spin-dependent fields in low-dimensional systems : the emergence of a helical phase, the appearance of anomalous charge currents, and the presence of Yu-Shiba-Rusinov states induced by a magnetic impurity in a non-conventional superconductor.

In Chapter 2, we present the main results of the Ginzburg-Landau theory and of Gor'kov reformulation of the BCS theory. The aim of this chapter is to briefly introduce some of the fundamental concepts needed to understand the rest of this work.

Chapter 3 is an introduction to inhomogeneous superconductivity through the description of the FFLO and helical phases. Using qualitative arguments, we explain the emergence of both phases. Moreover, we present the Green's function formalism which will be used in the next chapter and applying it to a superconducting system in the presence of a Zeeman field, we provide the FFLO field-temperature phase diagram.

In Chapter 4, we study the helical phase and anomalous currents stemming from the interplay between Zeeman and Rashba spin-orbit interactions in two distinct quasi one-dimensional superconductors. We first show that it is possible to predict the form of the anomalous currents in terms of the spin fields using the SU(2)-covariant formalism. Then, using the Green's function formalism introduced in Chapter 3, we derive the complete expression of such currents together with the self-consistent order parameter, in the limit of weak spin-orbit interaction with respect to the critical temperature, and show that the ground state corresponds indeed to a zero-current state. Finally, the field-temperature phase diagram is obtained in the limit of strong spin-orbit coupling with respect to the critical temperature  $T_c$ .

In Chapter 5, we investigate the magnetoelectric effects stemming from a Néel skyrmion proximity coupled to a superconducting thin film. In the presence of strong spin-orbit interaction, we show that the skyrmion induces charge currents at the interface between both layers, and a magnetic field which may lead to the generation of a vortex. From the expression of the free energy of the system, we derive the necessary condition for the appearance of this vortex, and compute the magnetic field and current distributions in the superconductor.

Finally, Chapter 6 is devoted to the building of effective models in order to understand qualitatively the coupling between magnetic impurities and superconductivity in non-conventional superconductors like  $\beta$ -Bi<sub>2</sub>Pd. To this purpose, we study two models in which 1D electronic bands are represented by wires : A one-dimensional superconductor with helical dispersion and a two wire model with a quadratic dispersion in which the impurity is coupled only to the upper superconductor.



## Chapter 2

# Brief survey of theories of superconductivity

AFTER THE EXPERIMENTAL DISCOVERY OF SUPERCONDUCTIVITY by H. Kamerlingh Onnes in 1911 [33], different phenomenological theories were developed to explain the main properties of superconductors. In 1935, Fritz and Heinz London built a theory based on electrodynamics to explain the perfect diamagnetism observed in superconducting materials [34], generalized to non-local treatment by Brian Pippard in 1953 [35]. However, the most complete phenomenological description of superconductivity was realized by Vitaly Ginzburg and Lev Landau in 1950 [36]. Associating electromagnetism and thermodynamics, this approach allowed to describe Meissner effect, and highlighted the two superconducting characteristic lengths, namely the magnetic field penetration length, already obtained by London, and the coherence length.

It was not until 1957 that the first microscopic description of superconductivity was developed by John Bardeen, Leon Cooper and Robert Schrieffer [37]. This BCS theory is based on the fact that in the superconducting state, two electrons with opposite spins and momenta are coupled via an effective attractive interaction mediated by phonons, forming the so-called Cooper pairs [38]. This theory is in fact a many-body theory describing the behaviour of Cooper pairs. It recovers the main characteristics of conventional superconductors : The Meissner effect, the penetration length or specific heats.

However, BCS formalism can be quite complicated to use, specifically to describe inhomogeneous superconductivity, where the superconducting order parameter is spatially dependent. This problem was solved in two different ways : Bogoliubov-De Gennes method consists in diagonalizing the BCS Hamiltonian [39], whereas Lev Gor'kov reworked the BCS formalism in term of Green's functions [40]. One of the most remarkable result coming from this last reformulation was the demonstration that the Ginzburg-Landau theory corresponds to a limiting case of the BCS theory, valid near the critical temperature  $T_c$  [41].

In this chapter, we first introduce the main results of the Ginzburg-Landau theory. Specifically, we derive the Ginzburg-Landau free energy and equations which contains the two superconducting characteristic lengths. In a second part, after a very brief introduction to the BCS Hamiltonian, we present the Gor'kov Green's function formalism. In particular, we derive the self-consistency equation, which will be used in Chapter 4. Notice that this chapter is only an introduction to some fundamental concepts of superconducting theories, which are needed to understand the rest of this thesis. To get access to a more complete description, in particular for the BCS theory which is

not detailed here, the reader could refer, for example, to Refs. [42, 43].

## 2.1 Ginzburg-Landau approach

The Ginzburg-Landau theory was developed in the continuity of Landau's second order phase transition theory [44, 45]. This one describes the transition from a high symmetry state to a reduced symmetry state, characterized by a parameter called the order parameter : In the high symmetry state, this parameter vanishes, and becomes finite when the symmetry breaks. Landau's theory is based on the expansion of the free energy in powers of the order parameter near the transition.

Following Landau's theory, Ginzburg and Landau described the transition between normal and superconducting states at temperatures close to the critical temperature  $T_c$ . They assumed a complex superconducting order parameter  $\Psi(\vec{r}) = \Psi_0 e^{i\varphi(\vec{r})}$  describing the superconducting electrons and derived an expansion of the free energy in powers of  $|\Psi|$ . Then, by the mean of variational calculations, they obtained two differential equations, the so-called Ginzburg-Landau equations, which allow to define the superconducting current and to determine the two characteristic lengths of the superconducting state.

The triumph of this theory is related to several results and predictions, specifically the spatial variation of the superconducting electron density and the classification of superconductors in two types, predicting the mixed phase where the superconducting and normal phase coexist.

Next, we present the Ginzburg-Landau free energy. Then, from variational treatment, we derive the so-called Ginzburg-Landau equations, leading to the definition of two characteristic lengths : The penetration length and the coherence length. Finally, we show how the ratio between these two lengths allow to classify superconductors in two types.

### 2.1.1 The Ginzburg-Landau free energy

At temperatures close to the critical temperature  $T_c$ , where the transition between the normal and the superconducting states happens, the free energy density can be expanded over powers of  $|\Psi|$  [44, 45] :

$$f_S = f_N + a |\Psi|^2 + \frac{b}{2} |\Psi|^4 + \frac{1}{2m^*} \left| \left( \frac{\hbar}{i} \vec{\nabla} + e^* \vec{A} \right) \Psi \right|^2 + \frac{\vec{B}^2}{2\mu_0}, \quad (2.1)$$

where  $\mu_0$  is the vacuum permeability,  $a$  and  $b$  are temperature-dependant parameters and  $f_N$  is the free energy density of the normal state,  $\vec{A}$  is the vector potential and  $\vec{B} = \vec{\nabla} \times \vec{A}$  is the magnetic induction.

To understand the transition between the normal and superconducting states, we first study the difference of free energy density  $f_N - f_S$  in the absence of gradient and magnetic field :

$$\Delta f = a \Psi_0^2 + \frac{b}{2} \Psi_0^4. \quad (2.2)$$

The minimization of  $\Delta f$  with respect to  $\Psi_0$  imposes that  $b$  must be positive. Indeed, if we take  $b$  negative, the minimum of the free energy would occur for very large values of  $\Psi_0^2$ , which makes the expansion inadequate. This minimization gives  $a + b \Psi_0^2 = 0$ ,

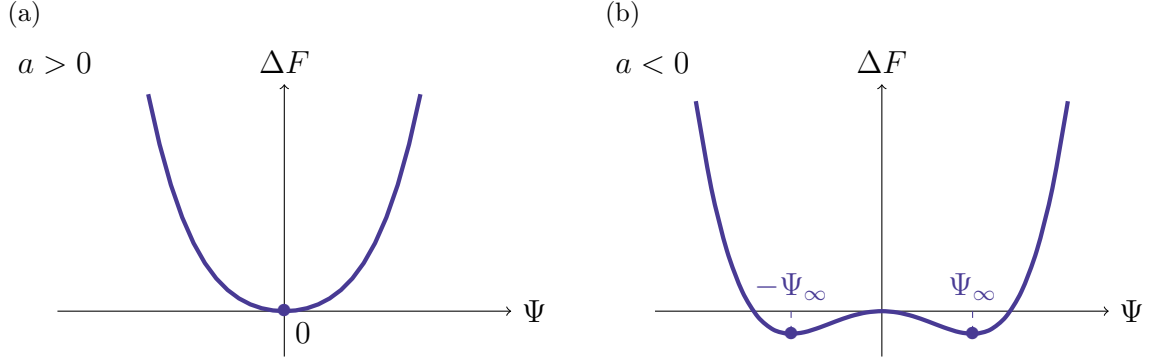


FIGURE 2.1 – Ginzburg-Landau free energy density in : (a) the normal state ( $T > T_c$ ) (b) the superconducting state ( $T < T_c$ ).

thus leading to the following expression for the order parameter amplitude :

$$\Psi_0^2 = -\frac{a}{b}. \quad (2.3)$$

Then, two situations arise depending on the sign of the parameter  $a$ , as illustrated in Fig. 2.1. If  $a > 0$ ,  $\Psi_0^2$  is negative and the only possible solution is  $\Psi_0^2 = 0$ . This is the normal state. On the other hand, if  $a < 0$ , the order parameter  $\Psi_0^2$  is finite and positive : This is the superconducting state. The minimum of energy is reached for  $\Delta F = -a^2/2b$  and the equilibrium value of the order parameter is called  $\Psi_\infty$ . The transition between the normal and superconducting states being related to the sign of  $a$ , we thus define it as  $a = a_0(T - T_c)$ , where  $a_0$  is positive and the temperature  $T$  is close to  $T_c$ .

### 2.1.2 The Ginzburg-Landau equations

The free energy density Eq. (2.1) is a functional of two variables : The order parameter  $\Psi$  and the potential vector  $\vec{A}$ . Standard variational calculations lead to the Ginzburg-Landau differential equations :

$$a\Psi + b|\Psi|^2\Psi + \frac{1}{2m^*} \left( -i\hbar\vec{\nabla} + e^*\vec{A} \right)^2 \Psi = 0, \quad (2.4)$$

and

$$\vec{j} = \frac{i\hbar e^*}{2m^*} \left( \Psi^*\vec{\nabla}\Psi - \Psi\vec{\nabla}\Psi^* \right) - \frac{e^{*2}}{m^*} \vec{A} |\Psi|^2. \quad (2.5)$$

By comparing the expression (2.5) with the usual quantum-mechanical current, one can identify the mass and the charge of the superconducting charge carriers, the so-called Cooper pairs :  $m^* = 2m$  and  $e^* = 2e$ , where  $m$  and  $-e$  are respectively the mass and the charge ( $e > 0$ ) of the electron. Eq. (2.5) can also be written :

$$\vec{j} = \frac{e}{m} \Psi_0^2 \left( \vec{\nabla}\varphi + 2e\vec{A} \right) = 2e\Psi_0^2 \vec{v}_s, \quad (2.6)$$

where  $\vec{v}_s = \frac{1}{2m} \left( \vec{\nabla}\varphi + 2e\vec{A} \right)$  is the velocity of the superconducting electrons in a gauge-invariant form. This equation allows to identify the modulus of the superconducting order parameter with the density of superconducting electrons  $n_s$  :

$$\Psi_0^2 = \frac{1}{2} n_s. \quad (2.7)$$

### 2.1.3 Two characteristic lengths : Penetration length and coherence length

A superconducting material is characterized by two lengths, namely the London penetration length and the coherence length. They can be derived from the Ginzburg-Landau equations (2.4) and (2.5).

#### Coherence length

In the absence of magnetic field, Eq. (2.4) reads :

$$a \Psi + b |\Psi|^2 \Psi - \frac{\hbar^2}{4m} \Delta \Psi = 0 . \quad (2.8)$$

Near the critical temperature, one can neglect higher order in  $|\Psi|^2$ , leading to the following differential equation :

$$\Delta \Psi - \frac{1}{\xi} \Psi = 0 . \quad (2.9)$$

This equation involves the coherence length  $\xi$  defined by :

$$\xi(T) = \frac{\xi_0}{\sqrt{1 - \frac{T}{T_c}}} , \quad (2.10)$$

where  $\xi_0 = \sqrt{\frac{\hbar^2}{4m a_0 T_c}}$  is the coherence length at zero temperature. This characteristic length can be interpreted as the average distance between the two electrons of the Cooper pairs.

#### London penetration length

At equilibrium in the superconducting state,  $\Psi = \Psi_\infty$  and the current Eq. (2.5) reads :

$$\vec{j} = -\frac{e^2 n_s}{m} \vec{A} . \quad (2.11)$$

Replacing  $\vec{j}$  in the Maxwell-Ampere equation  $\mu_0 \vec{j} = \vec{\nabla} \times \vec{B} = -\Delta \vec{A}$ , we obtain the London equation :

$$\Delta \vec{A} - \frac{1}{\lambda} \vec{A} = 0 , \quad (2.12)$$

where we have defined the London penetration length  $\lambda$  :

$$\lambda = \sqrt{\frac{m}{\mu_0 e^2 n_s}} . \quad (2.13)$$

This characteristic length describes the exponential decreasing of a magnetic field in a superconducting material, which explains the Meissner effect. Notice that contrary to the London theory, in the Ginzburg-Landau formalism  $\lambda$  is a function of the temperature :  $n_s = -2 a_0 (T - T_c) / b$ .

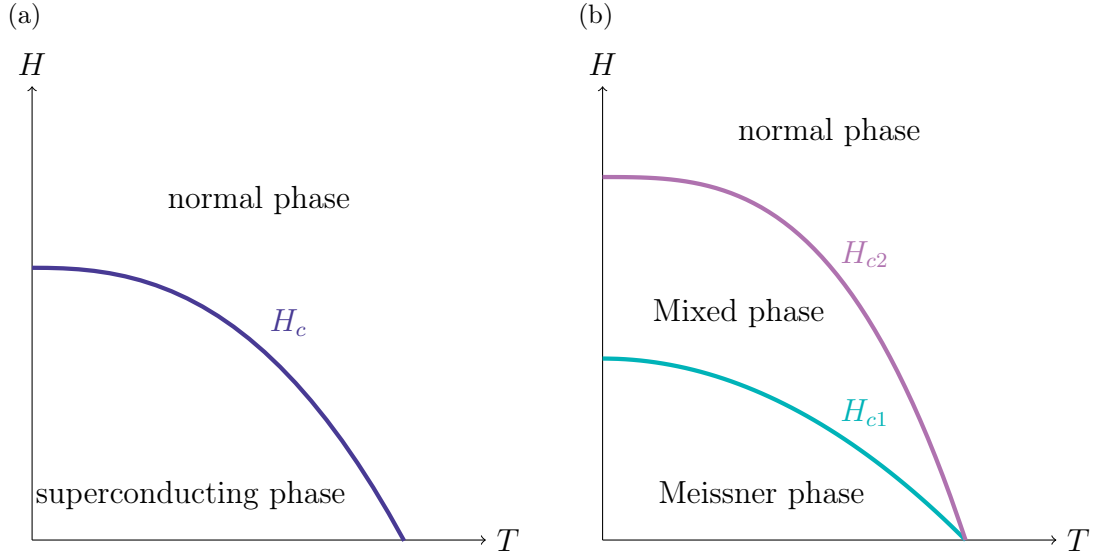


FIGURE 2.2 – Temperature-field phase diagrams of superconductors : (a) Type-I superconductor. When the magnetic fields exceeds  $H_{c1}$ , the material becomes normal. (b) Type-II superconductor. In the mixed phase  $H_{c1} < H < H_{c2}$ , the superconducting and normal states coexist, forming Abrikosov vortices.

### 2.1.4 Two types of superconductors

Both characteristic lengths  $\lambda(T)$  and  $\xi(T)$  are connected by a parameter called the Ginzburg-Landau parameter  $\kappa$  :

$$\kappa = \frac{\lambda(T)}{\xi(T)}, \quad (2.14)$$

which is independent of the temperature near  $T_c$ . The value of this parameter defines the two types of superconductors :

- if  $\kappa < \frac{1}{\sqrt{2}}$ , we have a superconductor of type I;
- if  $\kappa > \frac{1}{\sqrt{2}}$ , we talk about type-II superconductivity.

These two types of superconductors exhibit really different properties. Type-I superconductors are characterized by a perfect diamagnetism until a critical magnetic field  $H_c$ , where the metal becomes normal. From an energetic point of view, these superconductors present a positive surface energy between the normal and superconducting states.

On the other hand, type-II superconductors display a negative surface energy, namely normal and superconducting states can coexist in the same material. In this case, we observe two critical fields  $H_{c1}$  and  $H_{c2}$ . For magnetic fields smaller than the first critical field  $H_{c1}$ , the superconductor behaves like a perfect diamagnet. When the applied magnetic field exceeds  $H_{c2}$ , the material becomes normal. However, between these two values a new state appears, called the mixed phase or Shubnikov phase. It is characterized by the appearance of normal areas where the magnetic field penetrate the material, and surrounded by circulating supercurrents : The so-called Abrikosov vortices [16]. More details concerning vortices are provided in Chapter 5.

In conclusion to this section, we have presented the main results of the Ginzburg-Landau theory : The Ginzburg-Landau differential equations, the penetration and coherence lengths and the classification of superconductors in two groups. In the following, we introduce the Gor'kov Green's function formalism of the microscopic BCS theory.

## 2.2 Gor'kov formalism for the BCS theory

It was shown in 1956 by Leon Cooper that in the superconducting state, electrons were coupled by pairs, forming the so-called Cooper pairs [38]. The effective attractive interaction between two electrons is mediated by phonons : Qualitatively, an electron polarizes the ions of the crystal lattice along its trajectory, thus creating positive charges, which in turn attract a second electron. This last one is therefore connected to the first electron by an effective attractive interaction, forming a Cooper pair.

The Fermi sea is unstable against the creation of Cooper pairs, which condense until equilibrium, forming a Bose-like condensate of Cooper pairs. Bardeen, Cooper and Schrieffer described this condensate state in a historical paper by the mean of many-body and mean-field theories, recovering the main experimental results of superconductivity [37]. To this purpose, they introduced the following effective mean-field Hamiltonian<sup>1</sup> :

$$\begin{aligned} \mathcal{H}_{\text{BCS}} = & \int d^3\vec{r} \psi_{\alpha}^{\dagger}(\vec{r}) \left[ -\frac{\hbar^2}{2m} \vec{\nabla}^2 - \mu + V(\vec{r}) \right] \psi_{\alpha}(\vec{r}) + \Delta^{\star}(\vec{r}) \int d^3\vec{r} \psi_{\downarrow}(\vec{r}) \psi_{\uparrow}(\vec{r}) \\ & + \Delta(\vec{r}) \int d^3\vec{r} \psi_{\uparrow}^{\dagger}(\vec{r}) \psi_{\downarrow}^{\dagger}(\vec{r}) , \end{aligned} \quad (2.15)$$

where the summation over repeated indices is implicit, and the creation and annihilation operators  $\psi_{\alpha}^{\dagger}(\vec{r})$  and  $\psi_{\alpha}(\vec{r})$  of an electron at position  $\vec{r}$  and spin  $\alpha$  follow the anti-commutation relations<sup>2</sup> :

$$\{\psi_{\alpha}(\vec{r}), \psi_{\beta}(\vec{r}')\} = \{\psi_{\alpha}^{\dagger}(\vec{r}), \psi_{\beta}^{\dagger}(\vec{r}')\} = 0 ; \quad (2.16a)$$

$$\{\psi_{\alpha}(\vec{r}), \psi_{\beta}^{\dagger}(\vec{r}')\} = \delta_{\alpha\beta} \delta(\vec{r} - \vec{r}') . \quad (2.16b)$$

The first term of Eq. (2.15) describes the energy of a single electron, which includes a kinetic term  $-\frac{\hbar^2}{2m} \vec{\nabla}^2 - \mu$ , where  $\mu$  is the chemical potential, and a potential term  $V(\vec{r})$ . The two other terms represent the energy associated to the superconducting pairing, where we define the superconducting order parameter  $\Delta(\vec{r})$  as :

$$\Delta(\vec{r}) = \gamma \langle \psi_{\downarrow}(\vec{r}) \psi_{\uparrow}(\vec{r}) \rangle . \quad (2.17)$$

In the case of a constant order parameter, most of the characteristics of s-wave homogeneous superconductors can be obtained from Eqs. (2.15) and (2.17).

Shortly after the publication of the BCS theory, researchers began to investigate inhomogeneous superconductivity. To simplify the BCS treatment of such problems, Lev P. Gor'kov reworked the equations of motions of annihilation and creation operators involved in the BCS theory in terms of Green's functions [40]. Gor'kov formalism allows

1. Readers interested in details can refer to Refs. [42, 43].

2. Notice that in this thesis, we kept the most common denominations, *i.e.*  $\Psi(\vec{r})$  refers to the superconducting order parameter of the Ginzburg-Landau theory (which is called  $\Delta(\vec{r})$  in the BCS theory), whereas  $\psi$  corresponds to the annihilation operator of the BCS theory.

to get access to some information about the system, like the energy spectrum or the field-temperature phase diagram, in a rather simple way. This is the main subject of the present section : We present the Gor'kov Green's function formalism, which will be used in Chapters 3 and 4 to describe superconductivity in the presence of spin-dependent fields.

### 2.2.1 Gor'kov equations

The main idea of Gor'kov was to formulate the BCS theory in terms of Green's functions. In this case, the equations of motion, called Gor'kov equations, can be solved exactly, thus allowing to have the expression of the Green's functions. From these expressions, we can have access to fundamental characteristics of the superconductor like the energy spectrum, as we will see in this section, or the field-temperature phase diagram (see Sec. 2.2.2 and Chapter 3). To illustrate how Gor'kov formalism works, we consider an isolated superconductor with potential  $V(\vec{r}) = 0$  and a constant order parameter  $\Delta$ . From the BCS Hamiltonian written in momentum space, we derive the evolution equations of annihilation and creation operators and then write them in terms of Green's functions. Finally, we solve these equations and derive the energy spectrum of the system.

In momentum space, the BCS Hamiltonian Eq. (2.15) reads :

$$\mathcal{H}_{\text{BCS}} = \int d^3\vec{p} \left[ \xi \psi_{\alpha}^{\dagger}(\vec{p}) \psi_{\alpha}(\vec{p}) + \Delta^* \psi_{\downarrow}(\vec{p}) \psi_{\uparrow}(-\vec{p}) + \Delta \psi_{\uparrow}^{\dagger}(\vec{p}) \psi_{\downarrow}^{\dagger}(-\vec{p}) \right] \quad (2.18)$$

where  $\xi = \frac{p^2}{2m} - \mu$  is the quasiparticle energy. Although we did not mention it explicitly until now, the annihilation and creation operators are functions of the imaginary time  $\tau$  :  $\psi_{\alpha}(\vec{p}) = \psi_{\alpha}(\vec{p}, \tau)$ .

The evolution equations of creation and annihilation operators are given by the commutator of these operators with the BCS Hamiltonian :

$$\partial_{\tau} \psi_{\uparrow}(\vec{p}) = [\psi_{\uparrow}(\vec{p}), \mathcal{H}_{\text{BCS}}] = -\xi \psi_{\uparrow}(\vec{p}) - \Delta \psi_{\downarrow}^{\dagger}(-\vec{p}) ; \quad (2.19a)$$

$$\partial_{\tau} \psi_{\downarrow}^{\dagger}(\vec{p}) = [\psi_{\downarrow}^{\dagger}(\vec{p}), \mathcal{H}_{\text{BCS}}] = \xi \psi_{\downarrow}^{\dagger}(\vec{p}) - \Delta^* \psi_{\uparrow}(-\vec{p}) , \quad (2.19b)$$

where  $\partial_{\tau} = \partial/\partial\tau$ .

We now introduce two Green's functions as originally proposed by Gor'kov [40]. The first Green's function,  $G$ , is called normal Green's function and describes how an electron with momentum  $\vec{p}$  propagates during a time  $\tau$ . The second Green's function  $F^{\dagger}$  was introduced by Gor'kov to describe superconducting correlations, and is called anomalous Green's function :

$$G_{\alpha\beta}(\vec{p}, \tau) = -\langle T_{\tau} \psi_{\alpha}(\vec{p}, \tau) \psi_{\beta}^{\dagger}(\vec{p}, 0) \rangle ; \quad (2.20)$$

$$F_{\alpha\beta}^{\dagger}(\vec{p}, \tau) = \langle T_{\tau} \psi_{\alpha}^{\dagger}(\vec{p}, \tau) \psi_{\beta}^{\dagger}(-\vec{p}, 0) \rangle , \quad (2.21)$$

where  $T_{\tau}$  is the time-ordering operator and  $\alpha, \beta$  label the spin. The brackets  $\langle \dots \rangle$  represent the average value on the ground state at zero temperature, or a statistical average on the grand canonical Gibbs distribution at finite temperature.

The key point of this theory is that the evolution equations of the Green's functions (2.20) and (2.21) contain the time derivatives of the annihilation and creation operators

$\psi_{\uparrow}$  and  $\psi_{\downarrow}^{\dagger}$  :

$$\frac{\partial G_{\alpha\beta}}{\partial\tau} = -\delta_{\alpha\beta} - \langle T_{\tau} \frac{\partial\psi_{\alpha}(\vec{p}, \tau)}{\partial\tau} \psi_{\beta}^{\dagger}(\vec{p}, 0) \rangle ; \quad (2.22)$$

$$\frac{\partial F_{\alpha\beta}^{\dagger}}{\partial\tau} = \langle T_{\tau} \frac{\partial\psi_{\alpha}^{\dagger}(\vec{p}, \tau)}{\partial\tau} \psi_{\beta}^{\dagger}(-\vec{p}, 0) \rangle . \quad (2.23)$$

Therefore, after replacing Eqs. (2.19a) and (2.19b) into Eqs. (2.22) and (2.23) and taking the temporal Fourier transform, we obtain the so-called Gor'kov equations :

$$(i\omega_n - \xi) G + \Delta i\sigma_y F^{\dagger} = \mathbb{1} ; \quad (2.24a)$$

$$(i\omega_n + \xi) F^{\dagger} - \Delta^* i\sigma_y G = 0 , \quad (2.24b)$$

where  $G$  and  $F^{\dagger}$  are the spin matrices of components  $G_{\alpha\beta}(\vec{p}, \tau)$  and  $F_{\alpha\beta}^{\dagger}(\vec{p}, \tau)$ ,  $\sigma_y$  is a Pauli matrix, and  $\omega_n = 2\pi T \left( n + \frac{1}{2} \right)$  ( $n \in \mathbb{Z}$ ) are the Matsubara frequencies at temperature  $T$ .

These Gor'kov equations Eq. (2.24) can be solved exactly, leading to the expressions of  $G$  and  $F^{\dagger}$  :

$$G = -\frac{i\omega_n + \xi}{\omega_n^2 + \xi^2 + |\Delta|^2} \mathbb{1} ; \quad (2.25a)$$

$$F^{\dagger} = -\frac{\Delta^*}{\omega_n^2 + \xi^2 + |\Delta|^2} i\sigma_y . \quad (2.25b)$$

From the expression of the Green's functions Eq. (2.25), we can derive the energy spectrum  $\varepsilon$  of the system, which is given by the poles of the  $G$  and  $F^{\dagger}$  after performing the analytical continuation  $i\omega_n \rightarrow \varepsilon$  :

$$\varepsilon_{\pm} = \pm \sqrt{\xi^2 + |\Delta|^2} . \quad (2.26)$$

Therefore, we have seen that the Gor'kov equations allow to obtain the spectral properties of a superconductor in a simple way. However, to be fully equivalent to the BCS theory, these equations must be completed by the self-consistency relation, obtained from the expression of the superconducting order parameter Eq. (2.17), which gives access to macroscopic characteristics, like the critical magnetic field and temperature. This is the point of the following section.

## 2.2.2 The self-consistency relation

According to Gor'kov formulation, the superconducting order parameter  $\Delta(\vec{r})$  Eq. (2.17) can be expressed in terms of the anomalous Green's function  $F_{\downarrow\uparrow}$  :

$$\Delta(\vec{r}) = \gamma F_{\downarrow\uparrow}(\vec{r}, 0) , \quad (2.27)$$

where  $F_{\downarrow\uparrow}(\vec{r}, 0) = F_{\downarrow\uparrow}(\vec{r}, \vec{r}, 0)$  is written in time and position space. In frequency-momentum space, it reads :

$$\Delta^* = \gamma T \sum_{\omega_n} \int F_{\downarrow\uparrow}^{\dagger}(\vec{p}, \omega_n) \frac{d^3\vec{p}}{(2\pi)^3} , \quad (2.28)$$

where the summation is made over all Matsubara frequencies. This equation (2.28) is called self-consistency relation, and allows to have access to many properties of the superconductor.

To obtain the field-temperature phase diagram of a superconductor in the presence of a magnetic field as we do in Chap. 3 and 4, it is more convenient to reformulate the self-consistency relation Eq. (2.28) in a way which eliminates  $\gamma$ . In the following, we derive this second expression of the self-consistency relation in the specific case of 1D systems, which are studied in the next two chapters.

The superconducting order parameter being a constant, we can equalize this equation for two different temperatures :

$$T_c \sum_{\omega_n} \int_{-\infty}^{+\infty} \frac{F_{\downarrow\uparrow}^\dagger(p, \omega_n)}{\Delta^*} dp = T_{c0} \sum_{\omega_n^0} \int_{-\infty}^{+\infty} \frac{F_{\downarrow\uparrow}^\dagger(p, \omega_n^0)}{\Delta^*} dp, \quad (2.29)$$

where  $T_{c0}$  is the critical temperature of a uniform superconductor in the absence of fields, whereas  $T_c$  can be the critical temperature of a superconductor with a Zeeman field or spin-orbit coupling for example. For the isolated superconductor, the anomalous Green's function  $F_{\downarrow\uparrow}^\dagger(p, \omega_n^0)$  is given by Eq. (2.25b). Considering that the chemical potential is the largest energy involved in the problem, namely  $\mu \gg T_{c0}$ , and since  $F^\dagger$  only depends on  $\xi$ , one can transform the  $p$  integral of the right part of Eq. (2.29) into a  $\xi$  integral, following<sup>3</sup> :

$$\int_{-\infty}^{+\infty} dp \approx 2N(0) \int_{-\infty}^{+\infty} d\xi, \quad (2.30)$$

where  $N(0) = 1/v_F$  is the density of states at the Fermi level, and  $v_F$  is the Fermi velocity. We can then use the residue technique to integrate  $F_{\downarrow\uparrow}^\dagger(p, \omega_n^0)$  over  $\xi$ , leading to :

$$T_c \sum_{\omega_n} \int_{-\infty}^{+\infty} \frac{F_{\downarrow\uparrow}^\dagger(p, \omega_n)}{\Delta^*} dp = \frac{2}{v_F} T_{c0} \sum_{\omega_n^0} \frac{\pi}{|\omega_n^0|}, \quad (2.31)$$

By adding and subtracting the term  $\frac{2}{v_F} T_c \sum_{\omega_n} \frac{\pi}{|\omega_n|}$  to Eq. (2.31), and noticing that

the sum over all Matsubara frequencies of the anomalous Green's function  $F_{\downarrow\uparrow}^\dagger(p, \omega_n)$  is equal to twice the sum over positive Matsubara frequencies of the real part of  $F_{\downarrow\uparrow}^\dagger(p, \omega_n)$ , we arrive to the following equation :

$$\ln\left(\frac{T}{T_{c0}}\right) = T_c \sum_{\omega_n \geq 0} \left[ \frac{v_F}{2} \int_{-\infty}^{+\infty} \text{Re}\left(\frac{F_{\downarrow\uparrow}^\dagger(p, \omega_n)}{\Delta^*}\right) dp - \frac{\pi}{\omega} \right], \quad (2.32)$$

which is the expression of the self-consistency relation that we will use in Chapters 3 and 4 to determine the field-temperature phase diagram. Indeed, if we consider a superconductor in the presence of a Zeeman field  $h$ , which is taken into account in the anomalous Green's function  $F_{\downarrow\uparrow}^\dagger$ , it is quite easy to extract  $h$  as a function the temperature  $T$  from Eq. (2.32). Moreover, this relation allows to describe also inhomogeneous superconductors, characterized by a spatially dependent order parameter. This last point will be specifically detailed in Chapter 3.

3. As we will see in Chapter 4, the integration becomes more complicated in the presence of spin-orbit interaction.

## 2.3 Conclusion

The goal of this chapter was to present briefly the main ideas of two theories of superconductivity, namely the phenomenological Ginzburg-Landau theory, and the Gor'kov reformulation of the microscopic BCS theory.

From the expression of the Ginzburg-Landau free energy, we derived differential equations, the so-called Ginzburg-Landau equations, which led to some important results : The expression of the two characteristic lengths and the classification of superconductors in two groups.

Then, we introduced the Gor'kov formalism, and derived the self-consistency relation. This reformulation of the BCS theory in terms of Green's function is particularly adapted to study inhomogeneous superconductivity, and will be used in Chapters 3 and 4.

# Chapter 3

## Introduction to inhomogeneous superconductivity

**T**HE PRESENT CHAPTER provides an introduction to inhomogeneous superconductivity, a topic which will be addressed in Chapter 4 for 1D superconductors in the presence of spin-orbit interaction. We focus specifically on two types of non-uniform superconducting states : The Fulde-Ferrell-Larkin-Ovchinnikov (FFLO) phase [1, 2], which was the first inhomogeneous phase predicted, and the helical phase, which appears in the presence of spin-orbit interaction [46].

These non-uniform states emerge in s-wave superconductors in the presence of a Zeeman field, and are both characterized by a spatially dependent order parameter, leading to a critical magnetic field enhancement with respect to the critical field of uniform superconductors, where the order parameter is constant. However, they have different physical origins. The FFLO state stems from the Pauli paramagnetic effect : when a Zeeman field is applied on a superconductor, it can induce a finite momentum of the Cooper pairs, which in turn involves spatial oscillations of the order parameter. On the other hand, the helical state originates from the interplay between spin-orbit and Zeeman interactions, which also yields a finite momentum of the Cooper pairs. This state has been largely investigated in 2D and 3D superconductors due to the variety of resulting phenomena : magnetoelectric effects [11, 12, 14, 47, 48, 49, 50], triplet pairing [51, 52], and critical field enhancement larger than in the FFLO state [4, 5].

In a first section, we present the main characteristics of the FFLO phase. After a brief description of the two pair-breaking effects, namely the orbital and the Pauli paramagnetic effects, we qualitatively explain how the second one can induce the FFLO phase. Then, we use the Gor'kov formalism introduced in the previous chapter to study the self-consistency relation of a one-dimensional superconductor in the presence of a magnetic field, and we provide its field-temperature phase diagram. Recent experimental evidences of the FFLO phase are also briefly presented. The second section of this chapter is devoted to the helical phase. By the mean of spectral and phenomenological arguments, we briefly explain why this phase appears in superconductors in the presence of spin-orbit interaction.

This chapter allows to introduce methods that will be used in Chapter 4 to study inhomogeneous superconductivity in the presence of spin-orbit interaction. Moreover, the FFLO state will be exploited as a reference, with which we will always compare the helical phase obtained in Chapter 4.

## 3.1 First prediction of inhomogeneous superconductivity : The FFLO state

The FFLO state was predicted in 1964 by Peter Fulde and Richard Ferrell, and by Anatoly Larkin and Yurii Ovchinnikov in two different works for s-wave superconductors in the presence of a Zeeman magnetic field [1, 2].

Generally, in type-II superconductors, the presence of a magnetic field stronger than the critical field destroys superconductivity in two mechanisms : The orbital pair-breaking effect, responsible for the appearance of superconducting vortices, and the Pauli paramagnetic pair-breaking effect. This last one originates from the interaction between the magnetic field and the spin of the superconducting electrons, called Zeeman interaction, which induces a spin polarization breaking Cooper pairs if the field is sufficiently strong. However, it exists a critical value of the magnetic field larger than the critical field of the uniform superconducting state under which Cooper pairs are not broken : The finite momentum of the pairs induced by Zeeman effect is compensated by spatial oscillations of the superconducting order parameter. This is the FFLO state.

In this section, we first briefly introduce the two pair-breaking effects and qualitatively explain the origin of the FFLO state. Then, using the Gor'kov formalism introduced in Chapter 2, we derive the self-consistency equation of a superconductor in the presence of a Zeeman field, allowing for a spatially dependent order parameter. We show how the appearance of the FFLO phase can be deduced from the self-consistency relation and provide the field-temperature phase diagram. Finally, we present recent experimental evidences of the existence of the FFLO state.

### 3.1.1 Two pair-breaking mechanisms

When a magnetic field  $\vec{B}$  is applied on a superconductor, Cooper pairs can be destroyed in two ways. The first one is the orbital pair-breaking effect, resulting from the Lorentz force  $\vec{F}_{\text{Lorentz}} = e (\vec{v} \times \vec{B})$ , where  $\vec{v}$  is the electron velocity. This force is opposite for each electron of the Cooper pair due to their opposite momenta  $\vec{p} = m \vec{v}$ , as illustrated in Fig 3.1a. If the magnetic field is sufficiently strong, the kinetic energy of the Cooper pair becomes higher than the one of two single electrons, and the pair breaks. This effect leads to the emergence of Abrikosov vortices (see Chapter 5), and superconductivity is destroyed at the second critical field  $H_{c2}^{\text{orb}} = \frac{\Phi_0}{2 \pi \xi^2}$ , where  $\Phi_0$  is the superconducting quantum of flux and  $\xi$  is the coherence length.

The second pair-breaking mechanism is the Pauli paramagnetic effect. It originates from the interaction between the magnetic field and the spin of electrons, called Zeeman interaction and described by the Hamiltonian operator

$$\hat{h}_{\text{Zeeman}} = \vec{h} \cdot \vec{\sigma}, \quad (3.1)$$

where  $\vec{\sigma}$  are the Pauli matrices and we used the notation  $\vec{h} = g \mu_B \vec{B}/2$ ,  $g$  being the gyromagnetic factor ( $g \approx 2$  for electrons) and  $\mu_B$  the Bohr magneton. The Zeeman interaction leads to a splitting of the energy bands between spin up and down, as illustrated in Fig. 3.2, which induces a spin polarization in the normal state. In the case of s-wave superconductivity, Cooper pairs are made of two electrons with opposite spins, and thus are not interacting with the field. However, if the magnetic field becomes larger than the second critical field  $H_{c2}^{\text{P}} = \sqrt{2} \frac{\Delta}{g \mu_B}$ , single electrons are energetically

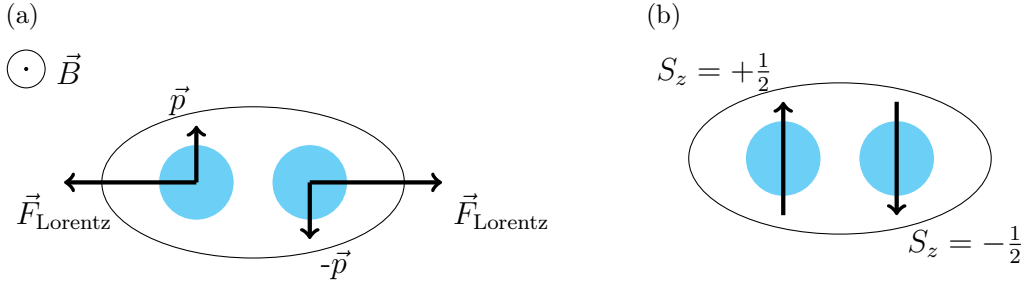


FIGURE 3.1 – (a) When we apply a magnetic field on Cooper pairs, the Lorentz force drives electrons in opposite directions because of their opposite momenta. (b) Electrons of Cooper pairs have opposite spins. The presence of a Zeeman field, which implies a spin polarization of electrons, can break the pair.

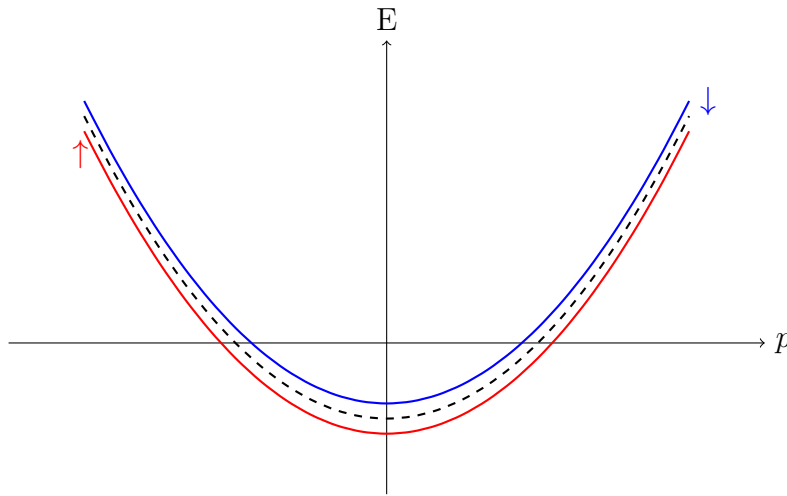


FIGURE 3.2 – Zeeman energy spectrum. The zero field energy band (dashed line) is split into two bands when we apply a magnetic field, one for spin-up electrons (red line) and the other for spin-down electrons (blue line).

more favorable than Cooper pairs, which are broken. The critical field  $H_{c2}^P$  is called the paramagnetic limit [53, 54].

The relative importance of both pair-breaking effects is determined by the Maki parameter [55] :

$$\alpha_M = \sqrt{2} \frac{H_{c2}^{\text{orb}}}{H_{c2}^P}. \quad (3.2)$$

This parameter is usually much smaller than unity, and thus the paramagnetic effect is negligible. However, in some materials like heavy fermion superconductors, 2D superconductors with an in-plane magnetic field or low-dimensional superconductors, this effect becomes predominant, and has been observed in thin superconducting films, like for example Al films [56]. Next, we explain qualitatively how the paramagnetic effect can lead to the FFLO state.

### 3.1.2 Qualitative arguments for the appearance of the FFLO state

In order to understand why the FFLO state appears, we study the simplest case of a one-dimensional (1D) superconductor at zero temperature in the presence of a

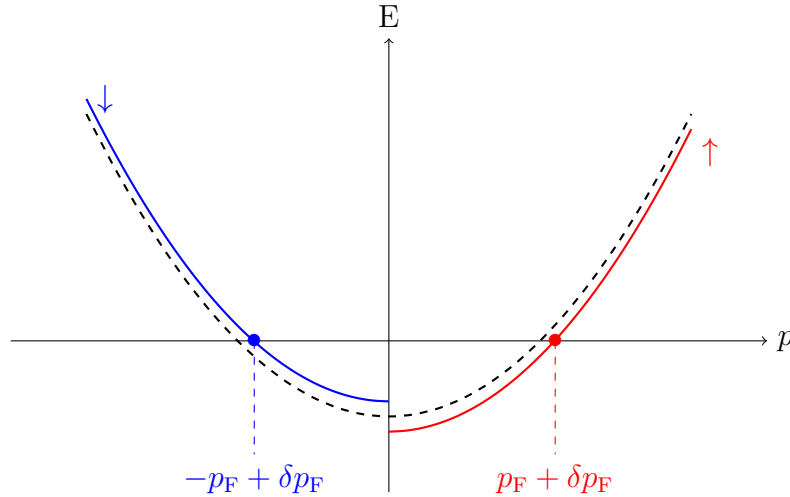


FIGURE 3.3 – In the presence of a magnetic field, the momentum of the Cooper pair electrons is shifted from  $p_F$  to  $p_F + \delta p_F$  for electrons with spin up, and from  $-p_F$  to  $-p_F + \delta p_F$  for electrons with spin down.

magnetic field, whose the orbital effect is neglected.

In the absence of magnetic field, Cooper pairs are formed by two electrons with opposite momenta  $p_F$  and  $-p_F$  at the Fermi surface. Therefore, the total momentum of a Cooper pair is zero. But when a magnetic field  $\vec{B}$  is applied on the superconductor, the Zeeman splitting implies momentum shifts from  $p_F$  to  $p_\uparrow = p_F + \delta p_F$  for the electron with spin up, and from  $-p_F$  to  $p_\downarrow = -p_F + \delta p_F$  for the electron with spin down, where  $\delta p_F = \mu_B B / v_F$  and  $v_F$  the Fermi velocity. This effect is illustrated in Fig. 3.3. The resulting momentum of the Cooper pair is then finite and equal to  $p_\uparrow + p_\downarrow = 2 \delta p_F$ . The presence of such a non-vanishing center-of-mass momentum implies that the superconducting order parameter exhibits a spatially dependent phase in real space such that :

$$\Delta(x) = \Delta e^{iqx}, \quad (3.3)$$

where the amplitude  $\Delta$  of the superconducting order parameter is a function of the temperature, as proposed by Fulde and Ferrel in 1964 [1]. Moreover, this description shows that at zero temperature, the FFLO phase is defined for all values of the magnetic field : The paramagnetic limit does not exist in 1D [57]. However, in 2D and 3D the wave vector  $\delta p_F$  depends on the direction of  $v_F$ . It is thus impossible to find a unique value of  $q$  which compensates exactly the Zeeman splitting for all the electrons of the Fermi surface. The paramagnetic limit is thus preserved. Notice nevertheless that the critical field of the FFLO phase is still higher than the uniform one at zero temperature.

This is a simple way to understand why the FFLO state can appear in superconductors in the presence of a field acting on spins. In the next section we provide a microscopically description of the effect at finite temperature. Specifically we present the Gor'kov equations of such a 1D superconductor in Nambu spin basis. From these equations, the self-consistency relation is deduced, which allows to present the field-temperature phase diagram.

### 3.1.3 Characteristics of the FFLO phase of a quasi-1D superconductor

In this section, we introduce the formalism which is used in the following chapter to describe non-uniform superconducting wires at finite temperature. In quasi-1D superconductors, electrons are confined in one direction, thus preventing the orbital effect. The effect of a magnetic field is then purely paramagnetic and one should expect the appearance of the FFLO phase. However, it has been demonstrated that quantum fluctuations would kill superconductivity in such low-dimensional systems [58]. Despite this, superconductivity has been reported in quasi-1D materials like some organic superconductors [57, 59, 60]. Such compounds consist of weakly coupled 1D chains. The interchain coupling is described by a hopping parameter  $t$ . If the hopping integral  $t \ll T_c$ , then the system can be described by a strictly 1D model. On the other hand, as it has been established in [61], the mean-field treatment is justified if  $t \gg T_c^2/\mu$ , where  $\mu$  is the chemical potential. So for  $T_c^2/\mu \ll t \ll T_c$ , the critical fluctuations of the superconducting order parameter are effectively suppressed, and the system can be treated as a strictly superconducting 1D wire.

The Hamiltonian of an infinite superconducting wire along the  $x$ -direction in the presence of a general Zeeman field  $\vec{h}$  (Eq. 3.1) with an oscillating superconducting order parameter  $\Delta(x) = \Delta e^{iqx}$  as introduced in Eq. (3.3) reads :

$$\mathcal{H} = \int dp \Psi^\dagger \left( \hat{h}_N + \hat{h}_{SC} \right) \Psi , \quad (3.4)$$

where  $\Psi = \left( \psi_\uparrow(p + q/2), \psi_\downarrow(p + q/2), -\psi_\downarrow^\dagger(-p + q/2), \psi_\uparrow^\dagger(-p + q/2) \right)^T$  is the spinor containing the annihilation and creation operators in Nambu spin basis. The Hamiltonian operator  $\hat{h}_N$  describes the system in the normal state :

$$\hat{h}_N = \left( \xi + \frac{q^2}{8m} \right) \tau_z + \frac{qp}{2m} + \vec{h} \cdot \vec{\sigma} . \quad (3.5)$$

Here  $\xi = \frac{p^2}{2m} - \mu$  is the quasiparticle energy, and  $\sigma_{x,y,z}, \tau_{x,y,z}$  are the Pauli matrices acting respectively in spin and Nambu space. The superconducting term  $\hat{h}_{SC}$  is expressed in Nambu basis as :

$$\hat{h}_{SC} = -\Delta \tau_x . \quad (3.6)$$

To compute the self-consistency equation, we use the Green's function formalism (see Chapter 2). Close to the normal-superconducting phase transition, and assuming that this phase is of second order,  $\Delta \ll T$ , one can expand the Green's function  $G$  in series of  $\Delta$ . At first order in  $\Delta$ ,  $G$  reads :

$$G \approx G_N + G_N \hat{h}_{SC} G_N , \quad (3.7)$$

where  $G_N$  is the normal state Green's function, obtained by solving the equation of motion for the Green's functions  $(i\omega_n - \hat{h}_N) G_N = \mathbb{1}$ . In Nambu space,  $G_N$  reads

$$G_N = \begin{pmatrix} G_- & 0 \\ 0 & G_+ \end{pmatrix} , \quad (3.8)$$

where the matrix  $G_\lambda$  ( $\lambda = \pm$ ) is defined in the spin basis :

$$G_\lambda = \frac{i\omega_n + \lambda\xi + \lambda\frac{q^2}{8m} - \frac{qp}{m} + \vec{h} \cdot \vec{\sigma}}{\left( i\omega_n + \lambda\xi + \lambda\frac{q^2}{8m} - \frac{qp}{m} \right)^2 - h^2} , \quad (3.9)$$

where  $h = |\vec{h}|$  is the modulus of the Zeeman field.

In this formalism, the self-consistency relation Eq. (2.32) derived in Chapter 2 can be written :

$$\ln \left( \frac{T_c}{T_{c0}} \right) = 2 T_c \sum_{\omega_n > 0} \left[ \frac{v_F}{8} \operatorname{Re} \left( \int_{-\infty}^{+\infty} \operatorname{Tr} \left( \frac{G}{\Delta} \tau_x \right) dp \right) - \frac{\pi}{\omega_n} \right]. \quad (3.10)$$

Assuming that the chemical potential is the largest energy involved in the problem,  $\mu \gg T_c, h$ , and noticing that  $G$  Eqs. (3.7 - 3.9) only depends on  $\xi$ , one can turn the  $p$  integration in Eq. (3.10) into  $\xi$  integration, using Eq. (2.30). A simple way of seeing the emergence of the FFLO phase is to expand Eq. (3.10) in series with respect to the wave-vector  $q$  :

$$\ln \left( \frac{T_c}{T_{c0}} \right) = -2 \pi T_c \sum_{\omega_n > 0} \left[ \frac{h^2}{\omega_n (\omega_n^2 + h^2)} + \frac{\omega_n (\omega_n^2 - 3 h^2)}{4 (\omega_n^2 + h^2)^3} v_F^2 q^2 \right]. \quad (3.11)$$

The equilibrium value of  $q$  is obtained by maximizing Eq. (3.11) with respect to  $q$ , which is the equivalent of minimizing the Ginzburg-Landau free energy [57]. The absence of linear term in  $q$  in the expansion of the self-consistency relation Eq. (3.11) implies that we need to expand it at higher order to derive the equilibrium value of the wave-vector. However, the sign of the second order term in  $q$ ,  $C = \sum_{\omega_n > 0} \frac{\omega_n (\omega_n^2 - 3 h^2)}{4 (\omega_n^2 + h^2)^3}$ , is sufficient to predict the behaviour of the superconductor, as illustrated in Fig. 3.4 :

- when  $C < 0$ , the maximum of Eq. (3.11) is obtained for  $q = 0$ , corresponding to the uniform phase ;
- when  $C > 0$ , the maximum of Eq. (3.11) corresponds to a finite value of  $q$ . This is the FFLO state.

The transition between the uniform and the FFLO states occurs when  $C$  vanishes, *i.e.* at coordinates ( $T^* = 0.56 T_{c0}$ ,  $h^* = 1.07 T_{c0}$ ), where  $T^*$  and  $h^*$  are the tricritical temperature and magnetic field.

The  $(h, T)$ -phase diagram of a 1D superconductor is presented in Fig. 3.5. For  $T > T^*$ , the modulated phase does not exist ( $q = 0$ ). However, for  $T < T^*$ , the critical field is larger for the modulated phase (solid line) than for the uniform one (dashed line) : The FFLO state is the most stable one. When  $T \rightarrow 0$ , the transition line between the FFLO and normal states diverges, due to the absence of paramagnetic limit in 1D highlighted in Sec. 3.1.2). Notice that this phase diagram does not depend on the direction of the magnetic field.

Finally, we have to emphasize an important point concerning the form of the space dependent order parameter  $\Delta(x)$ . For more convenience in the calculations, we used the form proposed by Fulde and Ferrel in 1964 (Eq. 3.3). However, another solution, proposed by Larkin and Ovchinnikov [2], gives the most stable inhomogeneous phase :  $\Delta(x) = \Delta \cos(qx)$ . Notice that due to this late expression of the order parameter, the FFLO phase is sometimes referred as multiple- $q$  phase.

In the next section, we provide some experimental evidences of the existence of the FFLO state. We briefly explain why this phase is complicated to detect, and present recent experiments on two types of potential candidates : Heavy fermion and layered organic superconductors.

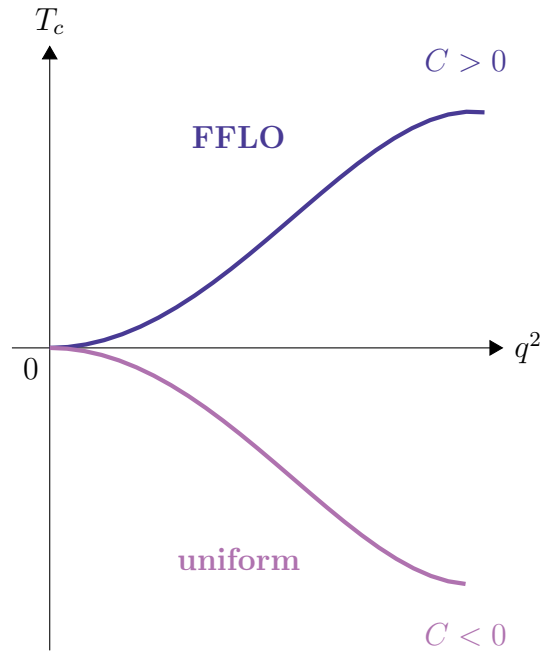


FIGURE 3.4 – The sign of the second order term in  $q$  of the expansion of the self-consistency relation is sufficient to determine the superconducting phase : If  $C < 0$ , this is the uniform phase, whereas  $C > 0$  corresponds to the modulated phase

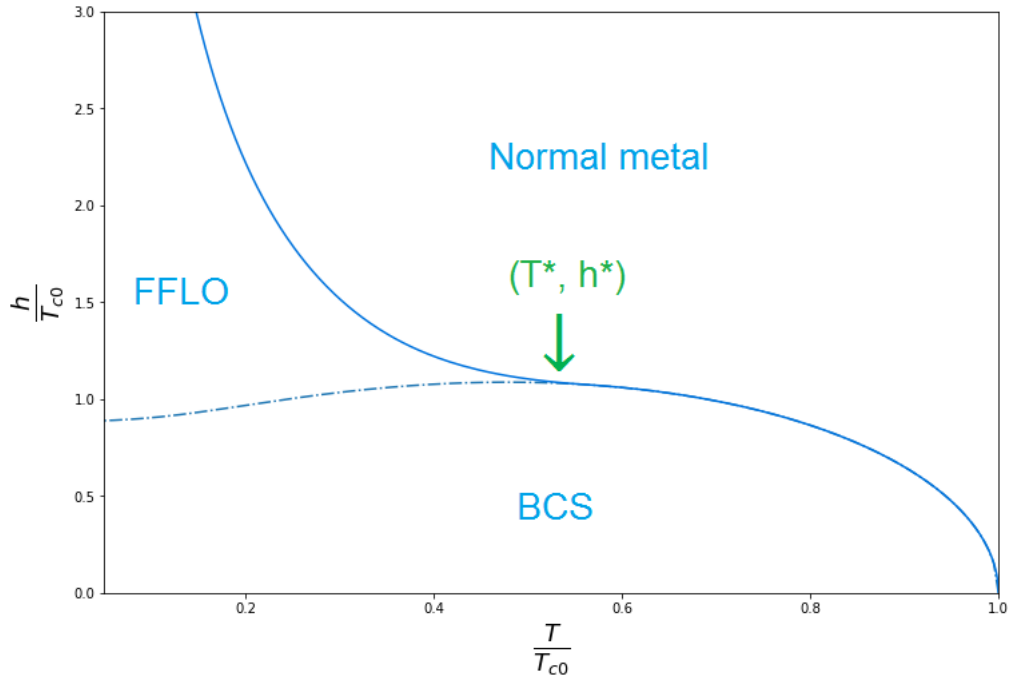


FIGURE 3.5 – Field-temperature phase diagram of a 1D superconductor. For  $T > T^* = 0.56 T_{c0}$ , the superconductor is in the uniform state. But for  $T < T^*$ , the transition line between the BCS and normal states (dashed line) has to be replaced by transition line between the FFLO and normal states (solid line).

### 3.1.4 Experimental evidence of the existence of the FFLO state

Despite its prediction more than 50 years ago, the FFLO state has been observed for the first time very recently [62]. Indeed, this inhomogeneous phase is not obvious to detect experimentally because of two requirements :

- As we explained in Sec. 3.1.1, the paramagnetic effect must be dominant over the orbital effect, which is not the case in most of the type-II superconductors.
- The superconductor must be very clean, because impurities are detrimental to the FFLO state [63].

Therefore, the material must display a very large Maki parameter  $\alpha_M \gg 1$ , and a mean free path larger than the coherence length  $\xi \ll l$ , which ensures that it is very clean. Among the possible candidates, two materials were widely investigated over the past twenty years : Heavy fermion superconductors and layered organic superconductors with an in-plane magnetic field.

#### Heavy fermion superconductors

Heavy fermion materials are intermetallic compounds containing a partly filled  $4f$  or  $5f$  energy band. At low temperature, the strongly interacting electrons can be described by weakly interacting fermionic quasiparticles, where the mass has been renormalized : The effective mass can be as high as  $1000 m$ , where  $m$  is the electronic mass. This high effective mass implies that the orbital field  $H_{c2}^{\text{orb}}$  and therefore the Maki parameter  $\alpha_M$  increase, thus leading to a dominant paramagnetic effect.

Several heavy electron superconductors were proposed as potential candidates for the FFLO state, in particular CeCoIn<sub>5</sub> [64], which satisfies both requirements ( $\alpha_M \gg 1$  and  $\xi \ll l$ ). Calorimetric measurements show indeed a transition between two superconducting phases at low temperature and high magnetic field [65], which could correspond to the transition between the BCS and the FFLO state. However, it was finally demonstrated that this transition corresponds to a spin-density wave ordering [66]. This is another aspect of the difficulties to observe the FFLO state : Such superconducting transitions and critical fields exceeding the paramagnetic limit are common features of unconventional superconducting states like the FFLO state or triplet superconductivity.

#### Layered organic superconductors

In quasi-2D (1D) organic superconductors, the orbital motion is restricted to the crystal plane (chain). Therefore, when a magnetic field is applied parallel to the layers (wires), the orbital effect is suppressed. Moreover, since these superconductors are very clean, they are perfect candidates for the FFLO detection. A critical field nearly diverging at low temperatures has been observed in several compounds, like  $\lambda$ -(BETS)<sub>2</sub>GaCl<sub>4</sub> or (TMTSF)<sub>2</sub>X, where the anion X can be PF<sub>6</sub> or ClO<sub>4</sub>. Such a feature can be interpreted as a strong evidence for the presence of the FFLO state.

More recently, the field-temperature phase diagram of the layered organic superconductor  $\kappa$ -(BEDT-TTF)<sub>2</sub>Cu(NCS)<sub>2</sub> has been experimentally established in the presence of an in-plane magnetic field [62] (Fig. 3.6). This result was obtained from heat capacity and magnetocaloric measurements, and compared with previous measurements : Nuclear magnetic resonance (NMR) [67, 68], rf penetration depth [69] and earlier specific heat measurements [70]. In this phase diagram, the FFLO state is clearly visible at low temperature ( $T < 4.13$  K) and high magnetic field ( $B > 20.7$  T).

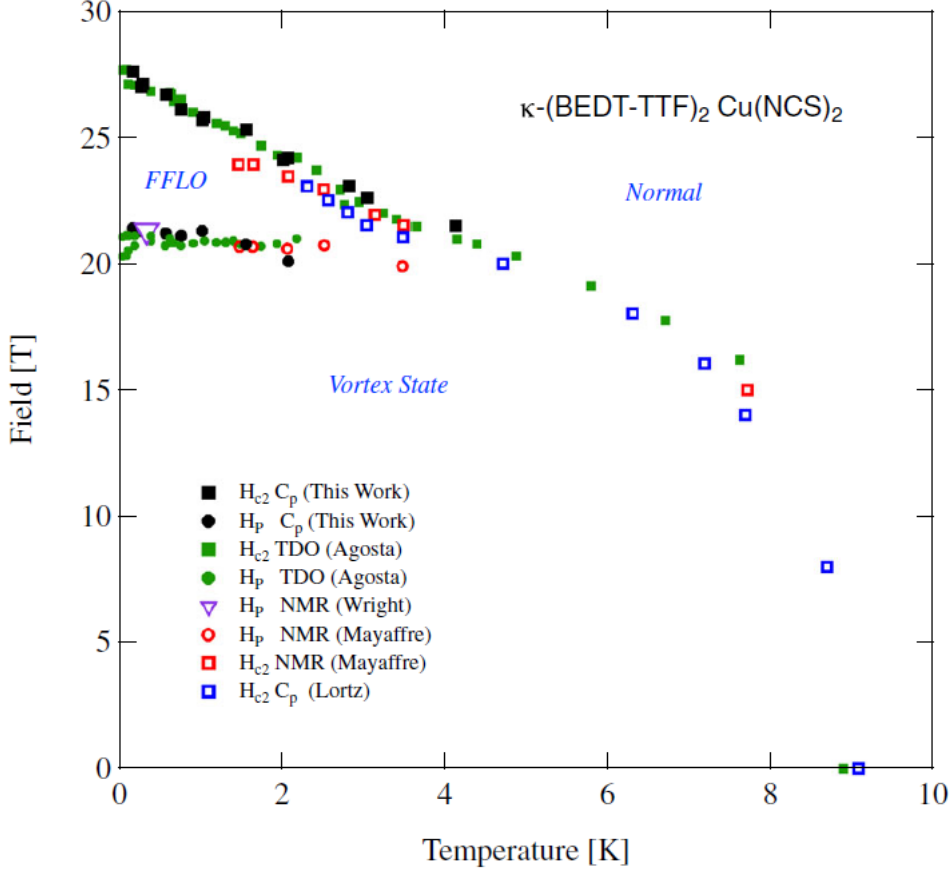


FIGURE 3.6 – Field-temperature phase diagram of the organic superconductor  $\kappa$ -(BEDT-TTF)<sub>2</sub>Cu(NCS)<sub>2</sub> in the presence of an in-plane magnetic field, obtained from calorimetric measurements (black points) [62]. Data points from other works are included for comparison : rf penetration depth (green) [69], NMR (purple and red) [67, 68] and previous calorimetric (blue) [70] measurements. The FFLO phase is clearly visible.

In the next section, we briefly introduce another type of inhomogeneous superconductivity, which appears in the presence of spin-orbit interaction : the helical state.

## 3.2 Another type of inhomogeneous superconductivity : The helical state

In the previous section, we described the FFLO phase stemming from the paramagnetic effect in a superconductor in the presence of a Zeeman magnetic field. Now, we consider that spin-orbit interaction is also present in the superconductor, leading to a new type of modulated phase called the helical phase. In this section, we qualitatively explain the origin of this phase, which will be investigated at the microscopical level for quasi-1D superconductors in Chap. 4.

The helical phase appears due to the interplay between the Zeeman (Eq. 3.1) and spin-orbit (SO) interactions. In particular, Rashba-type SO coupling, which is considered in the next chapter, is described by the following Hamiltonian operator :

$$\hat{h}_{\text{so}} = \alpha (\vec{\sigma} \times \vec{p}) \cdot \vec{n} , \quad (3.12)$$

where  $\alpha$  is the spin-orbit coupling constant and  $\vec{n}$  is a unit vector along the polar axis.

To illustrate the following explanations, we consider a 2D system in the  $(x, y)$ -plan with a Zeeman field  $\vec{h}$  applied parallel to the surface<sup>1</sup>. In this case, the SO interaction described by Eq. (3.12) reads :  $\hat{h}_{\text{so}} = \alpha (p_y \sigma_x - p_x \sigma_y)$ . The presence of both spin-orbit and Zeeman fields leads to split the energy spectrum into two helical bands represented in Fig. 3.7 and characterized by the energy :

$$E_\lambda(p) = \xi + \lambda \sqrt{h^2 + \alpha^2 p^2 + 2\alpha (\vec{p} \times \vec{e}_z) \cdot \vec{h}} , \quad (3.13)$$

where  $\lambda = \pm$  labels the bands and  $\vec{e}_z$  is the unit vector in the direction normal to the surface.

In the limit of large spin-orbit  $\alpha p_F \gg h$ , the energy Eq. (3.13) can be expanded at first order in  $h$  :

$$E_\lambda(p) \approx \xi + \lambda \alpha p_F + \lambda \alpha (\vec{p} \times \vec{e}_z) \cdot \vec{h} . \quad (3.14)$$

In the superconducting state for large SO, pairing occurs between two electrons with opposite spins in the same band, as we will demonstrate in Chap. 4 Sec. 4.3. Therefore, the interplay between SO and Zeeman interactions implies momentum shifts from  $\pm p$  to  $\pm p + q/2$  such that the paired states are degenerate :  $E_\lambda(p + q/2) = E_\lambda(-p + q/2)$ , where  $q = -2\alpha (\vec{p} \times \vec{e}_z) \cdot \vec{h}/v_F$  is obtained from Eq. (3.14). As in the FFLO state described in Sec. 3.1.2, Cooper pairs have a finite total momentum, which results in spatial oscillations of the superconducting order parameter such that  $\Delta(\vec{r}) = \Delta e^{i\vec{q}\cdot\vec{r}}$ .

From a phenomenological point of view, the appearance of the helical phase results from an additional term in the Ginzburg-Landau free energy Eq. (2.1) [10, 71]. This linear-in-gradient term is called Lifshitz invariant and reads for the previous 2D system<sup>2</sup> :

$$F_L = \varepsilon(\alpha) \vec{e}_z \cdot \left[ \vec{h} \times \left( \Psi^* \vec{\nabla} \Psi - \Psi \vec{\nabla} \Psi^* \right) \right] , \quad (3.15)$$

where  $\varepsilon(\alpha)$  is a function of the SO coupling constant  $\alpha$ . This Lifshitz invariant is finite only in the presence of a non-zero wave-vector  $\vec{q}$ , and allows to describe the magnetoelectric effects involved in a superconductor by the interplay between SO and Zeeman interactions [72]. Such an invariant is constructed in Chapter 4 in the context of one-dimensional systems. Notice that at the level of the Ginzburg-Landau free energy, the FFLO phase arises from a change of sign of the quadratic-in-gradient term (see Eq. 2.1), which is conceptually different from the helical state. Moreover, the competition between these two states has been studied in many references [4, 6, 7, 73, 74, 75, 76], and here we simply highlight the fact that when both helical and FFLO-like modulations coexist in a system, this involves two regions in the  $(h, T)$ -phase diagram with different magnitudes of  $q$ . This effect can be observed in the quasi-1D systems studied in Chapter 4.

---

1. Such arguments are more complicated to show in 1D systems. In this case it is necessary to take into account at least two components of the Zeeman field, one parallel and the other one normal to the SO vector,  $h_{\parallel}$  and  $h_{\perp}$ . Indeed, the normal component  $h_{\perp}$  ensures the hybridization of the bands describing up and down electrons into two helical bands, whereas the parallel component  $h_{\parallel}$  induces the shift in momentum between the two electrons of the Cooper pairs.

2. In the Ginzburg-Landau theory,  $\Psi$  corresponds to the superconducting order parameter.

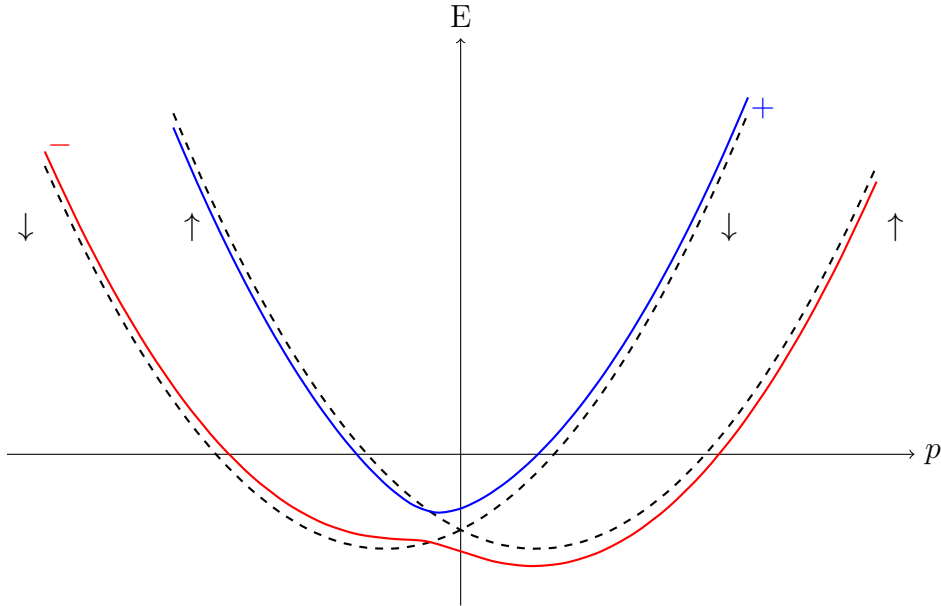


FIGURE 3.7 – Energy spectrum of a normal metal in the presence of spin-orbit interaction of Rashba type. SO coupling induces a shift between the bands of spin up and spin down electrons, represented by dashed lines. In the presence of a normal Zeeman field  $h_x$  (with respect to SO coupling), a gap is opened, leading to the appearance of the helical bands labeled + and -. The interplay between the parallel component of the Zeeman field  $h_z$  and SO interaction implies a shift in momentum at a given energy between up and down electrons.

### 3.3 Conclusion

In this chapter, we introduced two superconducting inhomogeneous phases, namely the FFLO and the helical states. Both appear in the presence of a Zeeman magnetic field, but have different physical origins.

The emergence of the FFLO phase can be understood from the paramagnetic effect caused by the Zeeman magnetic field. This effect induces a finite center-of-mass momentum for the Cooper pairs, which in turn implies a spatially oscillating superconducting order parameter. To illustrate this point, we derived the self-consistency equation for a 1D superconductor in the presence of a Zeeman field using the Green's function formalism in Nambu spin basis. This method will be used also in Chapter 4 for 1D superconductors in the presence of both Zeeman and spin-orbit interactions. From the self-consistency relation, we determined the tricritical point, namely the critical temperature and magnetic field where the FFLO phase appears, and represented the  $(h, T)$ -phase diagram of a 1D superconductor.

On the other hand, the helical phase originates from the interplay between spin-orbit and Zeeman interactions. Using spectral arguments, we explained how the combination of both interactions leads to finite-in-momentum Cooper pairs, involving a spatially dependent order parameter. We showed that from a phenomenological point of view, the interplay between both Zeeman and spin-orbit fields is described by an additional term in the Ginzburg-Landau energy, the Lifshitz invariant.

In the next chapter, we investigate this helical phase in low-dimensional superconductors. Using the  $SU(2)$ -covariant formalism, we derive an expression of the Lifshitz invariant for 1D systems in terms of  $SU(2)$  fields. Then, within the Green's function formalism introduced in Chapter 2, we explicitly compute the charge current related to this Lifshitz invariant together with the self-consistency relation, and provide the

$(h, T)$ -phase diagram in the limit of strong spin-orbit interaction.

# Chapter 4

## Helical state and magnetoelectric effects in superconducting wires

**S**UPERCONDUCTIVITY in low dimensional systems with spin-orbit coupling (SOC) and a Zeeman field has been intensively studied in the context of Majorana zero-energy modes [77, 78, 79, 80, 81, 82]. On the other hand the interplay between superconductivity and spin-dependent fields is also known to lead to striking phenomena as long-range triplet correlations [51, 52], critical field enhancement [4, 5] and magnetoelectric effects stemming from the coupling between charge and spin degrees of freedom [11, 12, 14, 47, 48, 49, 50]. This chapter is devoted to the study of the two latter effects, namely inhomogeneous superconductivity and the appearance of anomalous charge currents, for the particular case of quasi-1D systems. Two different setups are investigated : A single wire in which superconductivity, spin-orbit interaction and a Zeeman field coexist in the wire, and a double wire system in which superconducting pairing and the spin-dependant fields are spatially separated. In principle, these setups could be realized experimentally, from the organic superconductors mentioned in Chap. 3 for the single wire system, and using the two wire semiconducting systems presented in Refs. [83, 84, 85, 86] for the second setup, where one of the wires is a superconductor whose diameter is much smaller than the coherence length. However to fully describe this realistic system, the section of the wire must be taken into account in the calculations, which is beyond the scope of this chapter.

First, we briefly introduce the SU(2)-covariant formalism, in which the SOC and exchange field are written as the vector and scalar potentials respectively of the SU(2) magnetoelectric fields. With the help of this formulation we explore the appearance of the magnetoelectric effect, namely anomalous charge currents. We determine the condition under which such currents are allowed by symmetry for both setups, and express them in terms of the SU(2) electric and magnetic fields.

In a second part, we explicitly compute the anomalous currents together with the self-consistency equation and confirm the predictions made by the SU(2)-covariant consideration. Specifically we show that the combination of both spin-orbit and Zeeman fields results in the emergence of a modulated phase at low magnetic field and any temperature  $T < T_{c0}$ . We also demonstrate that the anomalous current is exactly compensated by the current coming from the wave-vector of the superconducting order parameter, leading to a zero-current ground state. Specifically, in the one wire case, a tilted Zeeman field  $\vec{h}$  with respect to the spin-orbit field must be present to generate the anomalous current and the enlarged modulated phase : If  $\vec{h}$  is purely parallel or normal to the spin-orbit field, no anomalous current is produced. For the two wire system, the

situation is rather different. The system behaves as a quasi two-dimensional system, and anomalous currents and high temperature inhomogeneous phase are present even when  $\vec{h}$  is parallel to the SOC. In the latter case the zero-current ground state corresponds in fact to two finite currents flowing in each wires in opposite directions.

Finally, we study the self-consistency equation in the regime of large spin-orbit coupling  $\alpha p_F$  with respect to the critical temperature  $T_c$  for the one-wire setup. In this case it is convenient to work in the helical basis. We show that increasing the spin-orbit field with respect to the Zeeman field changes the superconducting correlations from interband to intraband. Then we provide a complete field-temperature phase diagram for different orientations of the Zeeman field and several values of the spin-orbit coupling constant  $\alpha$ .

## 4.1 Spin-galvanic effects in superconducting wires

Magnetoelectric effects in the superconducting state are reminiscence of the widely studied spin Hall and Edelstein effects in normal conductors [87, 88, 89, 90]. These effects consist of generation of a spin current or spin density, respectively, by a charge current. In particular, the Edelstein effect has been theoretically demonstrated in 2D systems with Rashba SO interaction, and due to possible applications in spintronics, it has been largely investigated over the past few decades [91, 92, 93, 94, 95]. The inverse Edelstein effect, also known as spin-galvanic effect, describes the generation of an electric current via a spin density.

These effects also exist in the superconducting state [12, 14, 15, 72, 96, 97, 98]. They were first studied by Edelstein for 2D superconductors in the presence of Rashba spin-orbit coupling [72]. Specifically, the interplay between superconductivity, spin-orbit interaction and a Zeeman field leads to the appearance of anomalous charge currents. To understand this magnetoelectric effect from a general perspective, we briefly introduce the SU(2)-covariant formalism [99, 100] which describes systems with linear-in-momentum SOC, and provides a way to determine the conditions of appearance of anomalous currents.

### 4.1.1 Brief introduction to the SU(2)-covariant formalism

To understand the main outcome of the SU(2)-covariant formalism, let us introduce the general Hamiltonian operator of a system with a linear-in-momentum spin-orbit coupling and a Zeeman (or exchange) field :

$$\hat{h}_0 = \frac{p^2}{2m} - \mu + \vec{h} \cdot \vec{\sigma} - \Omega_i^a p_i \sigma^a , \quad (4.1)$$

where  $\mu$  is the chemical potential,  $\vec{h}$  is the Zeeman field,  $\sigma^a$  are the Pauli matrices and  $\Omega_i^a$  represents the SOC constant. Particular cases are :  $\Omega_x^y = -\Omega_y^x = \alpha$  in Eq. (4.1), which corresponds to Rashba SOC, or  $\Omega_x^x = -\Omega_y^y = \beta$  which describes the linear in momentum Dresselhaus spin-orbit interaction [101]. Notice that lower (upper) indices  $i = x, y, z$  label space (spin) variables and sum over repeated indices is implied.

Without any loss of generality, it is possible to write  $\hat{h}_0$  (Eq. 4.1) such that the linear-in-momentum SOC and the Zeeman field enter as a SU(2) gauge potential [99, 100] :

$$\hat{h}_0 = \frac{(p_i - \mathcal{A}_i)^2}{2m} - \tilde{\mu} + \mathcal{A}_0 , \quad (4.2)$$

where between Eqs. (4.1) and (4.2), the chemical potential has been shifted without physical consequences :  $\mu \rightarrow \tilde{\mu} = \mu - (\mathcal{A}_i^a)^2 / 8m$ . The SU(2) scalar potential  $\mathcal{A}_0 = \mathcal{A}_0^a \sigma^a / 2$  describes either a Zeeman magnetic field in a normal metal or an intrinsic exchange field in a ferromagnetic metal, whereas the vector potential  $\mathcal{A}_i = \mathcal{A}_i^a \sigma^a / 2$  represents spin-orbit interaction.

In analogy to usual electrodynamics, the Hamiltonian Eq. (4.2) is written in terms of a SU(2) four-potential  $\mathcal{A}_\mu$ , where  $\mu$  labels space ( $\mu = x, y, z$ ) via spin-orbit interaction and time ( $\mu = 0$ ) via the Zeeman field. This Hamiltonian is invariant under the gauge transformations  $\Psi \rightarrow \mathcal{U} \Psi$  and  $\mathcal{A}_\mu \rightarrow \mathcal{U} \mathcal{A}_\mu \mathcal{U}^{-1} - i(\partial_\mu \mathcal{U}) \mathcal{U}^{-1}$ , where  $\mathcal{U}$  is a SU(2) rotation matrix [99]. Following the analogy to electrodynamics one defines the SU(2) field strength tensor  $\mathcal{F}_{\mu\nu}$  as :

$$\mathcal{F}_{\mu\nu} = \partial_\mu \mathcal{A}_\nu - \partial_\nu \mathcal{A}_\mu - i[\mathcal{A}_\mu, \mathcal{A}_\nu] . \quad (4.3)$$

We consider now a superconductor at temperature close to its critical temperature  $T_c$ . Equilibrium properties can be described within the Ginzburg-Landau theory (see Chapter 2). Specifically the coupling between spin and charge degrees of freedom is described by an additional term in the Ginzburg-Landau free energy Eq. (2.1),  $F_L$ , the so-called Lifshitz invariant [10, 71]. For arbitrary linear-in-momentum SOC and dimension, the Lifshitz invariant can be written as [97, 102] :

$$F_L \sim T_i v_i , \quad (4.4)$$

where  $v_i \propto \partial_i \varphi$  is the superfluid velocity and  $T_i$  is a polar vector which is odd under time reversal and SU(2) gauge invariant. In other words this vector has to be expressed in terms of the SU(2) magnetic and electric fields and covariant derivatives  $\tilde{\nabla}_\mu = \partial_\mu \cdot - i[\mathcal{A}_\mu, \cdot]$ .

The anomalous current induced in a system is then proportional to the polar vector  $T_i$ . The latter can be constructed using SU(2) gauge symmetry arguments only. In Ref. [97], the Lifshitz invariant in the lowest order in the exchange field and in the SOC (this one being assumed to be homogeneous) was identified, and the anomalous current was found to be proportional to the following expression of the fields :

$$j_i \sim \mathcal{F}_{0k}^a \mathcal{F}_{ki}^a = E^a \times B^a , \quad (4.5)$$

where  $E_i^a = \mathcal{F}_{0i}^a$  and  $B_i^a = \epsilon_{ijk} \mathcal{F}_{jk}^a$  are the SU(2) electric and magnetic fields respectively, and  $\epsilon_{ijk}$  is the Levi-Civita symbol. From Eq. 4.3 , we can notice that the SU(2) magnetic field only exists in two-dimensional systems, which implies that the above result, Eq. 4.5, is only finite for 2D and 3D, but gives zero in 1D systems.

To illustrate the result of expression Eq. (4.5), let us consider a two-dimensional system in the  $x - y$  plane with homogeneous and time-independent Zeeman and Rashba spin-orbit fields. Specifically, the SOC is described by the Hamiltonian  $\mathcal{H}_{so} = \alpha (p_y \sigma^x - p_x \sigma^y)$  leading to a two component vector potential :  $\mathcal{A}_x^y = 2m\alpha = -\mathcal{A}_y^x$ . In this case, the electric field has two components  $\mathcal{F}_{0x} = m\alpha (\mathcal{A}_0^x \sigma^z - \mathcal{A}_0^z \sigma^x) / 2$  and  $\mathcal{F}_{0y} = m\alpha (\mathcal{A}_0^y \sigma^z - \mathcal{A}_0^z \sigma^y) / 2$ , whereas the magnetic field is given by  $\mathcal{F}_{xy} = m^2 \alpha^2 \sigma^z = -\mathcal{F}_{yx}$ . This leads to an in-plane current  $j_{x,y} \sim \pm m^3 \alpha^3 \mathcal{A}_0^{y,x}$  when the Zeeman field is applied in  $y$  or  $x$  direction respectively, in agreement with the Edelstein result, Ref. [71].

### 4.1.2 One dimensional systems

The situation is rather different in a one-dimensional system, for which the SU(2) magnetic field  $B^a$  is zero and therefore, according to Eq. (4.5) no anomalous current

should appear at first order in the exchange field. But, on the other hand, it is known that in wires with a 1D SOC such current can be finite [11, 48], namely, when at least two components of the magnetic field, one longitudinal and one transverse to the spin-orbit field, are finite. In order to understand this result we seek for an invariant of higher order in the exchange field (Eq. 4.4) : Clearly in a pure 1D system only the electric field is finite and the next leading order contribution to the current can be constructed as a product of covariant derivatives of the electric field. Specifically the first finite term in leading order of the fields is <sup>1</sup> :

$$j_i \sim \left( \tilde{\nabla}_k \mathcal{F}_{0k} \right)^a \left( \tilde{\nabla}_0 \mathcal{F}_{0i} \right)^a . \quad (4.6)$$

From Eq. (4.3), the electric field for a 1D system with time-independent fields is given by

$$\mathcal{F}_{0x} = -\partial_x \mathcal{A}_0 - i [\mathcal{A}_0, \mathcal{A}_x] . \quad (4.7)$$

The second term is the field induced, for example, by homogeneous exchange field and SOC. The first term is only finite if the exchange field is inhomogeneous exchange as in the case of a spin texture.

We first consider a homogeneous situation, for which the exchange field has an arbitrary direction and the SOC is, without loss of generality,  $\mathcal{H}_{\text{so}} = \alpha p \sigma^z$ , such that the vector potential has only one finite component  $\mathcal{A}_x^z = -2m\alpha$ . In this case  $\mathcal{F}_{0x} = -im\alpha \mathcal{A}_0^a [\sigma^a, \sigma^z] / 2$  and hence the anomalous current obtained from Eq. (4.6) reads :

$$j_x \sim -m^3 \alpha^3 \left[ (\mathcal{A}_0^x)^2 + (\mathcal{A}_0^y)^2 \right] \mathcal{A}_0^z . \quad (4.8)$$

This result coincides with the one obtained in Refs.[11, 48] in leading order in the exchange field.

A gauge equivalent situation to the previous one is a system without SOC but with an inhomogeneous exchange field that for example varies in only  $x$ -direction [52]. In such a case the electric field is finite due to the first term in Eq. (4.7). As a specific example we consider a spiral exchange such that the SU(2) scalar potential has three components  $\mathcal{A}_0^x = 2h \cos(Qx)$ ,  $\mathcal{A}_0^y = 2h \sin(Qx)$  and  $\mathcal{A}_0^z = 2h_z$ . In this case,  $\mathcal{F}_{0x} = Qh [\sin(Qx) \sigma^x - \cos(Qx) \sigma^y]$  and the anomalous current reads :

$$j_x \sim Q^3 h^2 h_z . \quad (4.9)$$

As expected the currents of Eqs. (4.8) and (4.9) coincides after identifying the gauge equivalence between the SOC parameter  $m\alpha$  and the wave vector  $Q$  of the magnetic texture.

### 4.1.3 The double wire setup : A quasi-2D system

In this section, we focus on the particular case of two spatially separated wires connected via a hopping term, as illustrated in Fig. 4.2. One of the wire is a superconductor, whereas the second one a normal metal with both parallel Zeeman and SOC fields. In a pure 1D system when the SOC and exchange field vectors are parallel, clearly no SU(2) fields are generated and hence no magnetoelectric effects can take place (Eq. 4.6). In other words, such situation implies that the SOC can be gauged out, and no current is generated. In the two wire system the situation is different, because strictly

---

1. I. V. Tokatly, private correspondence

speaking the system is not 1D and the coupling between the wires prevents such a pure gauge situation.

Namely, the fields depend not only on the spatial coordinate along the wires, but also on the one perpendicular to them denoted as  $z$  in Fig. 4.2, such that the system behaves as a 2D system. If we assume that SOC and exchange field are parallel, with the only non-zero components of the potentials being  $\mathcal{A}_x^z$  and  $\mathcal{A}_0^z$ , then according to Eq. (4.3) the SU(2) fields are finite and determined by  $\mathcal{F}_{0z}^z = -\partial_z \mathcal{A}_0^z$  for the electric field and  $\mathcal{F}_{zx}^z = \partial_z \mathcal{A}_x^z$  for the magnetic field. Therefore, from the above symmetry arguments, specifically from Eq. (4.5) one expects a finite anomalous current even when the SOC and exchange fields are parallel. The amplitude of such a current will be linear in both fields :  $j_x \sim \alpha h_z$ .

The above analysis only explains whether the anomalous currents are allowed by symmetry or not. However, it is important to emphasize that in systems in which superconductivity and spin-dependent fields spatially coexist, one should compute the superconducting order parameter self-consistently allowing for a spatially dependent phase, as done for the FFLO case in Chapter 3. The ground-state corresponds to a zero-current state [6] and therefore the anomalous current obtained above has to be compensated by the current induced by the phase gradient of the condensate wave function. In the next section we compute explicitly the equilibrium value of the wave-vector  $q$  and the currents for weak spin fields, and show that the ground-state is indeed a zero-current state.

## 4.2 Self-consistent order parameter for weak spin-orbit coupling

In this section, we derive the self-consistency equation in terms of the Green's functions in Nambu spin basis using the model introduced in Chapter 3. The system is studied in the limit of weak spin-orbit interaction and small wave-vector  $q$ . We then compute the anomalous charge current induced in the wire, and compare the result from those obtained by the above symmetry arguments. Finally, we show explicitly that in the ground-state the anomalous current is exactly compensated by the current induced by the spatial dependence of the superconducting phase.

### 4.2.1 Single wire system

Let us consider the particular case of an infinite superconducting wire along the  $x$ -direction, in the presence of Rashba SOC and a Zeeman field (Fig. 4.1).

#### Model and Hamiltonian

The Hamiltonian describing the system has the same form as Eq. 3.4, with an additional SOC term in the non-superconducting part  $\hat{h}_N$ . We assume that the Zeeman field  $\vec{h} = (h_x, 0, h_z)$  is applied in the  $x - z$  plane, and that the wire is on a substrate parallel to the  $x - z$  plane such that the SOC is along the  $z$ -direction :

$$\hat{h}_N = \left( \xi + \frac{q^2}{8m} + \alpha p \sigma_z \right) \tau_z + \frac{qp}{2m} + \frac{\alpha q}{2} \sigma_z + \vec{h} \cdot \vec{\sigma}. \quad (4.10)$$

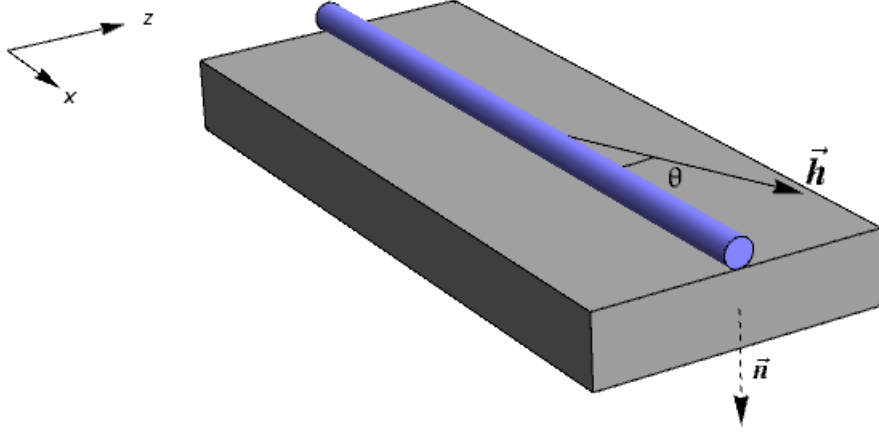


FIGURE 4.1 – The first setup is made of an infinite superconducting wire with SOC and a Zeeman field with two components, one longitudinal and one transverse to the spin-orbit field.

Here  $\xi = \frac{p^2}{2m} - \mu$  is the quasiparticle energy,  $\mu$  is the chemical potential,  $\alpha$  is the spin-orbit coupling constant and  $\sigma_{x,y,z}, \tau_{x,y,z}$  are the Pauli matrices acting respectively in spin and Nambu space. Throughout this chapter, we take  $\hbar = k_B = 1$ .

Near the second-order transition,  $\Delta \ll T$ , the Green's function  $G$  describing the system can be expanded in series of  $\Delta$ . At first order in  $\Delta$ ,  $G$  reads :

$$G \approx G_N + G_N \hat{h}_{SC} G_N, \quad (4.11)$$

where the superconducting hamiltonian  $\hat{h}_{SC}$  was introduced in Chapter 3, Eq. (3.6). The Green's function in the normal state  $G_N$  has the same form as Eq. (3.8) in Nambu space :

$$G_N = \begin{pmatrix} G_- & 0 \\ 0 & G_+ \end{pmatrix}, \quad (4.12)$$

where the matrix  $G_\nu$  ( $\nu = \pm$ ) now includes SOC :

$$G_\nu = \frac{i\omega_n + \nu\xi + \nu\frac{q^2}{8m} - \frac{qp}{2m} + \vec{h} \cdot \vec{\sigma} - \alpha\sigma_z (\nu p - \frac{q}{2})}{\left(i\omega_n + \nu\xi + \nu\frac{q^2}{8m} - \frac{qp}{2m}\right)^2 - (h_z - \nu\alpha p + \alpha\frac{q}{2})^2 - h_x^2}. \quad (4.13)$$

Next, we will use the expression of the Green's function  $G$  Eqs. (4.11 - 4.13) to write the self-consistency relation (Eq. 3.10), and derive the expression of the wave-vector  $q$  near the emergence of the modulated phase.

### Self-consistent order parameter

We recall the expression of the self-consistency relation given in Chapter 3, Eq. (3.10) :

$$\ln\left(\frac{T_c}{T_{c0}}\right) = 2T_c \sum_{\omega_n > 0} \left[ \frac{v_F}{8} \text{Re} \left( \int_{-\infty}^{+\infty} \text{Tr} \left( \frac{G}{\Delta} \tau_x \right) dp \right) - \frac{\pi}{\omega_n} \right]. \quad (4.14)$$

In the presence of spin-orbit interaction, the integral over  $p$  is more complicated to evaluate than in the FFLO case. Indeed, the Green's function  $G$  Eqs. (4.11 - 4.13) contains linear terms in  $p$  coming from SOC, thus preventing a straightforwardly transformation of the integral over  $p$  to an integral over  $\xi$  as we did in Chapter 3.

In order to compute the  $p$  integral in Eq. 4.14 we assume that both, the Zeeman field and SOC, are small such that  $h_x, h_z \ll T_c$  and  $\alpha p_F \ll T_c$  (where  $p_F$  is the Fermi momentum) and expand the Green's function  $G$  from Eq. (4.11) in series of  $h_x, h_z$  and  $\alpha p$ , after substitution of Eq. (4.12-4.13). Moreover, since the wave-vector  $q$  is small near the emergence of the modulation phase, we also expand  $G$  over  $q$ . Because of the integration over momentum, only terms even in  $p$  will contribute, allowing to transform the integral over  $p$  into an integral over the quasiparticle energy  $\xi$  following :

$$\int_{-\infty}^{+\infty} dp = 2 \int_{-\mu}^{+\infty} N(\xi) d\xi, \quad (4.15)$$

where  $N(\xi) = \sqrt{\frac{m}{2(\xi + \mu)}}$  is the density of states at energy  $\xi$ . We assume that the chemical potential is the largest energy involved in the problem :  $\mu \gg T_c, E_{so}$ , where  $E_{so} = \frac{1}{2} m \alpha^2$  and set the lower integration limit to  $-\infty$ . In the expansion of the Green's function  $G$  we keep terms up to order  $\alpha^3 p^4$ , where  $p^2 = 2 m (\xi + \mu)$ . This means that we have to keep terms up to  $(\xi/\mu)^2$  by expanding  $N(\xi)$ . Thus, the integral in Eq. (4.15) can be approximated as :

$$\int_{-\infty}^{+\infty} dp \rightarrow \frac{2}{v_F} \int_{-\infty}^{+\infty} \left( 1 - \frac{\xi}{2\mu} + \frac{3\xi^2}{8\mu^2} \right) d\xi, \quad (4.16)$$

where  $v_F = \sqrt{2m/\mu}$ . The  $\xi$  integration is then performed using the residue technique.

Therefore we obtain the following expression for the self-consistency relation :

$$\ln \left( \frac{T_c}{T_{c0}} \right) = 2 \pi T_c \sum_{\omega_n \geq 0} \left[ -\frac{h_x^2 + h_z^2}{\omega_n^3} + \frac{7 p_F^2}{\omega_n^7} h_x^2 h_z \alpha^3 q - \frac{v_F^2}{4 \omega_n^3} q^2 \right]. \quad (4.17)$$

Contrary to the FFLO case Eq. (3.11), the self-consistency relation Eq. (4.17) displays a linear term in  $q$ , ensuring that the modulated phase is more stable than the uniform phase for all temperatures  $T < T_{c0}$ . Indeed, the equilibrium value  $q_0$  of the wave-vector is obtained by maximizing Eq. (4.17) with respect to  $q$ , which is the equivalent of minimizing the Ginzburg-Landau free energy :

$$q_0 = 14 m^2 \alpha^3 h_x^2 h_z \frac{\Gamma_7}{\Gamma_3}, \quad (4.18)$$

where  $\Gamma_s = \sum_{\omega_n > 0} \frac{1}{\omega_n^s}$ . Hence the modulation requires both finite spin-orbit coupling and a tilted Zeeman field, which is neither perpendicular nor aligned with the SOC (both  $h_x$  and  $h_z$  need to be finite). This leads to anisotropic effects that must be observable when the Zeeman field is rotated with respect to the spin-orbit field.

Notice that the appearance of a wave-vector  $q$  proportional to  $\alpha^3$  occurs because of the compensation of the linear terms in  $\alpha$ , stemming from the expansion of the density of states  $N(\xi)$ , Eq. (4.16), in the limit of a large chemical potential  $\mu \gg T_c$ . The details of this calculation are provided in Appendix A. However, in the opposite limit, namely  $\mu \ll T_c$ , such compensation should not occur, which explains why in this

case, a linear-in- $\alpha$  current is found [48]. Finally, we emphasize that for a non-quadratic dispersion, this compensation of the linear-in- $\alpha$  terms would not be complete, leading to  $q \sim \alpha$ .

Next, we compute the charge current in the wire, and show that in the ground-state, the current coming from the superconducting wave-vector compensates exactly the anomalous current.

### Charge current

The charge current operator is proportional to the velocity operator  $\hat{v} = \frac{\partial \hat{h}_N}{\partial p}$ , such that in terms of the Green's function  $G$ , the charge current reads :

$$j = -\frac{eT_c}{2} \sum_{\omega_n} \int_{-\infty}^{+\infty} \frac{dp}{2\pi} \left[ \frac{p}{m} \text{Tr} G + \alpha \text{Tr} (G \sigma_z) + \frac{q}{2m} \text{Tr} (G \tau_z) \right], \quad (4.19)$$

where the second term in Eq. (4.19) stems from the anomalous velocity in the presence of SOC. To obtain a finite current from Eq. (4.19), the Green's function  $G$  has to be expanded up to second order in  $\Delta$  :

$$G \approx G_N + G_N \hat{h}_{SC} G_N + G_N \hat{h}_{SC} G_N \hat{h}_{SC} G_N, \quad (4.20)$$

where  $h_{SC}$  is given by Eq. (4.23) the normal state Green's functions  $G_N$  is obtained from Eqs. (4.12) and (4.13).

Using Eq. (4.16) to compute the integral over  $p$ , we obtain the following expression for the current :

$$j = 2eT_c \Delta^2 v_F (14 m^2 \alpha^3 h_x^2 h_z \Gamma_7 - q \Gamma_3). \quad (4.21)$$

The current in the ground-state is obtained by replacing  $q$  by its equilibrium value  $q_0$ . *i.e.* by substituting Eq. (4.18) in Eq. (4.21). This leads to a cancellation in the right hand side of Eq. (4.21). This is not surprising since the true ground-state has to be a zero-current state as demonstrated in Ref. [6] for a 2D system by minimization of the free energy with respect to  $q$ .

Moreover, at  $q = 0$ , one finds that this result is in agreement with the one obtained in Sec. 4.1 from the SU(2) covariant formulation Eq. (4.8) and with previous works [11, 48] : In leading order in SOC and Zeeman field, the anomalous current is proportional to  $\alpha^3 h_x^2 h_z$ .

### 4.2.2 Double wire system

In this section we consider a different setup made of two infinite wires coupled via a hopping term, as illustrated Fig. 4.2. Experimentally, such double wire systems have been realized in semiconducting systems, as for example GaAs wires separated by an insulating AlGaAs barrier [83, 84, 85, 86]. In our case, one of the wires is a superconductor, and may exhibit a spatially oscillating order parameter  $\Delta(x) = \Delta e^{iqx}$ , which could be done in the realistic systems described above if the superconducting wire has a diameter much smaller than the coherence length. The second wire is in the normal state and has a SOC and local exchange field. We assume that these fields are parallel to each other.

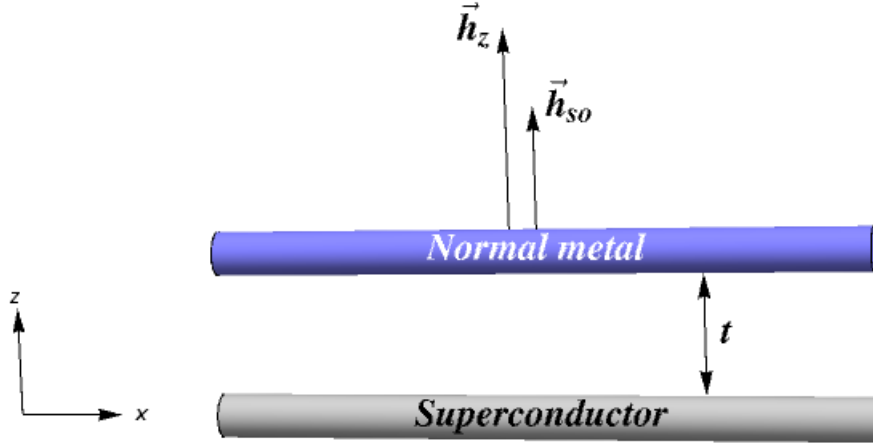


FIGURE 4.2 – In the second system, superconducting and magnetic correlations and fields are spatially separated into two different wires, coupled via a hopping term. We consider the case where the spin-orbit and Zeeman fields are parallel.

### Model and Hamiltonian

The Hamiltonian of the system has the same form as Eq. (3.4) enlarged over the wire space and taking into account the additional SOC term, such that :

$$\hat{h}_N = \left( \xi + \frac{q^2}{8m} \right) \tau_z + \frac{qp}{2m} + t \tau_z \eta_x + \left( \alpha p \tau_z + \frac{\alpha q}{2} + h_z \right) \sigma_z \frac{\eta_0 + \eta_z}{2}, \quad (4.22)$$

where  $t$  is the hopping energy and  $\eta_{x,y,z}$  are the Pauli matrices acting in wire space. To simplify, we have considered that the quasiparticle energy  $\xi$  is the same in both wires. In this basis, the superconducting Hamiltonian operator  $\hat{h}_{SC}$  is expressed as :

$$\hat{h}_{SC} = -\Delta \tau_x \frac{\eta_0 - \eta_z}{2}. \quad (4.23)$$

As we did for the one wire system, we assume that the temperature is closed to the critical temperature  $T_c$ , such that  $\Delta \ll T$  and can be treated perturbatively. At first order in  $\Delta$  the Green's function describing the double wire system is obtained from Eq. (4.11), where  $G_N$  can be written in Nambu-spin basis as

$$G_N = \begin{pmatrix} G_{--} & 0 & 0 & 0 \\ 0 & G_{-+} & 0 & 0 \\ 0 & 0 & G_{+-} & 0 \\ 0 & 0 & 0 & G_{++} \end{pmatrix}, \quad (4.24)$$

where  $G_{\nu\kappa}$  are  $2 \times 2$  matrices in the wire space, and  $\nu = \pm 1$  ( $\kappa = \pm 1$ ) corresponds to the Nambu (spin) indices. Specifically,

$$G_{\nu\kappa} = \frac{i\omega_n + \nu \left( \xi + \frac{q^2}{8m} \right) - \frac{qp}{2m} + \kappa \left( h_z - \nu \alpha p + \frac{\alpha q}{2} \right) \frac{\eta_0 - \eta_z}{2} + \nu t \eta_x}{\left[ i\omega_n + \nu \left( \xi + \frac{q^2}{8m} \right) - \frac{qp}{2m} \right] \left[ i\omega_n + \nu \left( \xi + \frac{q^2}{8m} \right) - \frac{qp}{2m} + \kappa \left( h_z - \nu \alpha p + \frac{\alpha q}{2} \right) \right] - t^2}. \quad (4.25)$$

The total Green's function is then obtained by substituting Eqs. (4.24, 4.25) into Eq. (4.11). Next we use the self-consistency relation written in terms of the Green's function  $G$  to derive the expression of the wave-vector  $q$  near the emergence of the modulated phase.

### Self-consistent order parameter

In Nambu spin wire basis, the self-consistency equation for the superconducting order parameter reads :

$$\ln \left( \frac{T_c}{T_{c0}} \right) = 2 T_c \sum_{\omega_n > 0} \left[ \frac{v_F}{8} \operatorname{Re} \left( \int_{-\infty}^{+\infty} \operatorname{Tr} \left( \frac{G}{\Delta} \tau_x \frac{\eta_0 - \eta_z}{2} \right) dp \right) - \frac{\pi}{\omega_n} \right], \quad (4.26)$$

where  $T_{c0}$  is the critical temperature of the isolated superconducting wire, i.e. for  $t = 0$ .

As we explained for the one wire system, the presence of spin-orbit interaction prevents to directly transform the  $p$  integral of Eq. 4.26 into a  $\xi$  integral, as it has been done in the FFLO case, Chapter 3. Therefore, we assume that the Zeeman and spin-orbit interactions, as well as tunneling are small such that  $t, h_z, \alpha p_F \ll T_c$ , and again that the chemical potential is the largest energy involved :  $\mu \gg T_c, E_{\text{so}}$ . We then expand the Green's function  $G$  in Eq. (4.11) in series of  $h_z, \alpha p$  and  $t$ , after replacing Eqs. (4.24, 4.25). Moreover, since the wave-vector  $q$  is small near the emergence of the modulation phase, we also expand  $G$  over  $q$ .

Only terms even in momentum survive the momentum integration in Eq. (4.26). As in Sec. 4.2.1, we can then change the integration variable to  $\xi$ , see Eq. (4.15). To keep consistently all terms with same power of the small parameter  $\xi/\mu$  one has to expand  $N(\xi)$  up to first order. Then the self-consistency equation reduces to :

$$\ln \left( \frac{T_c}{T_{c0}} \right) = -2\pi T_c \sum_{\omega_n > 0} \left[ \frac{t^2}{2\omega_n^3} + \frac{3}{8\omega_n^5} \alpha h_z t^2 q + \frac{v_F^2}{4\omega_n^3} q^2 \right]. \quad (4.27)$$

As we already mentioned in Sec. 4.2.1, the presence of a linear term in  $q$  in the self-consistency relation Eq. 4.27 implies that the modulated phase is more stable than the uniform one for all temperatures  $T < T_{c0}$ . The calculation details of this linear term are provided in Appendix B. The equilibrium value  $q_0$  of the superconducting wave vector is obtained by maximizing Eq. (4.27) with respect to  $q$ , which is the equivalent of minimizing the Ginzburg-Landau free energy. We obtain :

$$q_0 = -\frac{3}{4v_F^2} \alpha h_z t^2 \frac{\Gamma_5}{\Gamma_3}. \quad (4.28)$$

Contrary to the single wire system, the  $x$ -component of the field is not needed to generate the inhomogeneous phase. Indeed the two wire system behaves as quasi 2D, as we will discuss next, and therefore one expects to get a magnetoelectric effect also in the case of parallel SOC and exchange field. In the next section we determine the anomalous charge currents that appear when  $q = 0$  and, as we shown in Sec. 4.1 are allowed by symmetry.

### Anomalous charge current

The total charge current in the two wire system of Fig. 4.2 is given by the sum of the current flowing in the superconducting wire,  $j_S$ , and in the normal wire,  $j_N$  :

$$j = j_S + j_N. \quad (4.29)$$

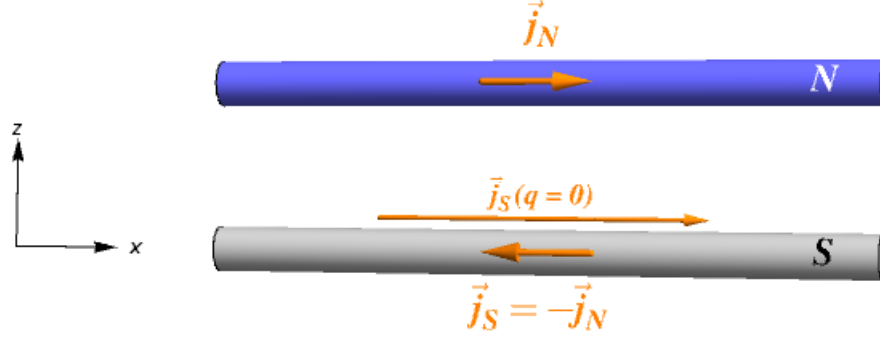


FIGURE 4.3 – In the ground state, each wire carries a finite current with opposite directions, corresponding to a zero current state. However, when the superconducting order parameter is constant ( $q = 0$ ), a finite current flows in each wire with the same direction. This is a finite current state, corresponding to an excited state.

In terms of the Green's function  $G$  expanded at second order in  $\Delta$  Eqs. (4.20, 4.24, 4.25), these components read :

$$j_S = -\frac{eT}{2} \sum_{\omega_n} \int_{-\infty}^{+\infty} \frac{dp}{2\pi} \left[ \frac{p}{m} \text{Tr} \left( G \frac{\eta_0 - \eta_z}{2} \right) + \frac{q}{2m} \text{Tr} \left( G \tau_z \frac{\eta_0 - \eta_z}{2} \right) \right] ; \quad (4.30)$$

$$j_N = -\frac{eT}{2} \sum_{\omega_n} \int_{-\infty}^{+\infty} \frac{dp}{2\pi} \left[ \frac{p}{m} \text{Tr} \left( G \frac{\eta_0 + \eta_z}{2} \right) + \frac{q}{2m} \text{Tr} \left( G \tau_z \frac{\eta_0 + \eta_z}{2} \right) + \alpha \text{Tr} \left( G \sigma_z \frac{\eta_0 + \eta_z}{2} \right) \right] . \quad (4.31)$$

Using Eq. (4.15) to compute the integrals over  $p$  as explained in the previous section, one obtains the following expressions for the currents :

$$j_S = -e T_c \Delta^2 \left( \frac{5}{4 v_F} \alpha h_z t^2 \Gamma_5 + 2 q v_F \Gamma_3 \right) ; \quad (4.32)$$

$$j_N = -e T_c \Delta^2 \frac{1}{4 v_F} \alpha h_z t^2 \Gamma_5 . \quad (4.33)$$

By replacing  $q$  by its equilibrium expression  $q_0$  from Eq. (4.28), one can easily check that the total current, Eq. (4.29), is zero in the ground-state. However, the current in each wire is finite with  $j_S = -j_N$ , as illustrated in Fig. 4.3. This is a remarkable result that shows that even though the ground state corresponds to a zero total current state, finite currents may flow in each of the wires.

The anomalous current predicted in Sec. 4.1.3 is obtained by imposing  $q = 0$ . It is finite and linear in  $\alpha$  and  $h_z$  :

$$j = -\frac{3}{2 v_F} e T_c \Delta^2 \alpha h_z t^2 \Gamma_5 . \quad (4.34)$$

This result is in agreement with the symmetry arguments discussed in Sec. 4.1.3.

### 4.3 Superconducting wire with a strong spin-orbit coupling

In the previous section, the self-consistency relation was derived in the case of weak spin-orbit interaction :  $\alpha p_F \ll T_c$ . In this section, we study the one wire system

illustrated in Fig. 4.1 in the opposite case, namely a strong spin-orbit coupling  $\alpha p_F \gg T_c$ . In this case, it is convenient to rewrite the normal Hamiltonian in the diagonal basis, the so-called *helical basis*. From the knowledge of the helical Hamiltonian, we derive the expression of the normal Green's function describing the system in the helical basis, from which we obtain the self-consistency equation by neglecting interband pairing contributions. We then determine the expression of the superconducting wave-vector  $q$  near the emergence of the modulated phase, in the limit of small Zeeman field  $h_x, h_z \ll T_c$ . We show that in the same way as the small spin-orbit case, the necessary condition for the appearance of the inhomogeneous phase at all temperatures  $T < T_{c0}$  is the presence of a tilted Zeeman field with respect to the spin-orbit field. We finally present the  $(h_x, h_z, T)$ -phase diagram for various orientations of the Zeeman field and various values of the spin-orbit coupling constant.

### 4.3.1 Normal state Green's functions in the helical basis

In the limit of strong spin-orbit interaction,  $T_c \ll \alpha p_F$  (but still  $E_{so} = m \alpha^2 / 2 \ll \mu$ ), it is convenient to study the single wire system (Fig. 4.1) in the diagonal basis. We first consider this system in the absence of superconductivity, and derive the diagonal Hamiltonian and the corresponding Green's function. In a second part, we deduce the expression of the Green's function describing the system in the presence of superconductivity from the normal Green's function.

The Hamiltonian operator describing the wire in the absence of superconductivity in Nambu spin space is defined by Eq. (4.10) by setting the wave-vector  $q = 0$  :

$$\hat{h}_N = (\xi + \alpha p \sigma_z) \tau_z + \vec{h} \cdot \vec{\sigma}, \quad (4.35)$$

where  $\sigma_{x,y,z}$  and  $\tau_{x,y,z}$  are the Pauli matrices acting in spin and Nambu space, and  $\xi$  is the quasiparticle energy.

To diagonalize the Hamiltonian Eq. (4.35), it is necessary to define a rotation matrix  $\mathcal{U}$  such that  $\hat{h}_N \rightarrow \hat{h}_{\text{hel}} = \mathcal{U}^\dagger \hat{h}_N \mathcal{U}$ , where  $\hat{h}_{\text{hel}}$  is the Hamiltonian operator in the helical basis :

$$\hat{h}_{\text{hel}} = \xi \tau_z - \frac{\lambda}{2} [(\varepsilon_+ + \varepsilon_-) \tau_0 + (\varepsilon_+ - \varepsilon_-) \tau_z], \quad (4.36)$$

where  $\varepsilon_\pm = \pm \sqrt{h_x^2 + (h_z \pm \alpha p)^2}$ ,  $\tau_0$  is the identity matrix and  $\lambda = \pm$  labels the two energy bands. The matrix  $\mathcal{U}$  reads in the Nambu basis :

$$\mathcal{U} = \begin{pmatrix} \tilde{\mathcal{U}}(\phi_p) & 0 \\ 0 & \tilde{\mathcal{U}}(\pi + \phi_{-p}) \end{pmatrix}, \quad (4.37)$$

where the matrix  $\tilde{\mathcal{U}}$  is defined in the spin basis by :

$$\tilde{\mathcal{U}}(\phi_p) = e^{-i \frac{\phi_p}{2} \sigma_y}, \quad (4.38)$$

and the phase  $\phi_p$  is such that :

$$\phi_p = \arccos \left( \frac{h_z + \alpha p}{\sqrt{h_x^2 + (h_z + \alpha p)^2}} \right). \quad (4.39)$$

From the expression of the normal Hamiltonian Eq. (4.35), it is possible to derive the expression of the normal Green's function  $\mathcal{G}_N$  in the helical basis by solving the equation of motion for the Green's functions  $(i\omega_n - \hat{h}_{\text{hel}}) \mathcal{G}_N = \mathbb{1}$  :

$$\mathcal{G}_N = \begin{pmatrix} \mathcal{G}_\lambda(p, \omega_n) & 0 \\ 0 & -\mathcal{G}_\lambda(-p, -\omega_n) \end{pmatrix}, \quad (4.40)$$

where  $\mathcal{G}_\lambda$  corresponds to the normal Green's function associated with the band  $\lambda$  :

$$\mathcal{G}_\lambda(p, \omega_n) = \frac{1}{i\omega_n - \xi + \lambda \sqrt{h_x^2 + (h_z + \alpha p)^2}}. \quad (4.41)$$

Notice that to distinguish Green's functions between spin and helical spaces, we use capital letters  $G$  in the spin basis, and scripted letters  $\mathcal{G}$  for the helical basis.

From the knowledge of the normal Green's function in the helical basis  $\mathcal{G}_N$  (Eq. 4.40), we can derive the expression of the Green's function of the system in the presence of superconductivity. Near the transition between the normal and superconducting states,  $\Delta \ll T_c$  and the Green's function  $\mathcal{G}$  can be expanded at first order in  $\Delta$ . In spin basis, the expansion of the Green's function  $G$  is given by Eq. (4.11). Using the relation between  $G$  and  $\mathcal{G}$ , namely  $G = \mathcal{U}^S \mathcal{G} (\mathcal{U}^S)^\dagger$ , Eq. (4.11) can be written in the following way :

$$\mathcal{G} = \mathcal{G}_N^S - \Delta \mathcal{G}_N^S (\mathcal{U}^S)^\dagger \tau_x \mathcal{U}^S \mathcal{G}_N^S. \quad (4.42)$$

The rotation matrix in the presence of superconductivity  $\mathcal{U}^S$  is obtained from the expression of  $\mathcal{U}$  (Eqs. 4.37 - 4.38), where the momentum is shifted by a factor  $q/2$ , such that  $\pm p \rightarrow \pm p + q/2$  :

$$\mathcal{U}^S = \begin{pmatrix} \tilde{\mathcal{U}}(\phi_{p+\frac{q}{2}}) & 0 \\ 0 & \tilde{\mathcal{U}}(\pi + \phi_{-p+\frac{q}{2}}) \end{pmatrix}. \quad (4.43)$$

In the same way,  $\mathcal{G}_N^S$  corresponds to normal Green's function where the momentum has been shifted by  $q/2$  :

$$\mathcal{G}_N^S = \begin{pmatrix} \mathcal{G}_\lambda(p + \frac{q}{2}, \omega_n) & 0 \\ 0 & -\mathcal{G}_\lambda(-p + \frac{q}{2}, -\omega_n) \end{pmatrix}. \quad (4.44)$$

Next, we write the expression of the self-consistency relation in terms of the helical Green's function  $\mathcal{G}$  Eqs. (4.42 - 4.44), and derive the expression of the wave-vector  $q$  near the emergence of the modulated phase.

### 4.3.2 Emergence of the modulated phase

Let us now consider the self-consistency relation Eq. (4.14). Using the transformation  $G = \mathcal{U}^S \mathcal{G} (\mathcal{U}^S)^\dagger$ , we can derive its expression in terms of the helical Green's function  $\mathcal{G}$  :

$$\ln \left( \frac{T_c}{T_{c0}} \right) = 2 T_c \sum_{\omega_n > 0} \left[ \frac{v_F}{8} \text{Re} \left( \int_{-\infty}^{+\infty} \text{Tr} \left( \frac{\mathcal{G}}{\Delta} (\mathcal{U}^S)^\dagger \tau_x \mathcal{U}^S \right) dp \right) - \frac{\pi}{\omega_n} \right]. \quad (4.45)$$

Using the expression of  $\mathcal{G}$  Eqs. (4.42 - 4.44), we can compute the expression of the trace in Eq. (4.45), which contains two finite terms :

$$\begin{aligned} \text{Tr} \left( \frac{\mathcal{G}}{\Delta} (\mathcal{U}^S)^\dagger \tau_x \mathcal{U}^S \right) = & 2 \left[ \sin^2 \left( \frac{\eta}{2} \right) \sum_{\lambda} \mathcal{G}_{\lambda} \left( p + \frac{q}{2}, \omega_n \right) \mathcal{G}_{\lambda} \left( -p + \frac{q}{2}, -\omega_n \right) \right. \\ & \left. + \cos^2 \left( \frac{\eta}{2} \right) \sum_{\lambda \neq \lambda'} \mathcal{G}_{\lambda} \left( p + \frac{q}{2}, \omega_n \right) \mathcal{G}_{\lambda'} \left( -p + \frac{q}{2}, -\omega_n \right) \right], \end{aligned} \quad (4.46)$$

where  $\eta = \phi_{-p+q/2} - \phi_{p+q/2}$ . The first term of Eq. (4.46) describes intraband pairing correlations, whereas the second one corresponds to interband pairing. In the regime of strong spin-orbit interaction,  $\alpha p_F \gg h_x, h_z, T_c$  and  $E_{so} = m \alpha^2 / 2 \ll \mu$ , the phase difference  $\eta \rightarrow \pi$  at zeroth order in the Zeeman field, thus allowing to neglect interband pairing terms. Therefore, the self-consistency relation Eq. (4.45) becomes :

$$\ln \left( \frac{T_c}{T_{c0}} \right) = T_c \sum_{\omega_n \geq 0, \lambda} \left[ \frac{v_F}{2} \text{Re} \left( \int_{-\infty}^{+\infty} \mathcal{G}_{\lambda} \left( p + \frac{q}{2}, \omega_n \right) \mathcal{G}_{\lambda} \left( -p + \frac{q}{2}, -\omega_n \right) dp \right) - \frac{\pi}{\omega_n} \right]. \quad (4.47)$$

The method used to perform the  $p$  integration in Eq. (4.47) is quite different from the one used in Sec. 4.2.1 for the small spin-orbit limit. Indeed in the regime of strong spin-orbit interaction, we consider only intraband pairing terms, which allows to treat each band separately. Therefore, it is possible to compute the integral in the customary way [103] : Because the Green's functions  $\mathcal{G}_{\lambda}$  are peaked around the Fermi energy  $p_F^{\lambda}$ , we can turn the  $p$  integral into a  $\xi$  integral as we did in Eq. (2.30) but for each band separately :

$$\int dp \rightarrow \frac{1}{v_F} \int d\xi, \quad (4.48)$$

and we can approximate the momentum  $p$  by  $p_F^{\lambda}$  in the  $\alpha p$  and  $qp$  terms, where

$$p_F^{\lambda} = \lambda m \alpha + \sqrt{2 m \mu + m^2 \alpha^2}, \quad (4.49)$$

is the Fermi momentum of the band  $\lambda$ , obtained by neglecting the Zeeman contribution with respect to the SOC :  $h_x, h_z \ll \alpha p_F$ . In such a way the  $\xi$  integration can be performed straightforwardly.

Finally the self-consistency relation Eq. (4.47) reads :

$$\ln \left( \frac{T_c}{T_{c0}} \right) = 2 \pi T_c \sum_{\omega_n \geq 0, \lambda} \left[ \frac{2 \omega_n}{4 \omega_n^2 + \left[ q v_F^{\lambda} - \lambda \left( \sqrt{h_x^2 + (h_z + \alpha p_F^{\lambda} + \alpha q/2)^2} - \sqrt{h_x^2 + (h_z - \alpha p_F^{\lambda} + \alpha q/2)^2} \right) \right]^2} - \frac{1}{2 \omega_n} \right]. \quad (4.50)$$

To see the emergence of the modulated phase, we consider that the Zeeman field and the wave-vector  $q$  are small :  $h_x, h_z \ll T_c$  and  $q \ll p_F$ . Therefore, the self-consistency relation Eq. (4.50) can be expanded over  $h_x, h_z$  and  $q$  :

$$\ln \left( \frac{T_c}{T_{c0}} \right) = 2 \pi T_c \sum_{\omega_n \geq 0} \left[ -\frac{h_z^2}{\omega_n^3} + \frac{3 h_x^2 h_z}{2 \omega_n^3 \alpha p_F^2} q - \frac{v_F^2}{4 \omega_n^3} q^2 \right]. \quad (4.51)$$

Be aware that the self-consistency relation Eqs. (4.50) and (4.51) was obtained by considering only intraband pairing. In this case, we can notice that when  $h_z = 0$ , Eq.

(4.51) leads to  $T_c = T_{c0}$ , which seems to indicate that superconductivity is not affected by the Zeeman field when this one is normal to the spin-orbit interaction. However, we have to keep in mind that taking interband correlations into account in Eq. (4.46) would modify this result by terms of order  $h_x^2/\alpha^2 p_F^2$  in Eq. (4.51).

As expected from the weak spin-orbit case, the self-consistency relation Eq. (4.51) displays a linear term in  $q$  which leads to the emergence of an inhomogeneous superconducting state at wave-vector

$$q_0 = \frac{3 h_x^2 h_z}{4 \alpha \mu^2}, \quad (4.52)$$

where  $q_0$  is estimated by maximizing Eq. (4.51) with respect to  $q$ , as we did in Sec. 4.2.1. Similarly to Eq. (4.18),  $q_0$  is proportional to both longitudinal and transverse components of the Zeeman field, then inducing a modulated phase for each temperature  $T < T_{c0}$  as long as  $h_x$  and  $h_z$  are finite.

In the next section, we solve the self-consistency equation for general values of  $q$ ,  $h_x$  and  $h_z$  (Eq. 4.50) and obtain the  $(h_x, h_z, T)$ -phase diagrams for different orientations of the Zeeman field and different values of the spin-orbit constant  $\alpha$ .

### 4.3.3 Field-temperature phase diagrams

We now consider general values of the wave-vector  $q$  and solve numerically the self-consistency relation Eq. (4.50). To this purpose, we proceed in the following way : First, the temperature is extracted from the self-consistency relation Eq. (4.50) as a function of both magnetic field modulus  $h$  and wavevector  $q$ . The wave-vector  $q$  is then determined such that it maximizes the temperature at a given  $h$ , which is equivalent to minimize the Ginzburg-Landau free energy.

Following this procedure we plot in Fig. 4.4a the  $(h_x, h_z, T)$ -phase diagram for different orientations of the field for  $\alpha = 0.05 v_F$  ( $\alpha p_F = 100 T_{c0}$ ). One can first observe the anisotropy induced by spin-orbit interaction : At fixed critical field (temperature), the critical temperature (field) increases when  $\theta$  decreases,  $\theta$  corresponding to the angle between the field and the wire (see Fig. 4.1). This means that the superconducting phase is widened when the field tends to be normal to the SOC. As expected from Eq. (4.51), the purely parallel  $h = h_z$  ( $\theta = \pi/2$ ) or purely perpendicular  $h = h_x$  ( $\theta = 0$ ) to the spin-orbit field correspond to particular cases in which the linear term in  $q$  in Eq. (4.51) is zero.

When the field is longitudinal ( $h_x = 0$ ), we get back to the FFLO case : The modulated phase emerges at the tricritical point ( $T^* = 0.56 T_{c0}$ ,  $h^* = 1.07 T_{c0}$ ). This effect was already predicted in Sec. 4.1 : when the spin-orbit and Zeeman fields are parallel, the SOC can be gauged out, and we obtain an effective Hamiltonian equivalent to Eq. (3.4), leading to the FFLO state.

In the opposite case, namely when the Zeeman field is transverse to the SOC ( $h_z = 0$ ), we obtain a rather different effect : The wave-vector  $q$  vanishes, and  $T_c$  is not modified with respect to  $T_{c0}$  within leading order in  $h_x/\alpha p_F \ll 1$ . As we mentioned previously, this result comes from the fact that we neglect interband correlations in the self-consistency relation Eq. (4.50). However, including interband pairing requires to take into account the second line of Eq. (4.46), which is beyond the scope of the present calculation.

We can also compare the  $(h_x, h_z, T)$ -phase diagrams for different values of the spin-orbit coupling constant  $\alpha$  for  $h_x = h_z$ , as illustrated in Fig. 4.4b. The blue curve

represents the transition line between the normal and superconducting states in the absence of SOC, whereas the three others correspond to three finite values of  $\alpha$ . Globally, the presence of spin-orbit interaction enlarges the superconducting phase. The important gap between the line  $\alpha = 0$  and the lines  $\alpha \neq 0$  comes from the fact that in the second case we considered large values of  $\alpha$  :  $\alpha p_F \ll T_c$ . Let us focus on the transition lines corresponding to  $\alpha \neq 0$ . At temperatures  $T > T^* = 0.56 T_{c0}$ , these curves cannot be distinguished from each other due to the very small values of  $q$ . These ones can be estimated from Eq. (4.52) for a small Zeeman field : for example at  $h = 0.5 T_{c0}$ ,  $\theta = \pi/4$  and  $\alpha = 0.05 v_F$ ,  $q \approx 10^{-10} p_F$ , which weakly influences the critical temperature. But these values significantly increase for temperatures smaller than the tricritical temperature, related to the competition between helical and FFLO-like modulations that we mentioned in Chapter 3 : At large temperatures, the modulation coming from the helical state dominates, whereas below the tricritical temperature  $T^* = 0.56 T_{c0}$ , the modulation stems mainly from the FFLO-like state.

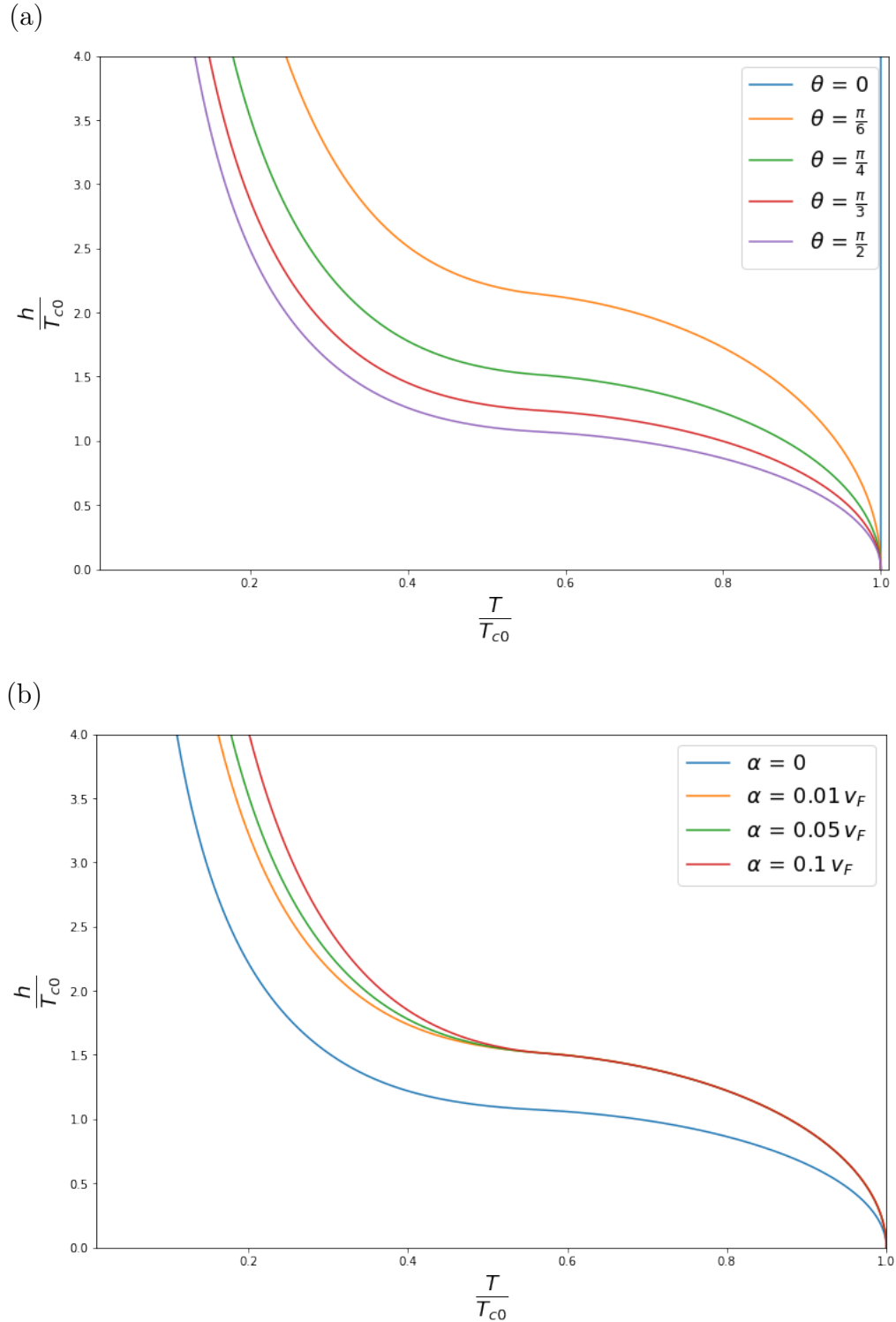


FIGURE 4.4 –  $(h, T)$ -phase diagrams for a one-dimensional superconductor with  $\mu = 10^3 T_{c0}$ . (a) Transition lines between the normal and the superconducting states in the presence of spin-orbit interaction  $\alpha = 0.05 v_F$  ( $\alpha p_F = 100 T_{c0}$ ), for different orientations of the Zeeman field;  $h = |\vec{h}|$  represents the modulus of the field, whereas  $\theta$  corresponds to the angle between  $\vec{h}$  and the wire. (b) Phase diagram for different values of the spin-orbit coupling constant :  $\alpha = 0$ ,  $\alpha = 0.01 v_F$  ( $\alpha p_F = 20 T_{c0}$ ),  $\alpha = 0.05 v_F$  ( $\alpha p_F = 100 T_{c0}$ ) and  $\alpha = 0.1 v_F$  ( $\alpha p_F = 200 T_{c0}$ ). The Zeeman field is taken such that  $h_x = h_z$  ( $\theta = \pi/4$ ).

## 4.4 Conclusion

In this chapter, we explored several effects related to the interplay between superconductivity and spin-dependent fields. Two systems were studied : A superconducting wire where both spin-orbit and Zeeman fields coexist (Fig. 4.1), and a double wire system in which superconducting pairing and spin-dependent fields are spatially separated (Fig. 4.2).

We first investigated the appearance of anomalous charge currents within the SU(2) covariant formulation, and determined the leading order contributions to  $j$  in the SOC and Zeeman field, in terms of the magnetic and electric SU(2) fields. In the case of a single wire we confirmed that a finite anomalous current can only appear when the Zeeman field has a component parallel and one orthogonal to the SOC [11, 48]. In the case of the two wires system, there is a finite SU(2) magnetic field and we predicted that a Zeeman field parallel to the spin-orbit field is sufficient to induce an anomalous current.

In Sec. 4.2, we derived the self-consistency equation for both setups in the presence of weak SOC  $\alpha p_F \ll T_c$ , using the Green's function formalism introduced in Chapter 3. Because of the presence of SOC, the integral in Eq. (4.14) has to be calculated with certain care by expanding the Green's function over the Zeeman field and SOC. For the one wire system, we found that the wave-vector  $q$  was finite only if both components of the Zeeman field, parallel and orthogonal to the SOC, were finite, thus involving an inhomogeneous superconducting phase for each temperature  $T < T_{c0}$ . In the case of the two wire setup, the parallel component of the field is sufficient to have a finite  $q$ .

In addition we computed the expression of the anomalous charge current for both systems and found that the ground-state corresponds in fact to a zero-current state, where the anomalous contribution is compensated by the contribution from the superconducting wave vector. However, if we impose  $q = 0$ , the anomalous charge current is finite and we obtain the results predicted in Sec. 4.1 by simple symmetry arguments. In the double wire system, the total zero-current state consists of two opposite currents flowing in each of the wires.

Sec. 4.3 was devoted to the self-consistency study of the single wire system in the presence of strong SOC  $\alpha p_F \gg T_c$ . To this purpose, it was convenient to introduce the helical basis. We showed that when the ratio  $\alpha p_F/h$  increases, superconducting correlations change from interband to intraband, which was also demonstrated in two dimensions in [9]. Thus, neglecting interband pairing, we derived the self-consistency relation, which allowed to obtain the  $(h_x, h_z, T)$ -phase diagram for different orientations of the Zeeman field and several values of the spin-orbit constant. We highlighted the anisotropy caused by SOC and showed that large values of  $\alpha$  and the ratio  $h_x/h_z$  allows for a more robust superconducting state. Moreover, we showed that when the spin-orbit and Zeeman fields are purely parallel, we recover the FFLO phase diagram, which can be explained by the fact that SOC can be gauged out.

In the next chapter, we investigate another effect resulting from the interplay between superconductivity and spin-dependent fields : We show that a skyrmion proximity coupled to a 2D superconductor can generate a superconducting vortex in the absence of external magnetic field.

# Chapter 5

## Generation of a superconducting vortex via Néel skyrmions

**S**UPERCONDUCTOR-FERROMAGNET HETEROSTRUCTURES [104, 105, 106, 107] in the presence of spin-orbit and exchange interactions are attracting great interest due to the possible realization of topological qubits based on Majorana fermions [77, 78, 79, 108, 109, 110, 111, 112] and the fact that such systems display unconventional magnetoelectric effects [11, 12, 14, 49, 97, 101, 113, 114, 115, 116, 117, 118, 119, 120, 121]. Similarly to the 1D systems studied in Chapter 4, the interplay between spin-orbit coupling and a homogeneous Zeeman or exchange field may lead to spontaneous supercurrents and hybrid structures.

From a  $SU(2)$ -covariant formulation of spin dependent fields, it is possible to show that a spin-orbit coupling and homogeneous Zeeman field is equivalent to an inhomogeneous magnetic texture that, in combination with superconducting correlations, may support spontaneous currents under certain symmetry conditions [12, 52, 122]. In this chapter, we investigate such a 2D heterostructure, namely a type-II superconducting layer proximity coupled to a ferromagnet hosting a Néel skyrmion. We show that the magnetoelectric effect induced by the skyrmion in the presence of a sufficiently strong spin-orbit interaction may lead to the nucleation of a vortex in the superconductor, without any external magnetic field.

First, we briefly present the two types of vortices involved in this problem, namely magnetic skyrmions and Abrikosov superconducting vortices. After a short description of the main properties of skyrmions, focusing more specifically on the case of a Néel skyrmion in a ferromagnetic layer, we discuss the structure of vortices in a thin superconducting film, which allows to introduce the method used next to study the nucleation of a vortex via Néel skyrmions. In a second part, we present the setup investigated in this chapter, namely a superconducting layer in contact with a Néel skyrmion, and derive the free energy describing the system. Then, we compute the magnetic field induced by the skyrmion, and show that its component normal to the layer can induce a vortex in the superconducting film. To this purpose, we minimize the free energy and obtain the condition which must be fulfilled for the vortex nucleation. We also show that for a sufficiently strong spin-orbit interaction, it is possible to stabilize a multiquanta vortex. Finally, we compute the magnetic field and current distributions in the superconducting layer in the presence of the vortex.

## 5.1 Two types of vortices : Magnetic skyrmions and Abrikosov superconducting vortices

In this section, we first give a brief overview of the physics of magnetic skyrmions, presenting in particular the case of a Néel skyrmion in a ferromagnetic layer. Then, we introduce the problem of a vortex in a superconducting thin film and from the expression of the free energy of the system, we compute the magnetic field and current distributions in the layer.

### 5.1.1 Néel skyrmion in a ferromagnetic layer

Although they were originally proposed to explain hadrons in nuclear physics [123], skyrmions turned out to be relevant in condensed matter physics. These inhomogeneous magnetic structures have attracted great interest because of their nanoscale dimension (1 - 100 nm), topological robustness and the low current density needed to move them. Such features make them good candidates as information carriers in future memory devices [124, 125, 126, 127, 128]. Moreover, it has been shown that skyrmions could be stabilized when proximity coupled to an s-wave superconductor [129, 130]. In this case, intriguing phenomena can be observed : spontaneous current generation [131], Majorana bound states [132, 133], Weyl points [134] or Yu-Shiba-Rusinov-like states [135].

Such structures, which can be seen as spin vortices, are characterized by the following spin profile [136] :

$$\vec{S}(\vec{r}) = (\cos \Phi(\theta) \sin \Theta(r), \sin \Phi(\theta) \sin \Theta(r), \cos \Theta(r)) , \quad (5.1)$$

where  $\vec{r} = (r \cos \theta, r \sin \theta)$  are the polar coordinates,  $\Theta(r)$  describes the boundary conditions and  $\Phi(\theta) = m\theta + \gamma$  encodes the topological properties of the skyrmion,  $m$  and  $\gamma$  being respectively the vorticity and the helicity. Those topological numbers characterize two kinds of magnetic skyrmions : Spiral (or Bloch) skyrmions, for which  $m = 1$  and  $\gamma = \pm \pi/2$ , and hedgehog (or Néel) skyrmions reading  $m = 1$  and  $\gamma = 0$  or  $\pi$ . These two possible structures are illustrated in Fig. 5.1. Notice that  $m = -1$  corresponds to anti-skyrmions.

Specifically in this chapter, we are interested in the case of a ferromagnet of thickness  $d_F$  hosting a Néel skyrmion (Fig. 5.3). From Eq. (5.1), the Néel skyrmion, with topological numbers  $m = 1$  and  $\gamma = 0$ , is characterized by the following spin profile :

$$\vec{S}(\vec{r}) = \eta \sin \Theta(r) \vec{e}_r + \cos \Theta(r) \vec{e}_z, \quad (5.2)$$

where  $\vec{e}_r$  is the radial unit vector and  $\vec{e}_z$  the unit vector normal to the layer. The profile function  $\Theta(r)$  must obey the boundary conditions  $\Theta(0) = \pi$  and  $\Theta(\infty) = 0$ . For the analytical calculations below, we assume that  $\Theta(r) = \pi(1 - r/R)$  for  $r < R$ , and otherwise 0, where  $R$  denotes the radius of the skyrmion. The constant  $\eta = \pm 1$  describes the skyrmion winding.

In the following we present the other physical object involved in our problem, namely a vortex in a superconducting thin layer.

### 5.1.2 Superconducting vortices in a thin film

When an external magnetic field  $\vec{B}$  is applied on a type-II superconductor such that  $H_{c1} < \mu_B B < H_{c2}$  where  $H_{c1}$  ( $H_{c2}$ ) is the lower (upper) critical field, a new

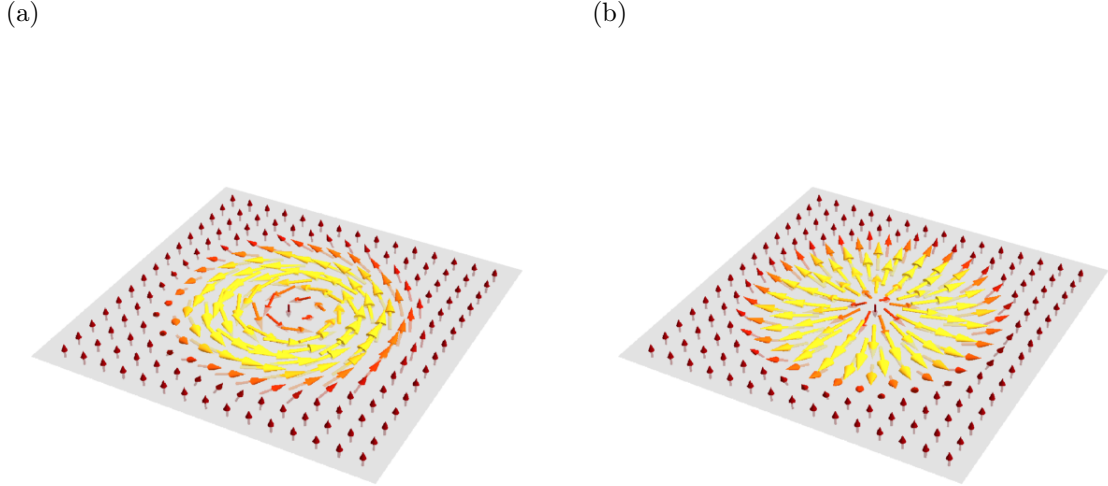


FIGURE 5.1 – (a) A Bloch skyrmion ( $\gamma = \pi/2$ ). (b) A Néel skyrmion ( $\gamma = 0$ ).

state called the mixed (or Shubnikov) state appears (see Chapter 2). In this case, the magnetic field screening decreases and the field penetrates partially the material through spatially separated tubes of magnetic flux, the so-called Abrikosov vortices [16].

In this section, we consider the particular case of a magnetic field applied normal to a superconducting thin film of thickness  $d_s$ , characterized by the coherence length  $\xi$  and the London penetration length  $\lambda \gg d_s$ . The magnetic field induces currents in the superconducting layer, leading to the appearance of a hard core vortex of radius  $\xi$ . Assuming that the superconductivity is well developed, *i.e.*  $T \ll T_c$ , we first derive the expression of the free energy using the London approach, which assumes that the current generated does not modify the modulus of the superconducting order parameter [39]. This is always the case for Abrikosov vortices, except the narrow core region. Then, we compute the expressions of the current and magnetic field distributions in the superconducting layer.

### Free energy of the system

The free energy of the superconducting layer can be written as

$$F = F_0 + F_{sc} + F_{mag} , \quad (5.3)$$

where  $F_0$  is the free energy in the absence of superconductivity and magnetic texture, and  $F_{sc}$  is the kinetic term related to the superconducting current energy, which reads :

$$F_{sc} = \int \frac{1}{2} m n_s v_s^2(\vec{r}, z) d^2\vec{r} dz , \quad (5.4)$$

where  $n_s$  and  $\vec{v}_s$  are respectively the density and the velocity of the superconducting electrons. Using the expression of  $\vec{v}_s$  defined in Chapter 2 Eq. (2.6) in the context of the Ginzburg-Landau theory, which can be transposed to the London approximation

by writing the superconducting order parameter  $\Psi$  such that  $\Psi = \Psi_0 e^{i\varphi}$  where  $\Psi_0$  is a constant and  $n_s = \Psi_0^2/2$ , and assuming that the density of superconducting current energy is nearly constant through the width  $d_S \ll \lambda$ , we obtain the following expression for  $F_{sc}$  :

$$F_{sc} = \int \frac{1}{2\mu_0 \lambda_{\text{eff}}} \left[ \vec{\phi}(\vec{r}) - \vec{A}(\vec{r}) \right]^2 d^2\vec{r}, \quad (5.5)$$

where  $\lambda_{\text{eff}} = \lambda^2/d_S$  is the effective screening length for the superconductor,  $\vec{\phi}$  is the gradient of the local superconducting phase (multiplied by  $\hbar/2e$ ), and  $\vec{A}(\vec{r})$  is the vector potential averaged over the thickness of the layer. In the presence of a vortex, the expression for the vector  $\vec{\phi}$  can be obtained from the London equation as [39] :

$$\vec{\phi}(r) = \frac{\Phi_0}{2\pi r} \vec{e}_\theta, \quad (5.6)$$

where  $\vec{e}_\theta$  is the unit orthoradial vector.

Finally, the last component  $F_{\text{mag}}$  of the free energy Eq. (5.3) represents the energy of the magnetic field  $\vec{B} = \vec{\nabla} \times \vec{A}$  :

$$F_{\text{mag}} = \int \frac{\vec{B}^2(\vec{r}, z)}{2\mu_0} d^2\vec{r} dz. \quad (5.7)$$

In order to compute the superconducting current density  $\vec{J} = -\partial f / \partial \vec{A}$  in the thin film, where  $f$  is the free energy density in the superconducting layer such that  $F = \int f d^2\vec{r}$ , it is necessary to derive the expression of the potential vector  $\vec{A}$ . This is the subject of the next section.

### Expression of the vector potential

Using the Maxwell-Ampere equation in the London gauge,  $\mu_0 \vec{j} = \vec{\nabla} \times \vec{B} = -\Delta \vec{A}$ , and the expression of the current density for  $d_S \ll \lambda$  in the plane  $z = 0$ , namely :

$$\vec{j} = -\frac{\partial f}{\partial \vec{A}} \delta(z) = \frac{1}{\mu_0 \lambda_{\text{eff}}} \left[ \vec{\phi}(\vec{r}) - \vec{A}(\vec{r}) \right] \delta(z), \quad (5.8)$$

it is possible to derive a differential equation for the vector potential  $\vec{A}$  :

$$-\Delta \vec{A}(\vec{r}, z) + \frac{1}{\lambda_{\text{eff}}} \vec{A}(\vec{r}) \delta(z) = \frac{1}{\lambda_{\text{eff}}} \vec{\phi}(\vec{r}) \delta(z). \quad (5.9)$$

To solve this equation and obtain the expression of  $\vec{A}$ , we work in Fourier space. To this purpose, we introduce the following three and two-dimensional Fourier transforms :

$$\vec{A}_{kl} = \int \vec{A}(\vec{r}, z) e^{i(\vec{k}\cdot\vec{r}+lz)} d^2\vec{r} dz; \quad (5.10)$$

$$\vec{A}_k = \frac{1}{2\pi} \int \vec{A}_{kl} dl = \int \vec{A}(\vec{r}) e^{i\vec{k}\cdot\vec{r}} d^2\vec{r}; \quad (5.11)$$

$$\vec{\phi}_k = \int \vec{\phi}(r) e^{i\vec{k}\cdot\vec{r}} d^2\vec{r} = i \frac{\Phi_0}{k} \vec{e}_\perp, \quad (5.12)$$

where the unit vector  $\vec{e}_\perp$  is represented in Fig. 5.2.

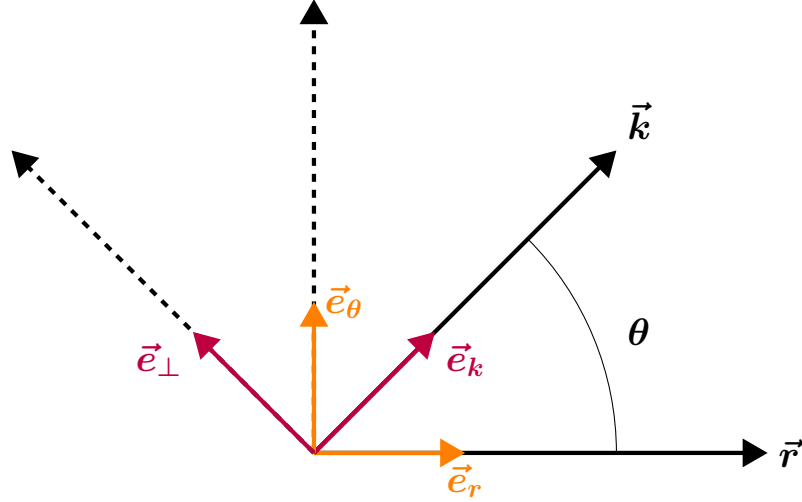


FIGURE 5.2 – The sets of coordinates  $(\vec{e}_r, \vec{e}_\theta)$  and  $(\vec{e}_k, \vec{e}_\perp)$ , respectively corresponding to the real space and the Fourier space.

Then, the Fourier transform of Eq. (5.9) is obtained from Eqs. (5.10 - 5.12), leading to the following equation :

$$\vec{A}_{kl} = \frac{1}{\lambda_{\text{eff}}} \frac{\vec{\phi}_k - \vec{A}_k}{k^2 + l^2}. \quad (5.13)$$

Therefore, the expression of  $\vec{A}_k$  can be obtained by performing the integration of Eq. (5.13) over  $l$  using Eq. (5.11) :

$$\vec{A}_k = \frac{\vec{\phi}_k}{1 + 2k\lambda_{\text{eff}}}. \quad (5.14)$$

It is now possible from Eq. (5.14) to derive the expression of the current density in the superconducting layer, as done in the following.

### Current distribution in the superconducting layer

The current distribution in the superconducting layer may be obtained from the free energy density<sup>1</sup> :

$$\vec{J}_v(\vec{r}) = -\frac{\partial f}{\partial \vec{A}} = \frac{1}{\mu_0 \lambda_{\text{eff}}} \left[ \vec{\phi}(\vec{r}) - \vec{A}(\vec{r}) \right]. \quad (5.15)$$

In the Fourier space and after replacing  $\vec{A}_k$  by its expression using Eq. (5.14), this equation becomes :

$$\vec{J}_k^v = \frac{2i}{1 + 2k\lambda_{\text{eff}}} \frac{\Phi_0}{\mu_0} \vec{e}_\perp. \quad (5.16)$$

The current density in position space may be recovered by performing the inverse Fourier transform of Eq. (5.16), taking into account that  $\vec{e}_\perp = -\sin\theta \vec{e}_r + \cos\theta \vec{e}_\theta$ , as illustrated in Fig. 5.2. In the limit  $\xi \ll r \ll \lambda_{\text{eff}}$ , it reads :

$$\vec{J}_v(\vec{r}) = \frac{\Phi_0}{2\pi\mu_0\lambda_{\text{eff}}r} \vec{e}_\theta, \quad (5.17)$$

1. The index v which appears in the current and magnetic field distributions will be useful in the next sections to make the difference between the contributions coming from the vortex or the skyrmion, labelled s.

Hence, we have shown that supercurrents induced by the normal magnetic field  $\vec{B}$  are present around the vortex, and decrease with distance. Next, we compute the density of magnetic field in the superconducting layer.

### Magnetic field distribution in the superconducting layer

The magnetic field distribution can be calculated using the relation  $\vec{B} = \vec{\nabla} \times \vec{A}$ , which reads in Fourier space :

$$\vec{B}_{kl}^v = -i k \left( \vec{e}_k \times \vec{A}_{kl} \right) - i l \left( \vec{e}_z \times \vec{A}_{kl} \right) , \quad (5.18)$$

which gives, after replacing  $\vec{A}_{kl}$  by its expression, derived from Eqs. (5.13) and (5.14) :

$$\vec{B}_{kl}^v = \frac{2}{1 + 2 k \lambda_{\text{eff}}} \frac{\Phi_0}{k^2 + l^2} (k \vec{e}_z - l \vec{e}_k) , \quad (5.19)$$

In order to obtain the magnetic field distribution in the superconducting layer, we integrate Eq. (5.19) over  $l$ . Since the external magnetic field is applied normal to the layer, only the normal component of  $\vec{B}_k^v$  is finite :

$$\vec{B}_k^v = \frac{\Phi_0}{1 + 2 k \lambda_{\text{eff}}} \vec{e}_z . \quad (5.20)$$

Finally, the magnetic field distribution in the thin film is obtained from the inverse Fourier transform of  $\vec{B}_k^v$  and reads in the limit  $\xi \ll r \ll \lambda_{\text{eff}}$  :

$$\vec{B}_v(r) = \frac{\Phi_0}{4 \pi \lambda_{\text{eff}} r} \vec{e}_z . \quad (5.21)$$

Therefore, from the free energy expressed in London approximation, we have derived the magnetic field and current distributions in a superconducting layer hosting a vortex.

In the next section, we investigate the formation of a composite topological excitation between a magnetic skyrmion and a superconducting vortex in a ferromagnet/superconductor (F-S) bilayer with Rashba spin-orbit coupling, in the absence of external magnetic field. In contrast to Ref. [137], the superconducting vortex is initially absent. We show that the generation of a vortex may occur via the magnetoelectric effect induced by the skyrmion in the presence of a sufficiently strong spin-orbit coupling. By evaluating the free energy of the system, we derive the conditions required for the creation of this vortex, and compute the current and magnetic field distributions in the superconductor.

## 5.2 Superconducting layer in contact with a Néel skyrmion : Free energy

We consider a type-II superconducting thin film of thickness  $d_S$ , characterized by the coherence length  $\xi$  and the London penetration length  $\lambda \gg d_S$ , as described in Sec. 5.1.2. The superconductor is in contact with a ferromagnet of thickness  $d_F$  hosting a Néel skyrmion of radius  $R$ , characterized by the spin profile Eq. (5.2), as illustrated in Fig. 5.3. We assume that a two-dimensional spin-orbit interaction is present in the ferromagnetic layer and described by the Rashba constant  $\alpha_R$ .

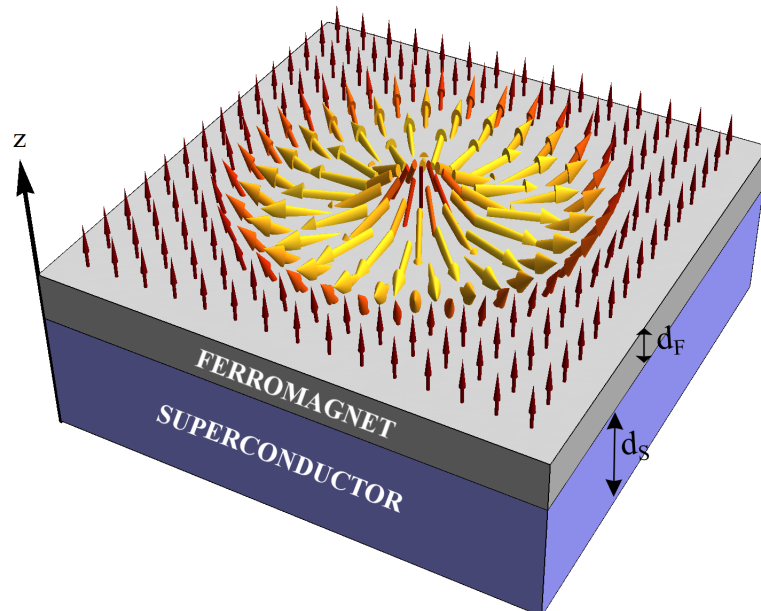


FIGURE 5.3 – A thin superconducting film proximity-coupled to a ferromagnetic layer hosting a Néel skyrmion. The F layer has thickness  $d_F$  and the S layer  $d_S$ .

In principle both the direct electromagnetic coupling between the skyrmion and the superconductor [138], and the magnetic proximity effect may result in the nucleation of a vortex. For a uniform ferromagnetic layer in contact with a superconductor, it is possible to avoid vortex formation via the standard electromagnetic interaction by designing the F and S layers such that  $\mu_0 M \ll H_{c1} d_S/d_F$ , which may be easily fulfilled if the ferromagnetic layer is much thinner than the superconducting one. Hence in this work, we neglect the direct electromagnetic effect and we only focus on the proximity effect by assuming that the exchange field and spin-orbit interaction penetrate the superconductor over the atomic thickness  $a$ , where  $a \ll d_S$ , as illustrated in Fig. 5.4. It induces a spin polarization in the superconductor, which gives rise to a supercurrent at the interface between F and S, and creates a magnetic field. If this magnetic field is sufficiently strong, a vortex is then generated below the skyrmion, without external magnetic field.

Let us consider temperatures for which superconductivity is well developed, i.e.,  $T \ll T_c$ . As we already did in Sec. 5.1.2 for vortices in a thin superconducting film, we derive the free energy of the system within the London approach, which assumes that the modulus of the superconducting order parameter is not modified by the current generated. The criterion of applicability of this formalism is well known (see for example Ref. [39]): the current density should be much smaller than the critical current density  $j_c \propto \Phi_0/\mu_0 \lambda^2 \xi$ . The computation of the current (see Sec. 5.4.2) shows that this approach is completely justified to describe the vortex generation by the skyrmion while  $R \gg \xi$ .

The free energy of the F/S bilayer can be written as

$$F = F_0 + F_{sc} + F_{mag} + F_L, \quad (5.22)$$

where  $F_0$  is the free energy in the absence of superconductivity and magnetic texture. In the following, we omit this term, which does not influence the generation of the vortex. The superconducting current energy  $F_{sc}$  and the energy of the magnetic field  $F_{mag}$  are given by Eqs. (5.5) and (5.7).

The last contribution to the free energy,  $F_L$  in Eq. (5.22), corresponds to the coupling energy between the superconductor and the magnetic order induced by the skyrmion. By proximity effect, the interplay between the exchange field and the Rashba spin-orbit interaction in the ferromagnetic layer induces a spin polarization in the superconducting film. This may give rise for example to a spontaneous current in the bulk superconductor near the interface to F, in the absence of an external magnetic field [49, 72]. For  $T$  close to  $T_c$ , such an interaction is described by the Lifshitz invariant [5, 71, 139]. At low temperatures and for  $d_S \ll \lambda$ , one can consider that the spin-orbit interaction is averaged over  $d_S$ . In this case the energy  $F_L$  can be written as (see Appendix C.1):

$$F_L = \int \vec{\alpha}(r) \cdot [\vec{\phi}(\vec{r}) - \vec{A}(\vec{r})] d^2\vec{r}, \quad (5.23)$$

where  $\vec{\phi}$  is given by Eq. (5.6) and  $\vec{\alpha}(r) = \alpha(r) \vec{e}_\theta = \eta \alpha_0 \sin \Theta(r) \vec{e}_\theta$ . The expression of the constant  $\alpha_0$  is also derived in Appendix C.1 and incorporates the Rashba constant  $\alpha_R$ , the exchange energy  $h_{ex}$ , the thickness of the superconducting film  $d_S$  and the proximity length  $a$ :

$$\alpha_0 \approx \frac{1}{4 \mu_0 e \lambda_{eff}} \frac{a}{d_S} \frac{\alpha_R h_{ex}}{v_F^2}. \quad (5.24)$$

In order to derive the vortex nucleation condition and the magnetic field and current distributions in the superconducting layer, it is necessary to get the expression of the

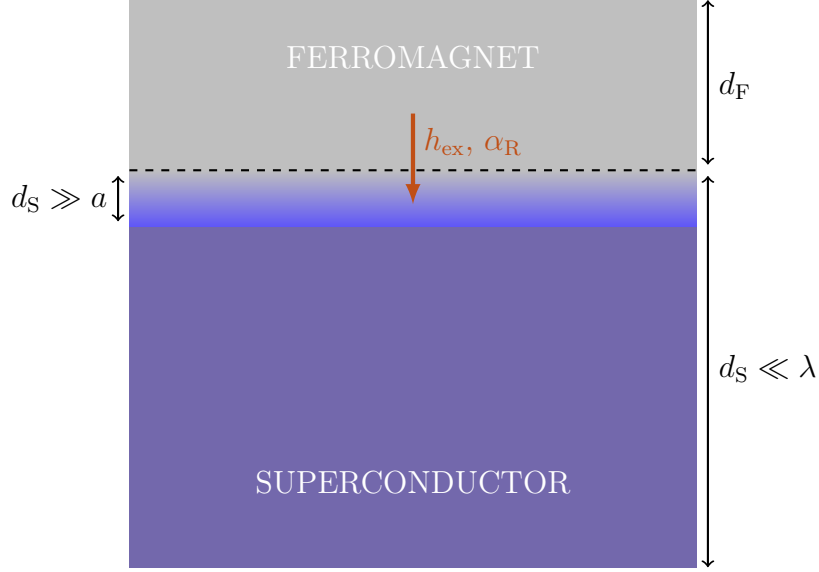


FIGURE 5.4 – By proximity effect, the exchange and spin-orbit interactions penetrate the superconductor over the atomic thickness  $a$ , generating a spin polarization which in turn may induce a supercurrent at the interface between the layers.

vector potential  $\vec{A}$ . Using the same method as in Sec. 5.1.2, we can derive a differential equation for  $\vec{A}$  from the Maxwell-Ampere equation and the current density for  $d_S \ll \lambda$  in the plane  $z = 0$  :

$$-\Delta \vec{A}(\vec{r}, z) + \frac{1}{\lambda_{\text{eff}}} \vec{A}(\vec{r}) \delta(z) = \frac{1}{\lambda_{\text{eff}}} \vec{\phi}(\vec{r}) \delta(z) + \mu_0 \vec{\alpha}(r) \delta(z). \quad (5.25)$$

This equation can be solved exactly in Fourier space. To this purpose, we use the Fourier transforms defined in Eqs. (5.10 - 5.12) and introduce the following one, acting on  $\vec{\alpha}(\vec{r})$  :

$$\vec{\alpha}_k = \int \vec{\alpha}(r) e^{i\vec{k}\cdot\vec{r}} d^2\vec{r} = i \alpha_k \vec{e}_\perp, \quad (5.26)$$

such that  $\alpha_k = 2\pi \int_0^\infty r \alpha(r) J_1(kr) dr$  where  $J_1(kr)$  is a Bessel function of first kind.

Solving Eq. (5.25) in Fourier space, we obtain the following expressions for  $\vec{A}_{kl}$  and  $\vec{A}_k$ , which are respectively the Fourier transforms of  $\vec{A}(\vec{r}, z)$  and  $\vec{A}(\vec{r})$  :

$$\vec{A}_{kl} = \frac{2k}{k^2 + l^2} \frac{1}{1 + 2k\lambda_{\text{eff}}} \left( \vec{\phi}_k + \mu_0 \lambda_{\text{eff}} \vec{\alpha}_k \right); \quad (5.27)$$

$$\vec{A}_k = \frac{1}{1 + 2k\lambda_{\text{eff}}} \left( \vec{\phi}_k + \mu_0 \lambda_{\text{eff}} \vec{\alpha}_k \right). \quad (5.28)$$

These expressions of  $\vec{A}_{kl}$  and  $\vec{A}_k$ , Eqs. (5.27) and (5.28), are similar to the ones obtained for the isolated superconducting layer (Eqs. 5.14 and 5.13), but enlarged with a term induced by the presence of the skyrmion, proportional to  $\vec{\alpha}_k$ . In the next section, we focus more particularly on these terms, and compute the expression of the magnetic field stemming from the Néel skyrmion. Then, by comparing the free energy Eq. (5.22) with and without vortex, we derive the condition for the vortex nucleation, and study the possibility that it carries more than one quantum of flux.

## 5.3 Creation of a superconducting vortex

This section is devoted to investigate the condition to nucleate a vortex in the superconducting layer. To this purpose, we first assume that there is no vortex, and compute the magnetic field distribution coming from the skyrmion.

### 5.3.1 Magnetic field induced by the skyrmion

Because of the spontaneous current generated by the skyrmion in the superconducting film, a magnetic field is created. We first consider that there is no vortex. In this case, the term proportional to  $\vec{\phi}_k$  in Eq. (5.28) is absent and we can derive the expression of the magnetic field distribution in the superconducting layer. Similarly to Eq. (5.18), the magnetic field stemming from the skyrmion,  $\vec{B}_{kl}^s$ , reads in Fourier space :

$$\vec{B}_{kl}^s = \frac{2k\lambda_{\text{eff}}}{1+2k\lambda_{\text{eff}}} \frac{1}{k^2+l^2} \mu_0 \alpha_k (k\vec{e}_z - l\vec{e}_k) , \quad (5.29)$$

Following the method introduced in Sec. 5.1.2, the magnetic field distribution in the superconducting layer is obtained from Eq. (5.29) after integrating over  $l$  and performing the inverse Fourier transform. Notice that only the normal component to the layer survives the  $l$  integration. Considering that the skyrmion is small compared to  $\lambda_{\text{eff}}$  and focusing on small distances  $r$  from the center of the skyrmion ( $r \ll \lambda_{\text{eff}}$ ), we finally obtain the normal component of the magnetic field distribution in the superconducting layer :

$$B_s(r) = \frac{1}{2} \eta \mu_0 \alpha_0 \int k \Gamma(k) J_0(kr) dk , \quad (5.30)$$

where  $\Gamma(k) = \int_0^R r \sin(\pi \frac{r}{R}) J_1(kr) dr$  and  $J_0(kr)$ ,  $J_1(kr)$  are Bessel functions of first kind. This field distribution is represented by the blue line in Fig. 5.5. As expected, outside of the skyrmion  $B_s(r)$  decreases and vanishes very fast. Moreover, one can check that the magnetic flux associated to  $B_s(r)$  is equal to zero.

Because of the presence of this magnetic field normal to the layer, a vortex may appear in the superconducting layer. Next, we investigate this vortex nucleation by minimization of the free energy.

### 5.3.2 Superconducting vortex generation

The condition for the superconducting vortex creation can be derived by comparing the free energy of the system with and without a vortex. We replace  $\vec{A}$  by its expression, (Eqs. 5.27 and 5.28), into the kinetic, magnetic and magnetoelectric terms Eqs. (5.5, 5.7 and 5.23) to the free energy. The resulting  $F$  can be written as a sum of three terms, derived in Appendix C.2, Eq. (C.17) :

$$F = F_v + F_s + F_{\text{int}} . \quad (5.31)$$

The first one, proportional to  $\Phi_0^2$ , describes the self-energy of the vortex. The second term, proportional to  $\alpha_R^2$ , describes the energy of the current induced by the skyrmion, whereas the third term, proportional to  $\Phi_0 \alpha_R$ , corresponds to the interaction energy between the vortex and such currents.

In the limit  $\xi \ll r \ll \lambda_{\text{eff}}$ , we can write the self-energy of the vortex in the following way :

$$F_v = \frac{1}{\pi \mu_0 \lambda_{\text{eff}}} \left( \frac{\Phi_0}{2} \right)^2 \ln \left( 2 \frac{\lambda_{\text{eff}}}{\xi} \right). \quad (5.32)$$

Moreover, by assuming  $R \ll \lambda_{\text{eff}}$ , the current energy and the interaction term read :

$$F_s = -\frac{\mu_0}{8\pi} \int \alpha_k^2 dk; \quad (5.33)$$

$$F_{\text{int}} = 2\eta \frac{\Phi_0 \alpha_0}{\pi} R. \quad (5.34)$$

The difference of free energy,  $\Delta F = F - F_s$ , between the states with and without vortex reads after replacing  $\alpha_0$  by its expression (Eq. 5.24) :

$$\Delta F = \frac{\Phi_0^2}{2\pi^2 \mu_0 \lambda_{\text{eff}}} \left[ \frac{\pi}{2} \ln \left( 2 \frac{\lambda_{\text{eff}}}{\xi} \right) + 0.180 \eta \frac{h_{\text{ex}}}{k_B T_c} \frac{a}{d_S} \frac{\alpha_R}{v_F} \frac{R}{\xi} \right], \quad (5.35)$$

where  $k_B$  is the Boltzmann constant,  $T_c$  is the critical temperature of the superconductor and the coherence length is given by  $\xi = 0.180 \hbar v_F / k_B T_c$ .

The condition for the vortex nucleation is determined by  $\Delta F < 0$ , which requires that  $\eta \alpha_R < 0$  : The vortex polarity is determined by the sign of  $\eta$ , combined with the Rashba constant  $\alpha_R$ . In the opposite case, namely if  $\eta \alpha_R > 0$ , the appearance of the vortex is energetically not favorable. We thus consider  $\alpha_R > 0$ , which implies  $\eta = -1$ . Therefore, the vortex generation condition reads :

$$\frac{h_{\text{eff}}}{k_B T_c} \frac{\alpha_R}{v_F} \frac{R}{\xi} > \frac{\pi}{0.36} \ln \left( 2 \frac{\lambda_{\text{eff}}}{\xi} \right), \quad (5.36)$$

where  $h_{\text{eff}} = h_{\text{ex}} a / d_S$  is the average effective exchange energy, with  $a \ll d$ .

The condition Eq.(5.36) gives the features of the ferromagnetic layer required to induce a vortex inside the superconducting film without any external magnetic field. Qualitatively, this result shows that if  $\alpha_R$  or  $R$  increase, so does the magnetic field  $B_s$  (Eq. 5.30), thereby favoring the appearance of the vortex.

Next, we discuss the possibility of nucleating a vortex carrying more than one superconducting flux quantum  $\Phi_0$ , which was not considered until now.

### 5.3.3 Multiquanta vortices

The free energy  $F_n$  in the presence of a  $n$ -quanta vortex, with  $n > 1$ , is given by :

$$F_n = n^2 F_v + F_s + n F_{\text{int}}. \quad (5.37)$$

The optimal value of  $n$  can be estimated by minimizing  $F_n$  with respect to  $n$  :

$$n_{\text{op}} \approx -\frac{F_{\text{int}}}{2F_v} = \frac{\pi}{0.72 \ln(2 \frac{\lambda_{\text{eff}}}{\xi})} \frac{h_{\text{eff}}}{k_B T_c} \frac{\alpha_R}{v_F} \frac{R}{\xi}. \quad (5.38)$$

Therefore, upon raising the Rashba coupling and/or the radius of the skyrmion, it is possible to stabilize a multiquanta vortex carrying the integer value of  $n_{\text{op}}$  superconducting flux quanta.

In the following, we investigate the magnetic field and current distributions in the superconducting layer. For simplicity, we assume that the spin-orbit interaction is too weak to have a vortex with vorticity larger than 1.

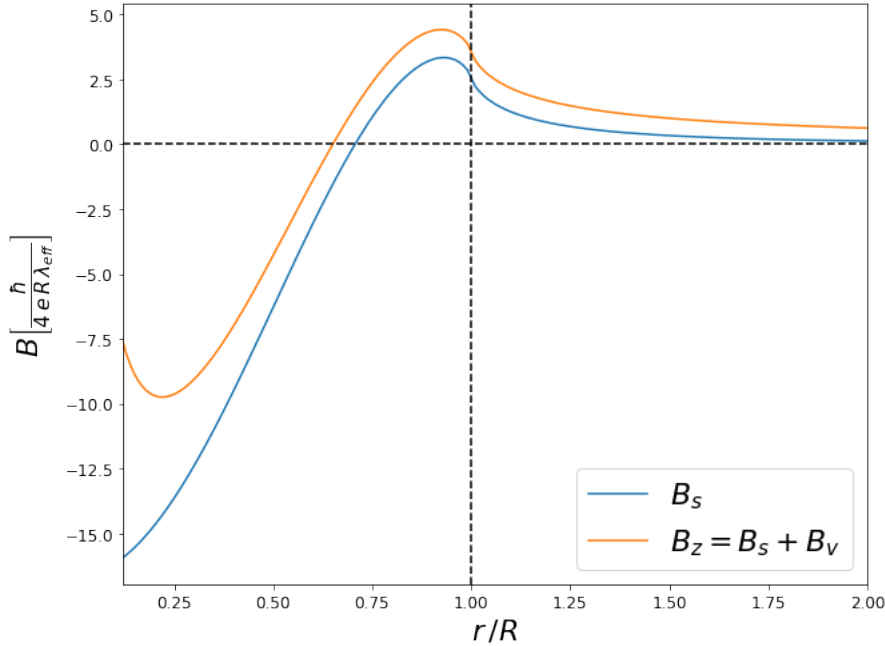


FIGURE 5.5 – Magnetic field distribution in the superconducting layer. The vortex nucleation condition for a vortex with vorticity 1 is fulfilled :  $R = 50 \xi$ ,  $\alpha_R = 0.1 v_F$  and  $h_{\text{eff}} = 20 k_B T_c$ . The blue line corresponds to the magnetic field distribution without vortex, whereas the orange one is in the presence of the vortex.

## 5.4 Magnetic field and current distributions

Here, we suppose that the vortex was nucleated in the superconducting layer, and that it carries only one quantum of flux. As it was shown in Sec. 5.1.2, the magnetic field and current distributions are modified by the vortex. We then derive these distributions and show how they compete with the magnetic field and current originating from the skyrmion.

### 5.4.1 Magnetic field distribution

The presence of the vortex modifies the magnetic field distribution. In addition to the component  $B_s$  (Eq. 5.30), stemming from the current induced by the skyrmion in the superconducting layer, there is a term originating from the vortex itself,  $B_v$ , determined in Sec. 5.1.2 (Eq. 5.21). The total magnetic field distribution normal to the layer can thus be written as

$$B_z(r) = B_s(r) + B_v(r) . \quad (5.39)$$

for  $\xi \ll r \ll \lambda_{\text{eff}}$ .

The magnetic field distribution  $B_z(r)$  is shown in Fig. 5.5 (orange line). It is assumed that the condition for the appearance of a vortex is fulfilled. As expected, both  $B_z$  and  $B_s$  follow the spin direction of the skyrmion, with a sinusoidal-like shape : it is negative near the center, and positive for  $r \gtrsim 0.65 R$ . At  $r = R$ , the amplitude of the magnetic field decreases away from the skyrmion. The component  $B_s$  tends to zero very fast, whereas  $B_z$  vanishes far from the center. It decreases slowly because of the presence of the vortex, whose component  $B_v$  is proportional to  $1/r$ .

Next, we investigate the current distribution in the superconducting layer.

## 5.4.2 Current distribution

As with the magnetic field distribution Eq. (5.39), the current  $\vec{J}$  in the superconducting layer can be written as the sum of two contributions : one induced directly by the skyrmion,  $\vec{J}_s$ , and a second stemming from the vortex,  $\vec{J}_v$ , which was derived in Sec. 5.1.2 (Eq. 5.17).

$$\vec{J}(r) = \vec{J}_s(r) + \vec{J}_v(r) , \quad (5.40)$$

where  $\vec{J}_s$  may be obtained by using the method introduced in Sec. 5.1.2 : We compute  $\vec{J}_v(\vec{r}) = -\partial f / \partial \vec{A}$ , where  $f$  is the density of free energy, in the absence of the vortex. Then, using the skyrmion part of the vector potential  $\vec{A}_k$  (Eq. 5.28), we derive the expression of the current density in Fourier space, which reads :

$$\vec{J}_k^s = i \frac{2 k \lambda_{\text{eff}}}{1 + 2 k \lambda_{\text{eff}}} \alpha_k \vec{e}_\perp . \quad (5.41)$$

The expression of  $\vec{J}_s$  is obtained after an inverse Fourier transform of Eq. (5.41). Under the same assumptions as before,  $\xi \ll r \ll \lambda_{\text{eff}}$  and  $R \ll \lambda_{\text{eff}}$ , it reads :

$$\vec{J}_s(r) = -\alpha_0 \int k \Gamma(k) J_1(k r) dk \vec{e}_\theta ; \quad (5.42)$$

The current lines in the film are shown in Fig. 5.6a. We used the same parameters as in (Fig. 5.5).

Around the vortex ( $r < 0.20 R$ ), the current is dominated by the contribution from the vortex and flows counterclockwise. As it can be seen in Fig. 5.6b, in this region the current is positive and decreases like  $1/r$ . For larger values of  $r$  within the skyrmion ( $0.20 R < r < 0.95 R$ ), the current distribution has a sinusoidal shape, and is dominated by the contribution from the skyrmion. In this region, the current loops are clockwise. Finally, for  $r > 0.95 R$ , the current is again dominated by the contribution from the vortex. It decreases slowly with distance, and tends to zero far from the skyrmion.

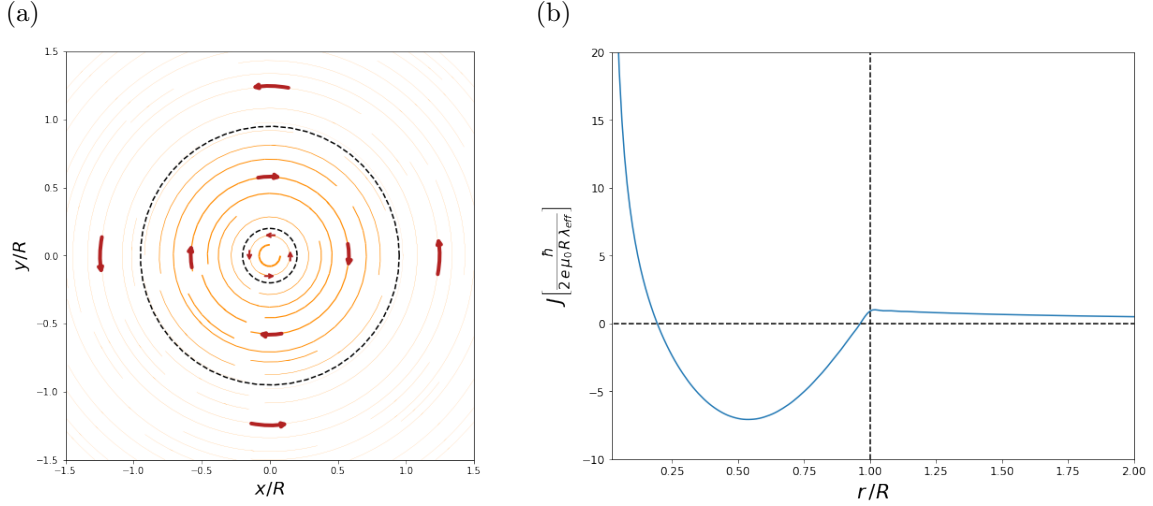


FIGURE 5.6 – (a) Current lines in the superconducting layer. The vortex nucleation condition for a vortex with vorticity 1 is fulfilled :  $R = 50 \xi$ ,  $\alpha_R = 0.1 v_F$  and  $h_{\text{eff}} = 20 k_B T_c$ . The dashed black lines represent the changes in the rotation direction of the current loops. The thickness of the lines represents the amplitude of the current. (b) Distribution of the current  $J$  in the superconducting layer.

## 5.5 Conclusion

In this chapter, we explored the magnetoelectric effects resulting from the interplay between a superconductor and a ferromagnetic layer hosting a Néel skyrmion. We assumed that the magnetization in the F layer was sufficiently weak to neglect the direct electromagnetic coupling, thus focusing only on the proximity effect between the layers. We showed that the magnetic texture of the skyrmion induces a current and a magnetic field in the superconducting layer, which may in turn lead to generate an Abrikosov vortex.

To this purpose, we derived the free energy of the system in the London approach. By minimization of this free energy, namely comparing the energy with and without vortex, we obtained the condition which must be fulfilled to generate a vortex in S : If the Rashba coupling exceeds a threshold value (given by Eq. 5.36), the skyrmion can nucleate a superconducting vortex by magnetoelectric proximity effect in the absence of an applied external field. Surprisingly, we also demonstrated that this vortex may carry more than one quantum of flux  $\Phi_0$  for a sufficiently strong spin-orbit interaction.

Finally, we investigated the magnetic field and current distributions in the superconducting layer. These distributions correspond in fact to the sum of two contributions, one stemming from the skyrmion, and the second coming from the vortex itself. We have emphasized the competition between them, which leads for example to several changes of the rotation direction of the current in the layer.

In the next chapter, we focus on another possible effect resulting from the interplay between superconductivity and spin-dependent fields : the appearance of Yu-Shiba-Rusinov bound states in the presence of paramagnetic impurities.

# Chapter 6

## Multiband superconductivity in the presence of magnetic impurities

**D**UE TO THEIR ANTAGONIST CHARACTERS, the coexistence between superconducting and magnetic orders has attracted numbers of investigations, leading for example to the prediction of the FFLO state introduced in Chapter 3. Another example of striking physics stemming from the interplay between magnetism and superconductivity is the effect of paramagnetic impurities on superconductivity. Such impurities break locally Cooper pairs, inducing bound states in the superconducting gap. First predicted in the late 1960's [27, 28, 29, 30], these so-called Yu-Shiba-Rusinov (YSR or Shiba) states were detected experimentally in 1997 thanks to the development of Scanning Tunneling Microscopy (STM) [31]. During the last decade, the interest on Shiba states was further enhanced by the discovery of Majorana zero modes in chains of magnetic atoms coupled to topological superconductors [18, 19, 20, 21, 22, 23, 24, 25, 26].

This chapter is motivated by a collaboration with the experimental group of José Ignacio Pascual from CIC-nanoGUNE. The focus of this collaboration is the study of the local spectral properties of the superconducting crystal  $\beta$ -Bi<sub>2</sub>Pd in the presence of Vanadium adatoms.  $\beta$ -Bi<sub>2</sub>Pd is known to display topologically protected surface states and suspected to host unconventional pairing [140, 141]. The recent experiments by J. Zaldívar and J. I. Pascual show an unexpected double period spatial oscillation of the LDOS at Shiba energy. The aim of this chapter is to provide simple effective models to identify the mechanisms at the origin of this double oscillation. Our simple models could be used to gain a first qualitative overview about the spectrum of multiband superconductors in the presence of magnetic impurities.

A possible approach to model electronic band structures is to use simulations based on tight-binding calculations. Although there are observations that point towards 2D surface bands (and even some bulk bands) involved in electron scattering of  $\beta$ -Bi<sub>2</sub>Pd [141], we have chosen to reduce the problem to a 1D system. Even though such a model will not give a complete description of the experiments, it provides a first fundamental understanding of the mechanisms at the origin of the spatial dependence of Shiba states. Specifically, our 1D models allow to answer two basic questions, namely whether a magnetic impurity coupled to a helical band may lead to Shiba spatial oscillations, and what is the minimal condition to observe a double period spatial oscillation of YSR states. To this purpose, the group of Alfredo Levy Yeyati from the Universidad Autónoma de Madrid, considered a 1D tight-binding model, which in the continuous limit can be represented by wires. In order to guide their simulations, we thus developed two effective 1D analytical models, which are presented in this chapter.

First, we briefly describe the main properties of YSR states in a superconducting wire in the presence of a magnetic impurity. From the Green's function of the system, we derive the energy of Shiba states and compute the non-polarized and spin-polarized local densities of states (LDOS) at Shiba energy. We highlight the presence of a spatial oscillation of the LDOS and the phase-shift between electron and hole components.

Then, after introducing the main experimental results obtained by J. Zaldívar and J. I. Pascual on  $\beta$ -Bi<sub>2</sub>Pd coupled to Vanadium adatoms, we develop a first effective model, made of a single superconducting wire with helical dispersion in order to reproduce the spin-polarization of  $\beta$ -Bi<sub>2</sub>Pd energy bands. We show that the Shiba states induced by a magnetic impurity do not produce any spatial oscillations of the non-polarized LDOS, thus failing to describe  $\beta$ -Bi<sub>2</sub>Pd.

The second model presented in this chapter is illustrated in Fig. 6.7. Two superconducting wires with quadratic dispersion are connected via a hopping term, and the magnetic impurity is coupled only to the upper wire. We demonstrate that the presence of the two wires is the minimal ingredient to obtain the double spatial oscillation of the LDOS at Shiba energy. In this case, the oscillation frequencies correspond respectively to the sum and difference of the Fermi momenta associated to each wire.

## 6.1 Introduction to Yu-Shiba-Rusinov bound states

Yu-Shiba-Rusinov bound states were predicted in the 1960's independently by three theoreticians, Luh Yu [27], Hiroyuki Shiba [28] and A. I. Rusinov [29, 30]. Their work focused on the effect of a single paramagnetic impurity embedded in an s-wave superconductor. Because of the Pauli paramagnetic pair-breaking effect presented in Chapter 3, the presence of such an impurity is detrimental to superconductivity. The interaction between the (classical) spin of the impurity and Cooper pairs leads to the appearance of a pair of bound states in the superconducting gap (Fig. 6.1) : These are the so-called YSR states [142, 143]. They are characterized by spatial oscillations of the LDOS at a specific energy, the Shiba energy, which allowed the first experimental detection of Shiba states in 1997 [31]. Yazdani et al. investigated the local density of states (LDOS) of a Niobium (Nb) crystal in the superconducting state (around 4 K), in the presence of single Manganese (Mn) and Gadolinium (Gd) adatoms. STM measurements revealed the presence of excitations in the superconducting gap, corresponding to the predicted Shiba states. Notice that the first observation of YSR states in two-dimensional superconductors was done very recently, in 2015 [144].

In this section, we derive the Shiba energy and the LDOS in the particular case of a 1D superconductor in the presence of a magnetic impurity.

### 6.1.1 Energy of the Shiba states

The Shiba energy at which YSR states appear can be obtained from the poles of the Green's function describing an s-wave superconductor in the presence of a magnetic impurity. To simplify the problem, we consider an infinite superconducting wire along the  $x$ -axis with a constant order parameter  $\Delta$  in the presence of a single localized magnetic impurity. We assume that the impurity interacts with the superconductor via a scalar potential  $V(x) = \vec{h} \cdot \vec{\sigma} \delta(x)$ , where  $\vec{h}$  is the exchange field of the impurity and  $\sigma_{x,y,z}$  are the Pauli matrices acting in spin space. In this case, the Green's function  $G$  of the impurity-superconductor system in position space is derived from the Dyson

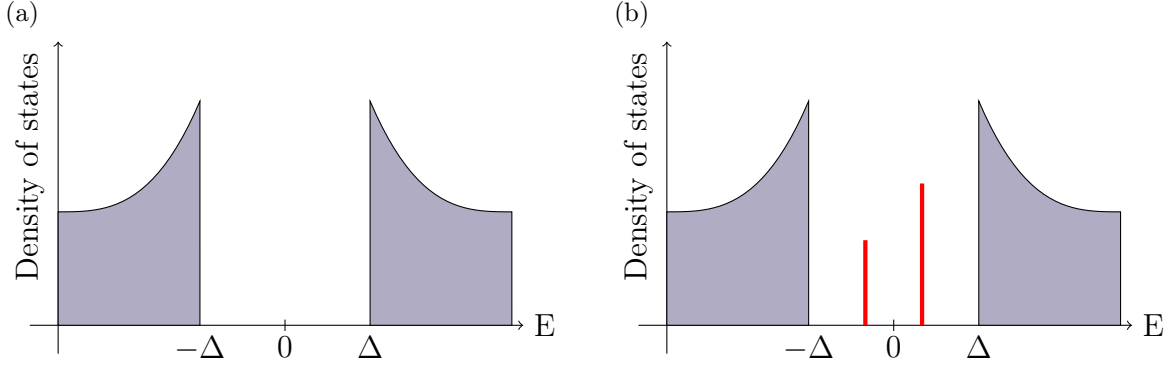


FIGURE 6.1 – In the absence of magnetic impurity, a superconductor is characterized by a gap at energy  $-\Delta < E < \Delta$  (left panel). In the presence of a single localized magnetic impurity (right panel), a pair of subgap bound states, the Shiba states, appears with opposite energies (red lines).

equation :

$$G(x', x) = G_0(x', x) + \int dy G_0(x', y) V(y) G(y, x), \quad (6.1)$$

where  $G_0$  is the Green's function of the superconductor in the absence of the impurity. We now explain how to obtain the expression of the local Green's function  $G(x, x)$ , which characterizes the system made by the impurity and the superconductor. After replacing  $V(y)$  by its expression, we can perform the integration and derive the general expression of  $G(x, x')$  :

$$G(x', x) = G_0(x', x) + G_0(x', 0) \vec{h} \cdot \vec{\sigma} G(0, x), \quad (6.2)$$

Taking  $x' = 0$  in Eq. (6.2), we obtain the expression of the Green's function  $G(0, x)$  :

$$G(0, x) = \left[ \mathbb{1} - G_0(0) \vec{h} \cdot \vec{\sigma} \right]^{-1} G_0(-x), \quad (6.3)$$

where we set  $G(0, 0) = G(0)$  and  $G(-x) = G(-x, 0)$ . Then, taking  $x' = x$  in Eq. (6.2) and replacing  $G(0, x)$  by its expression using Eq. (6.3), we obtain the general expression of the Green's function of the system :

$$G(x, x) = G_0(x, x) + G_0(x) \vec{h} \cdot \vec{\sigma} \left[ \mathbb{1} - G_0(0) \vec{h} \cdot \vec{\sigma} \right]^{-1} G_0(-x). \quad (6.4)$$

We are now able to extract the Shiba energy from Eq. (6.4). Moreover, we can notice that the poles of the Green's function  $G(x, x)$  are all contained in the term  $\left[ \mathbb{1} - G_0(0) \vec{h} \cdot \vec{\sigma} \right]^{-1}$ , and therefore we focus only on this term.

We first compute the Green's function  $G_0(0) = \int G_0(p) dp / 2\pi$ . In Nambu spin space, the Green's function  $G_0(p)$  describing the superconducting wire without impurity is obtained from the equation of motion  $(i\omega_n - \hat{h}_0) G_0 = \mathbb{1}$ , where the superconducting Hamiltonian operator is defined by

$$\hat{h}_0 = \xi \tau_z - \Delta \tau_x, \quad (6.5)$$

where  $\xi = \frac{p^2}{2m} - \mu$  is the quasiparticle energy and  $\tau_{x,y,z}$  are the Pauli matrices acting in Nambu space. Therefore, the Green's function  $G_0(p)$  reads :

$$G_0(p) = -\frac{i\omega_n + \xi\tau_z - \Delta\tau_x}{\omega_n^2 + \xi^2 + \Delta^2}, \quad (6.6)$$

where  $\omega_n$  are the Matsubara frequencies. Assuming that the chemical potential  $\mu$  is the largest energy involved in this problem and noticing that  $G_0(p)$  only depends on  $\xi$ , the calculation of  $G_0(0)$  is performed by transforming the  $p$  integration into a  $\xi$  integration, as we did in Chapter 2 (we set  $\hbar = 1$ ) :

$$G_0(0) \approx \frac{1}{\pi v_F} \int G_0(\xi) d\xi, \quad (6.7)$$

where  $v_F$  is the Fermi energy. Then, using the residue technique for the  $\xi$  integration, we obtain :

$$G_0(0) = -\frac{i\omega_n - \Delta\tau_x}{v_F \sqrt{\omega_n^2 + \Delta^2}}. \quad (6.8)$$

It is now straightforward to derive the expression of  $[\mathbb{1} - G_0(0)\vec{h} \cdot \vec{\sigma}]^{-1}$  :

$$\begin{aligned} & [\mathbb{1} - G_0(0)\vec{h} \cdot \vec{\sigma}]^{-1} = \\ & \frac{\omega_n^2(1+J^2) + \Delta^2(1-J^2) - 2i\omega_n J^2 \Delta \tau_x - \sqrt{\omega_n^2 + \Delta^2} [i\omega_n(1+J^2) - \Delta(1-J^2)\tau_x] \vec{J} \cdot \vec{\sigma}}{\omega_n^2(1+J^2)^2 + \Delta^2(1-J^2)^2}, \end{aligned} \quad (6.9)$$

where we took  $\vec{J} = \vec{h}/v_F$ . The energy of the Shiba states  $\varepsilon_s$  is obtained from the poles of Eq. (6.9) after performing the analytical continuation  $i\omega_n \rightarrow \varepsilon$  :

$$\varepsilon_s = \pm \Delta \frac{1 - J^2}{1 + J^2}. \quad (6.10)$$

We obtain two opposite values of the Shiba energy, which is a direct consequence of the electron-hole symmetry imposed by the Nambu basis. Notice that this energy does not depend on the impurity spin orientation nor on the dimensionality of the system. The variation of  $\varepsilon_s$  with the impurity strength  $J$  is illustrated in Fig. 6.2. At  $J = 1$ , the sign of the Shiba energy  $\varepsilon_s$  changes : A topological transition occurs, which modifies the superconducting ground state parity. Two important limits have to be taken into account when studying YSR states. Indeed, when  $J \gg 1$ , the impurity is sufficiently strong to modify the order parameter, which is not constant anymore and spatially oscillates. In the opposite limit, namely  $J \ll 1$ , Shiba physics occurs as long as the superconducting critical temperature  $T_c$  is larger than the Kondo temperature [145]. Otherwise, the system must be studied within the Kondo framework, where the impurity spin cannot be considered as classical. Notice that usually  $J \sim 1$  in STM measurements, thus avoiding these two problematic limits. These STM measurements give access to the polarized and non-polarized LDOS, characterized by spatial oscillations in the YSR states. Next, we analytically derive the LDOS of the 1D system considered in this part.

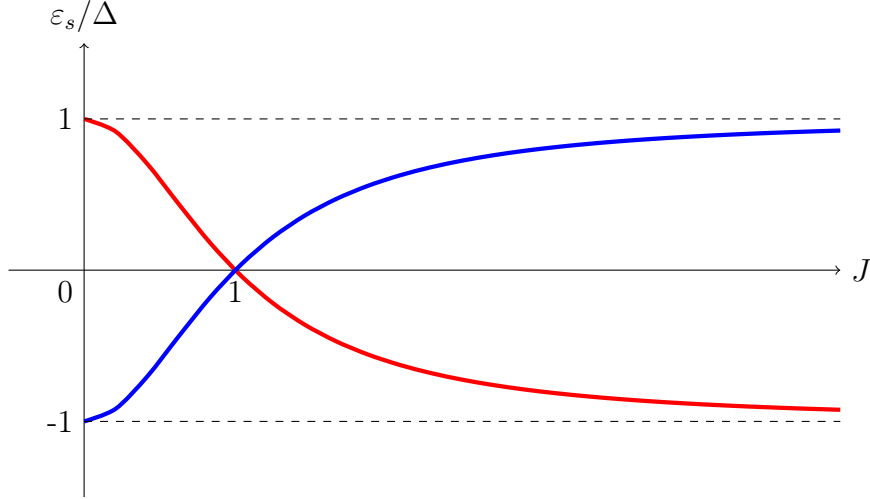


FIGURE 6.2 – Variation of the Shiba energy with the impurity strength  $J$ . The red curve represents the energy of the electron, whereas the blue one corresponds to the hole energy. At  $J = 1$ , the sign of the energy changes : A topological transition occurs.

### 6.1.2 Local density of states

The non-polarized and polarized LDOS,  $\nu(x)$  and  $S_n(x)$  respectively, where  $n = x, y, z$ , read in Nambu spin space :

$$\nu(x) = \frac{1}{4} \text{Tr}_\sigma G_{ii}(x, x) ; \quad (6.11)$$

$$S_n(x) = \frac{1}{4} \text{Tr}_\sigma (G_{ii}(x, x) \sigma_n) , \quad (6.12)$$

where  $\text{Tr}_\sigma$  corresponds to the trace over spins and  $i$  refers to the Nambu components of the matrix Green's function  $G(x, x)$ . The index  $i = 1$  gives access to the LDOS of electrons, whereas  $i = 2$  corresponds to holes. Since we are only interested in the spatially dependent part of the LDOS,  $\delta\nu(x)$  and  $\delta S_n(x)$ , we in fact derive the spin trace of  $\delta G_{ii}(x, x)$  in Eqs. (6.11, 6.12), where  $\delta G(x, x)$  corresponds to the spatially-dependent part of Eq. (6.4) :

$$\delta G(x, x) = G_0(x) \vec{h} \cdot \vec{\sigma} \left[ \mathbb{1} - G_0(0) \vec{h} \cdot \vec{\sigma} \right]^{-1} G_0(-x) . \quad (6.13)$$

The Green's function  $G_0(\pm x)$ , is given by the Fourier transform of  $G(p)$  :

$$G_0(\pm x) = \int e^{\pm i p x} G_0(p) \frac{dp}{2\pi} , \quad (6.14)$$

where in this case,  $G_0(p)$  is an even function of  $p$ , implying that  $G_0(x) = G_0(-x)$ .

As we already did in the previous part, we turn the  $p$  integration into  $\xi$  integration. To this purpose, we need to replace the  $p$  in the exponential by its expression with respect to  $\xi$  :  $p = \pm \sqrt{2m(\xi + \mu)} \approx p_F + \xi/v_F$ .

$$G_0(\pm x) = \int_{-\infty}^{+\infty} (e^{i(p_F + \xi/v_F)|x|} + e^{-i(p_F + \xi/v_F)|x|}) G_0(\xi) \frac{d\xi}{2\pi v_F} . \quad (6.15)$$

One can notice that the Green's function  $G_0(\xi)$  may be written as a sum of two com-

ponents  $G_{\text{even}}(\xi)$  and  $G_{\text{odd}}(\xi)$ , respectively even and odd in  $\xi$ , defined by :

$$G_{\text{even}}(\xi) = -\frac{i\omega_n - \Delta \tau_x}{\omega_n^2 + \xi^2 + \Delta^2} ; \quad (6.16)$$

$$G_{\text{odd}}(\xi) = -\frac{\xi \tau_z}{\omega_n^2 + \xi^2 + \Delta^2} . \quad (6.17)$$

Then, doing the change  $\xi \rightarrow -\xi$  in the negative exponential term, we finally obtain the following expression for  $G_0(\pm x)$  :

$$G_0(\pm x) = \frac{1}{\pi v_F} \left[ \cos(p_F |x|) \int_{-\infty}^{+\infty} e^{i|x|\xi/v_F} G_{\text{even}}(\xi) d\xi + i \sin(p_F |x|) \int_{-\infty}^{+\infty} e^{i|x|\xi/v_F} G_{\text{odd}}(\xi) d\xi \right] . \quad (6.18)$$

Performing the  $\xi$  integration using the residue technique,  $G_0(\pm x)$  reads :

$$G_0(x) = G_0(-x) = -N_F e^{-|x|/\zeta} \left[ \frac{i\omega_n - \Delta \tau_x}{\sqrt{\omega_n^2 + \Delta^2}} \cos(p_F |x|) - \tau_z \sin(p_F |x|) \right] , \quad (6.19)$$

where  $N_F = 1/v_F$  is the density of states at the Fermi level and we put  $\zeta = v_F/\sqrt{\omega_n^2 + \Delta^2}$ . Notice that we can also write this expression in a more condensed way :

$$G_0(x) = G_0(-x) = -i N_F e^{-|x|(1/\zeta - i p_F \hat{g})} \hat{g} \tau_z , \quad (6.20)$$

where  $\hat{g} = \frac{\omega_n \tau_z + \Delta \tau_y}{\sqrt{\omega_n^2 + \Delta^2}}$ .

Finally, replacing Eqs. (6.9) and (6.19) in Eq. (6.13) and taking the trace over spins, both at the positive Shiba energy  $\varepsilon \rightarrow \varepsilon_s = +\Delta(1 - J^2)/(1 + J^2)$ , we obtain the following expressions for the spatially-dependent parts of non-polarized and spin polarized LDOS :

$$\delta\nu(x) = \frac{N_F}{2} e^{-2|x|/\zeta_s} \frac{\varepsilon_s}{\varepsilon^2 - \varepsilon_s^2} \Delta \left[ 1 + \frac{\varepsilon_s}{\Delta} \cos(2p_F |x| \mp \theta) \right] \frac{J}{1 + J^2} ; \quad (6.21)$$

$$\delta S_n(x) = -\frac{N_F}{2} e^{-2|x|/\zeta_s} \frac{\varepsilon_s}{\varepsilon^2 - \varepsilon_s^2} \Delta \left[ 1 + \frac{\varepsilon_s}{\Delta} \cos(2p_F |x| \mp \theta) \right] J_n , \quad (6.22)$$

where  $\zeta_s = v_F(1 + J^2)/2J\Delta$  is the characteristic length describing the spatial decay of the LDOS at Shiba energy and  $2\theta$  represents the spatial shift between the LDOS of electrons and holes (the minus sign corresponds to electrons) such that

$$\theta = \begin{cases} \arctan\left(\frac{2J}{1-J^2}\right) & \text{when } J \neq 1 \\ \frac{\pi}{2} & \text{when } J = 1 \end{cases} . \quad (6.23)$$

The non-polarized LDOS is illustrated in Fig. 6.3. We can first notice that the LDOS, described by Eqs. (6.21) and (6.22), spatially oscillates, and second that it decays exponentially with distances, which means that Shiba states are localized around the impurity. Notice that the LDOS depends on the dimensionality of the system : It is multiplied by a factor  $1/p_F r$  in 2D and  $1/(p_F r)^2$  in 3D, where  $r$  is the distance from the impurity [32].

The first experimental detection of YSR states in 1997 was made using a STM [31]. Scanning a very pure Nb crystal in contact with a single magnetic impurity (Mn and Gd), Yazdani et al. obtained the tunneling spectra of the sample, which is proportional to the non-polarized LDOS [145]. This experiment clearly showed the phase shift

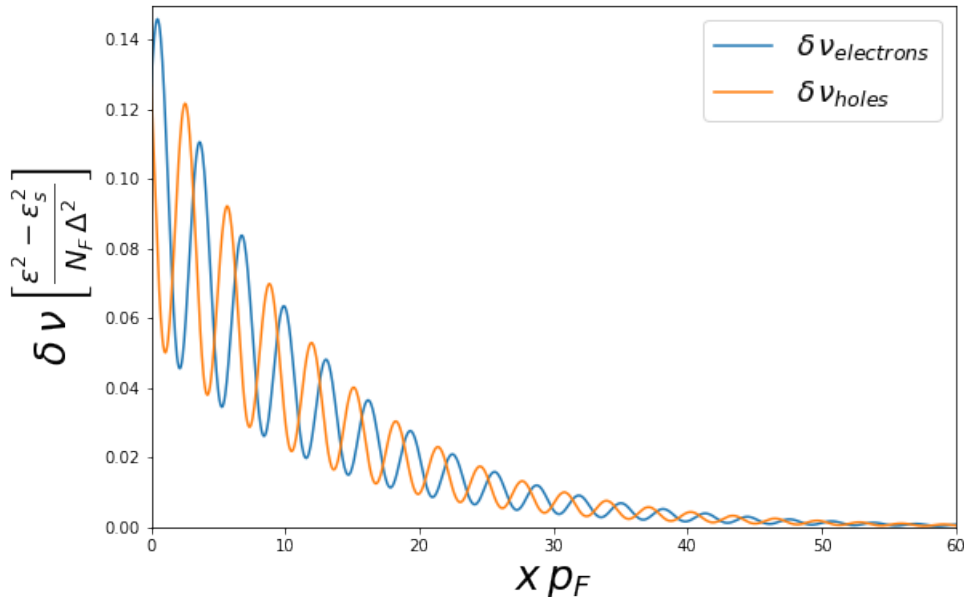


FIGURE 6.3 – Spatial dependence of the Shiba bound states with positive energy, highlighting the phase shift between electron and hole states. The LDOS vanishes at large distances  $x$  from the impurity, showing the localized character of YSR states. The parameters used for this figure are  $J = 0.6$  and  $\Delta/\mu = 0.1$ .

between electron and hole LDOS. It is also possible to have experimentally access to the polarized LDOS via a spin-polarized STM. In this case, the metallic tip used to scan the sample surface, made of normal metal, is replaced by a magnetized tip [146].

The recent progress of technologies has enabled to better characterize Shiba states properties, for example with higher energy resolution in STM measurements. Combined with the topological properties of YSR states, this has motivated new investigations in this field, both theoretical and experimental. For example, it has been demonstrated that one-dimensional chains of magnetic impurities on top of an s-wave superconductor lead to the appearance of Majorana bound states [18, 19, 20, 21, 22, 23, 24, 25, 26], which are possible candidates for the construction of topologically protected qubits.

In the next section, we present a very recent experiment on YSR states in  $\beta$ -Bi<sub>2</sub>Pd in the presence of Vanadium (V) adatoms, realized by J. Zaldívar and J. I. Pascual<sup>1</sup>. This experiment has motivated our investigations on the subject, presented in Secs. 6.3 and 6.4.

## 6.2 Superconducting crystal $\beta$ -Bi<sub>2</sub>Pd in the presence of Vanadium impurities

The recent observation of topologically protected surface states in the superconducting crystal  $\beta$ -Bi<sub>2</sub>Pd, whose structure is illustrated in Fig. 6.4, has attracted great interest on this material [140]. Moreover, it is suspected to host non-conventional superconducting pairing, involving both spin-singlet and spin-triplet components of the order parameter [141].

A possible way of detecting this unconventional pairing would consist in measuring the spin-polarized LDOS of Shiba states induced in  $\beta$ -Bi<sub>2</sub>Pd by a magnetic impurity,

1. CIC nanoGUNE, 20018 Donostia-San Sebastián, Spain

as proposed in Ref. [32]. Although in 3D materials YSR states are not easily detectable because of the fast decay of the LDOS spatial oscillations, it has been shown that in NbSe<sub>2</sub> bulk crystal the LDOS was spatially extended [144]. This feature was attributed to the 2D character of the electronic band structure. Therefore in  $\beta$ -Bi<sub>2</sub>Pd, one should also expect to have extended Shiba states, which could be used as a probe to determine the superconducting correlations.

Following this idea, J. Zaldívar and J. I. Pascual investigated experimentally the effect of the electronic band structure of  $\beta$ -Bi<sub>2</sub>Pd on the YSR states induced by Vanadium adatoms<sup>2</sup>. In this section, we give a brief report of their results :

- Three YSR excitations appear in the superconducting gap, labeled A, B and C as illustrated in Fig. 6.5a, which may be attributed to the three spin-polarized d-orbitals of Vanadium [147].
- The non-polarized LDOS of the Shiba state A (Shiba states B and C give essentially the same oscillatory pattern) is presented in Fig. 6.5b. We can observe spatial oscillations of this LDOS, with a phase shift between electron and hole-like excitations, as we predicted theoretically in Sec. 6.1. Moreover, the oscillatory pattern is developed over several nanometers from the impurity, resembling the extended LDOS found for Fe atoms in NbSe<sub>2</sub> [144], which seems to confirm the possibility of using the YSR states of  $\beta$ -Bi<sub>2</sub>Pd as a probe to detect unconventional superconducting pairing. Finally, Fig. 6.5b shows an unexpected double period spatial oscillation of the LDOS.
- We can also compare Shiba states with quasiparticle interferences (QPI), which are virtual bound states appearing in the normal state due to electron scattering. In Fourier space, we can see two peaks of the LDOS for the YSR state A, corresponding to the double oscillation observed in real space, whereas five peaks arise for the QPI, measured far from the superconducting gap. This result is presented in Fig. 6.6.

From these measurements, several open questions arise : How can we explain the double period spatial oscillation of the LDOS at Shiba energy ? Why in the normal state the number of oscillation periods of the LDOS is different from the superconducting state ? To answer these questions, a possible approach is to use numerical simulations based on tight-binding models describing the energy bands involved in the appearance of Shiba states. In order to simplify the analytical treatment of this problem, we have chosen to reduce the system to 1D, which obviously cannot provide a full description of the experiment, but should provide a first fundamental understanding of the mechanisms involved in the appearance of Shiba states in non-conventional superconductors in the presence of magnetic impurities. In the continuous limit, 1D tight-binding models can be approximated by 1D systems. This is why in the next two sections, we study analytically effective 1D models of superconductors in the presence of a magnetic impurity, which can be useful to guide simulations. Specifically, in this manuscript we choose to focus on the first problem : explain the double oscillation of the LDOS at Shiba energy.

---

2. To be published.

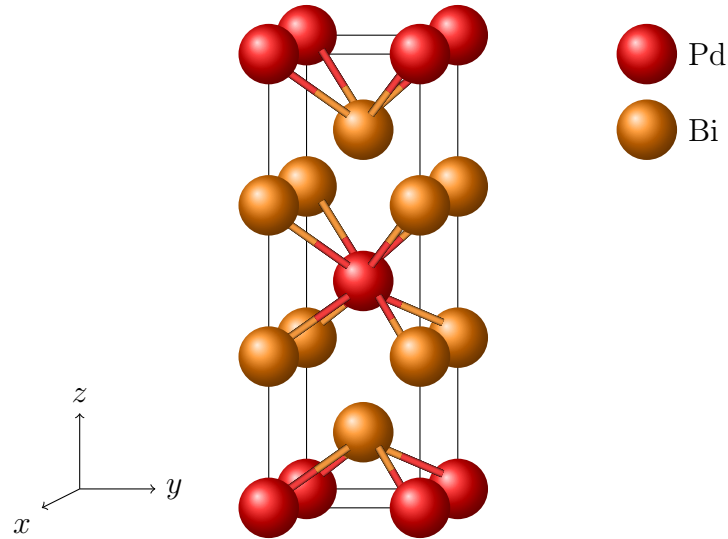


FIGURE 6.4 – Crystal structure of the superconductor  $\beta$ -Bi<sub>2</sub>Pd.

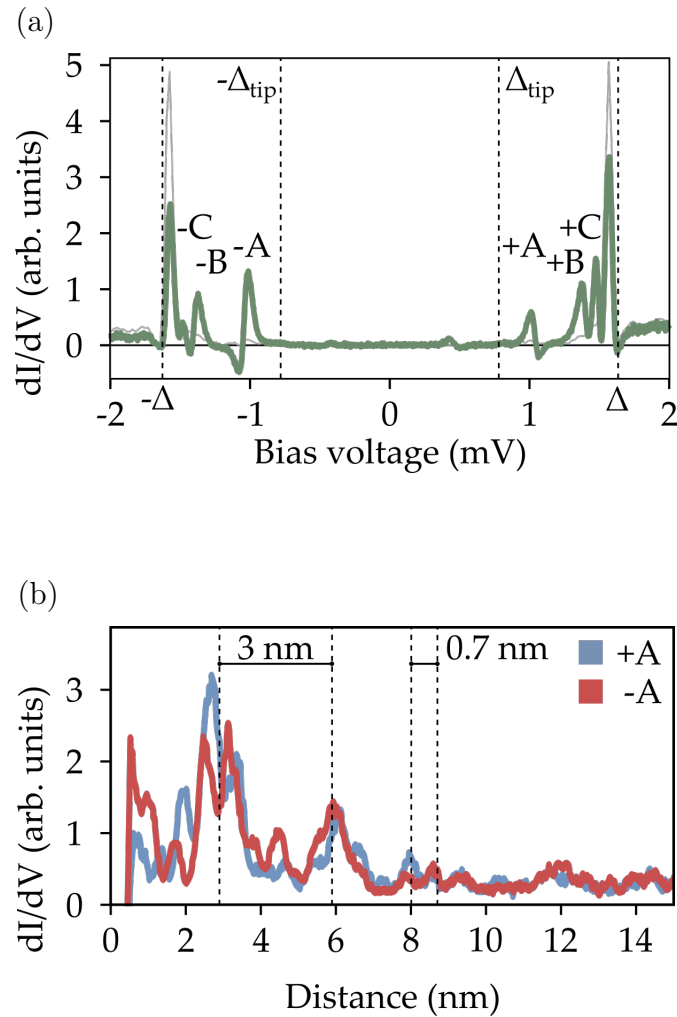


FIGURE 6.5 – Spectral and spatial properties of Yu-Shiba-Rusinov states in  $\beta$ -Bi<sub>2</sub>Pd, obtained by J. Zaldívar and J. I. Pascual from STM measurements. (a) Experimental spectra. Three YSR states are detected inside the superconducting gap, labelled A, B and C (from lower to higher energy). (b) Spatial variations of the electron (blue line) and hole-like (red line) Shiba state A, characterized by a double period oscillation.

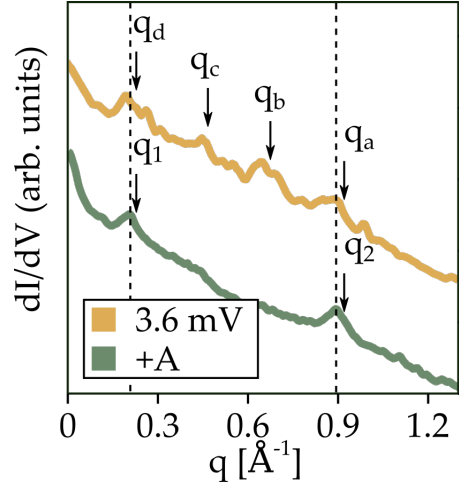


FIGURE 6.6 – Spectral comparison between the Shiba state A and QPI at energy 3.6 meV (above the superconducting gap). The YSR state is characterized by two peaks, whereas five peaks appear for QPI.

### 6.3 First model : Single superconducting band with helical dispersion

In order to understand the oscillatory pattern of the LDOS of Shiba states observed in  $\beta$ -Bi<sub>2</sub>Pd, we built effective models of one-dimensional superconductors in the presence of a magnetic impurity. The first model consists in a single superconducting wire with helical dispersion. First, we show that the presence of a magnetic impurity coupled to the helical wire induces Shiba states with the same energy as the one obtained in Sec. 6.1.1. Then, we demonstrate through the calculation of the non-polarized LDOS that Shiba spatial oscillations cannot be explained by purely chiral bands.

#### 6.3.1 Model

We consider an s-wave superconducting wire along the  $x$ -axis with helical dispersion and a constant order parameter  $\Delta$ . We suppose that a single localized magnetic impurity is coupled to the wire, described by the potential  $V(x) = \vec{h} \cdot \vec{\sigma} \delta(x)$ , where  $\sigma_{x,y,z}$  are the Pauli matrices acting in spin space. Notice that in the whole chapter we take  $\hbar = 1$ .

In Nambu spin space, the Hamiltonian without impurity  $\hat{h}_0$  reads :

$$\hat{h}_0 = (p v_F \sigma_z - \mu) \tau_z - \Delta \tau_x, \quad (6.24)$$

where the Pauli matrices  $\tau_{x,y,z}$  label Nambu space.

Using the equation of motion for the Green's functions  $(i\omega_n - \hat{h}_0) G_0 = 1$ , where  $\omega_n$  are the Matsubara frequencies, one can write the Green's function in the absence of impurity  $G_0$  in Nambu spin space :

$$G_0(p) = - \frac{[i\omega_n + (p v_F \sigma_z - \mu) \tau_z - \Delta \tau_x] [\omega_n^2 + \Delta^2 + (p v_F \sigma_z + \mu)^2]}{[\omega_n^2 + \Delta^2 + (p v_F - \mu)^2] [\omega_n^2 + \Delta^2 + (p v_F + \mu)^2]}. \quad (6.25)$$

In the next subsections, we compute the Shiba energy and the LDOS of states of this system, using the same method as in Sec. 6.1.

### 6.3.2 Shiba energy

The Shiba energy is given by the poles of the Green's function  $G(x, x)$  defined in Eq. (6.4), which are all contained in the term  $[\mathbb{1} - G_0(0) \vec{h} \cdot \vec{\sigma}]^{-1}$ . The Green's function  $G_0(0)$  is defined by the inverse Fourier transform of  $G_0(p)$  at  $x = 0$  (see Eq. 6.7), and can be computed directly by integrating Eq. (6.25) with respect to  $p$  using the residue method. Notice that in this case, because of the linear dispersion, we don't need to transform the  $p$  integral into a  $\xi$  integral as we did until now. Therefore, the Green's function  $G_0(0)$  reads :

$$G_0(0) = -\frac{1}{2v_F} \frac{i\omega_n - \Delta\tau_x}{\sqrt{\omega_n^2 + \Delta^2}}, \quad (6.26)$$

where  $v_F$  is the Fermi velocity.

Therefore, the term  $[\mathbb{1} - G_0(0) \vec{h} \cdot \vec{\sigma}]^{-1}$  reads :

$$\begin{aligned} [\mathbb{1} - G_0(0) \vec{h} \cdot \vec{\sigma}]^{-1} &= \frac{1}{\omega_n^2 (1 + J^2)^2 + \Delta^2 (1 - J^2)^2} [\omega_n^2 (1 + J^2) + \Delta^2 (1 - J^2) \\ &\quad - 2i\omega_n J^2 \Delta \tau_x - \sqrt{\omega_n^2 + \Delta^2} (i\omega_n (1 + J^2) - (1 - J^2) \Delta \tau_x) \vec{J} \cdot \vec{\sigma}], \end{aligned} \quad (6.27)$$

where  $\vec{J} = \vec{h}/2v_F$ . The poles of Eq. (6.27) give the Shiba energy  $\varepsilon_s$  after performing the analytical continuation  $i\omega_n \rightarrow \varepsilon$  :

$$\varepsilon_s = \pm \Delta \frac{1 - J^2}{1 + J^2}. \quad (6.28)$$

Except the expression of the impurity strength  $J$  with respect to the exchange field  $h$ , we obtain exactly the same expression for the energy as Eq. (6.10). This energy is a characteristic of YSR states and does not depend on the direction of the impurity magnetization.

Next, we derive the non-polarized and polarized LDOS of this system.

### 6.3.3 Local density of states

The spatially dependent part of the non-polarized and polarized LDOS  $\delta\nu(x)$  and  $\delta S_n(x)$ , where  $n = x, y, z$ , is given by Eqs. (6.11) and (6.12), where we take the spin trace of  $\delta G(x, x)$  instead of  $G(x, x)$  :

$$\delta\nu(x) = \frac{1}{4} \text{Tr}_\sigma \delta G_{ii}(x, x); \quad (6.29)$$

$$\delta S_n(x) = \frac{1}{4} \text{Tr}_\sigma (\delta G_{ii}(x, x) \sigma_n), \quad (6.30)$$

where  $\delta G(x, x)$  is given by Eq. (6.13) and the index  $i$  labels the component of  $\delta G(x, x)$  in Nambu space;  $i = 1$  corresponds to the LDOS of electrons, whereas  $i = 2$  corresponds to hole LDOS.

To compute the Green's function  $G_0(\pm x)$ , let us write  $G_0(p)$  as a sum of two terms,

one even in  $p$  and the other one odd in  $p$  :  $G_0(p) = G_{\text{even}}(p) + G_{\text{odd}}(p)$ , where

$$G_{\text{even}}(p) = -\frac{(i\omega_n - \Delta\tau_x)(\omega_n^2 + \Delta^2 + p^2 v_F^2 + \mu^2) - \mu\tau_z(\omega_n^2 + \Delta^2 - p^2 v_F^2 + \mu^2)}{[\omega_n^2 + \Delta^2 + (p v_F - \mu)^2][\omega_n^2 + \Delta^2 + (p v_F + \mu)^2]} ; \quad (6.31)$$

$$G_{\text{odd}}(p) = -p v_F \frac{(\omega_n^2 + \Delta^2 + p^2 v_F^2 - \mu^2)\tau_z + 2\mu(i\omega_n - \Delta\tau_x)}{[\omega_n^2 + \Delta^2 + (p v_F - \mu)^2][\omega_n^2 + \Delta^2 + (p v_F + \mu)^2]} \sigma_z . \quad (6.32)$$

Then, using Eq. (6.14) together with the residue method, we can compute  $G_{\text{even}}(x)$  and  $G_{\text{odd}}(x)$ , and finally obtain the expression of  $G_0(\pm x)$  :

$$G_0(\pm x) = G_{\text{even}}(x) \pm i G_{\text{odd}}(x) , \quad (6.33)$$

where

$$G_{\text{even}}(x) = -\frac{e^{-|x|/\zeta}}{2\sqrt{\omega_n^2 + \Delta^2} v_F} \left[ (i\omega_n - \Delta\tau_x) \cos\left(\frac{2\mu|x|}{v_F}\right) - \sqrt{\omega_n^2 + \Delta^2} \tau_z \sin\left(\frac{2\mu|x|}{v_F}\right) \right] ; \quad (6.34)$$

$$G_{\text{odd}}(x) = -i \frac{e^{-|x|/\zeta}}{2\sqrt{\omega_n^2 + \Delta^2} v_F} \left[ (i\omega_n - \Delta\tau_x) \sin\left(\frac{2\mu|x|}{v_F}\right) - \sqrt{\omega_n^2 + \Delta^2} \tau_z \cos\left(\frac{2\mu|x|}{v_F}\right) \right] \sigma_z , \quad (6.35)$$

where  $\zeta = v_F/\sqrt{\omega_n^2 + \Delta^2}$ . Replacing Eqs. (6.33 - 6.35) and (6.27) in  $\delta G(x, x)$  (Eq. 6.13), we finally obtain the spatially dependent part of the non-polarized and polarized LDOS at positive Shiba energy  $\varepsilon_s = +\Delta(1 - J^2)/(1 + J^2)$  for electrons and holes from Eqs. (6.29) and (6.30) :

$$\delta\nu(x) = \frac{N_F}{2} e^{-2|x|/\zeta_s} \frac{\varepsilon_s}{\varepsilon^2 - \varepsilon_s^2} \frac{J}{1 + J^2} \Delta ; \quad (6.36)$$

$$\delta S_x^\pm(x) = -\frac{N_F}{2} e^{-2|x|/\zeta_s} \frac{\varepsilon_s}{\varepsilon^2 - \varepsilon_s^2} \frac{\sqrt{J_x^2 + J_y^2}}{1 + J^2} \Delta \cos\left(\frac{2\mu|x|}{v_F} + \theta_x^\pm\right) ; \quad (6.37)$$

$$\delta S_y^\pm(x) = -\frac{N_F}{2} e^{-2|x|/\zeta_s} \frac{\varepsilon_s}{\varepsilon^2 - \varepsilon_s^2} \frac{\sqrt{J_x^2 + J_y^2}}{1 + J^2} \Delta \cos\left(\frac{2\mu|x|}{v_F} - \theta_y^\pm\right) ; \quad (6.38)$$

$$\delta S_z(x) = -\frac{N_F}{2} e^{-2|x|/\zeta_s} \frac{\varepsilon_s}{\varepsilon^2 - \varepsilon_s^2} \frac{J_z}{1 + J^2} \Delta , \quad (6.39)$$

where  $\zeta_s = v_F(1 + J^2)/2J\Delta$  is the spatial decay of the LDOS and  $N_F = 1/v_F$  is the density of states at Fermi energy. The angles  $\theta_{x,y}^\pm$  show the shift between electron and holes polarized LDOS and are such that  $\tan\theta_x^\pm = \frac{(1 - J^2)J_y \mp 2JJ_x}{(1 - J^2)J_x \pm 2JJ_y} = 1/\tan\theta_y^\pm$ , where  $\theta_{x,y}^+$  corresponds to electrons and  $\theta_{x,y}^-$  corresponds to holes.

Due to its helical dispersion, this system presents a peculiar behaviour : The spatial oscillations that we should normally observe in the non-polarized LDOS Eq. (6.36) are absent. Therefore, this model cannot explain the experimental results obtained in Sec. 6.2. Interestingly, the polarized LDOS  $S_x$  and  $S_y$  (Eqs. 6.37 and 6.38) present a spatial oscillation and a phase shift between electron and hole states, which could be measured using STM with magnetic tips.

In the next section, we present a second effective model, made of two superconducting wires connected via a hopping term.

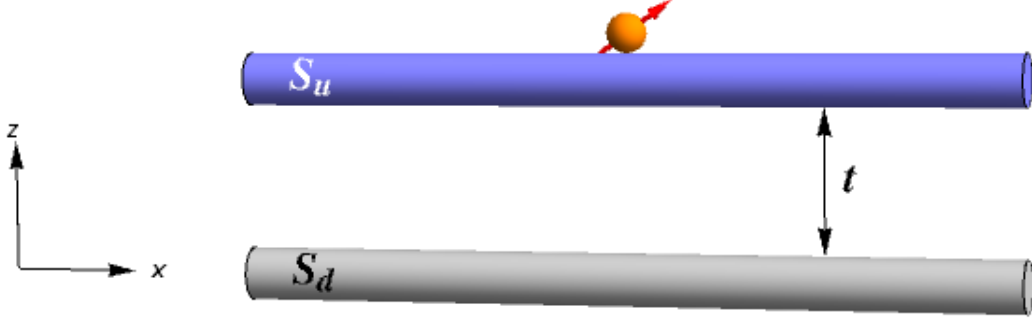


FIGURE 6.7 – The second effective model is made of two superconducting wires  $S_u$  and  $S_d$  with quadratic dispersion, connected via a hopping term. A magnetic impurity is coupled to  $S_u$ .

## 6.4 Second model : Two superconducting wires coupled via a hopping term

We have seen in the previous section that a single helical wire cannot involve spatial oscillations of the non-polarized Shiba LDOS. Here, we consider a two wire model : Two superconducting wires with a quadratic dispersion are connected via a hopping term. A magnetic impurity is coupled to one of the wires, involving YSR states. We demonstrate that in this case the LDOS presents a double spatial oscillation, with frequencies corresponding respectively to the sum and difference of the Fermi momenta of each wire. By showing that the presence of two (non chiral) coupled bands is the minimal condition to observe Shiba double period oscillation, this model is a first step in the understanding of the mechanisms leading to the appearance of YSR states in  $\beta$ -Bi<sub>2</sub>Pd (Sec. 6.2).

### 6.4.1 Model

We consider two identical infinite s-wave superconducting wires  $S_u$  and  $S_d$  along the  $x$ -axis, connected via a hopping term  $t$  as illustrated in Fig. 6.7. We assume that a magnetic impurity is coupled to  $S_u$ , described by the potential  $V(x) = \vec{h} \cdot \vec{\sigma} \delta(x) (\mathbb{1}_\eta + \eta_z) / 2$ , where  $\sigma_{x,y,z}$ ,  $\eta_{x,y,z}$  are the Pauli matrices acting respectively on spin and wire spaces, and  $\mathbb{1}_\eta$  is the identity matrix in wire space.

In Nambu-wire space, the Hamiltonian without impurity  $\hat{h}_0$  reads :

$$\hat{h}_0 = (\xi \tau_z - \Delta \tau_x) \mathbb{1}_\eta + t \tau_z \eta_x , \quad (6.40)$$

where  $\xi = p^2/2m - \mu$  is the quasiparticle energy,  $\mu$  is the chemical potential and  $\Delta$  is the superconducting order parameter, which is assumed to be constant. The Pauli matrices  $\tau_{x,y,z}$  label Nambu space.

Using the equation of motion for the Green's functions  $(i\omega_n - \hat{h}_0) G_0 = \mathbb{1}$  where  $\omega_n$  are the Matsubara frequencies, one can write the zeroth-order Green's function  $G_0$  in Nambu-wires space :

$$G_0(p) = - \frac{(i\omega_n - \Delta \tau_x) (\omega_n^2 + \Delta^2 + \xi^2 + t^2 - 2\xi t \eta_x) + [(\xi + t \eta_x) (\omega_n^2 + \Delta^2) + (\xi - t \eta_x) (\xi^2 - t^2)] \tau_z}{t^4 + 2t^2 (\omega_n^2 + \Delta^2 - \xi^2) + (\omega_n^2 + \Delta^2 + \xi^2)^2} . \quad (6.41)$$

In the next to subsections, we compute the Shiba energy and the LDOS of states of this two wire model, using the same method as in Sec. 6.1.

### 6.4.2 Shiba energy

The Shiba energy is given by the poles of the Green's function  $G(x, x)$  defined in Eq. (6.4), enlarged over the wire space :

$$G(x, x) = G_0(x, x) + G_0(x) \vec{h} \cdot \vec{\sigma} \frac{\mathbb{1}_\eta + \eta_z}{2} \left[ \mathbb{1} - G_0(0) \vec{h} \cdot \vec{\sigma} \frac{\mathbb{1}_\eta + \eta_z}{2} \right]^{-1} G_0(-x). \quad (6.42)$$

The poles of  $G(x, x)$  are therefore all contained in the term  $\left[ \mathbb{1} - G_0(0) \vec{h} \cdot \vec{\sigma} (\mathbb{1}_\eta + \eta_z) / 2 \right]^{-1}$  of Eq. (6.42). The Green's function  $G_0(0)$  is defined by the inverse Fourier transform of  $G_0(p)$  at  $x = 0$  :  $G_0(0) = \int G_0(p) dp / 2\pi$ . Assuming that the chemical potential  $\mu$  is the largest energy involved in this problem, namely  $\xi \ll \mu$ , and noticing that  $G_0(p)$  only depends on  $\xi$ , it is possible to turn the  $p$  integral into a  $\xi$  integral using Eq. (6.7). Then, the  $\xi$  integral is calculated from the residue technique :

$$G_0(0) = -\frac{1}{v_F} \frac{i\omega_n - \Delta \tau_x}{\sqrt{\omega_n^2 + \Delta^2}}, \quad (6.43)$$

where  $v_F$  is the Fermi velocity.

We can then compute the term  $\left[ \mathbb{1} - G_0(0) \vec{h} \cdot \vec{\sigma} (\mathbb{1}_\eta + \eta_z) / 2 \right]^{-1}$ , which gives in wire basis :

$$\left[ \mathbb{1} - G_0(0) \vec{h} \cdot \vec{\sigma} (\mathbb{1}_\eta + \eta_z) / 2 \right]^{-1} = \begin{pmatrix} \hat{M} & 0 \\ 0 & \mathbb{1} \end{pmatrix}, \quad (6.44)$$

where the matrix  $\hat{M}$  is defined in spin Nambu space by :

$$\hat{M} = \frac{\omega_n^2 (1 + J^2) + \Delta^2 (1 - J^2) - 2i\omega_n J^2 \Delta \tau_x - \sqrt{\omega_n^2 + \Delta^2} [i\omega_n (1 + J^2) - \Delta (1 - J^2) \tau_x] \vec{J} \cdot \vec{\sigma}}{\omega_n^2 (1 + J^2)^2 + \Delta^2 (1 - J^2)^2}, \quad (6.45)$$

with  $\vec{J} = \vec{h}/v_F$ . Let us notice that the matrix  $\hat{M}$  is exactly equal to Eq. (6.9) which gives the Shiba energy in the one wire system with quadratic dispersion, described in Sec. 6.1. From the form of Eq. (6.44), we can see that the Shiba states are localized in the upper wire  $S_u$ , which is coupled to the impurity. The energy of the YSR states  $\varepsilon_s$  is thus exactly the same as Eq. (6.10) :

$$\varepsilon_s = \pm \Delta \frac{1 - J^2}{1 + J^2}. \quad (6.46)$$

This energy does not depend on the hooping between the wires  $t$ , and is independent of the direction of the impurity exchange field  $\vec{h}$ .

In the following, we derive the expression of the LDOS of this two-wire model at the Shiba energy.

### 6.4.3 Local density of states

The spatially dependent part of the non-polarized and spin polarized LDOS  $\delta\nu(x)$  and  $\delta S_n(x)$ , where  $n = x, y, z$ , is given by Eqs. (6.29) and (6.30), enlarged to take into account the presence of both wires :

$$\delta\nu(x) = \frac{1}{4} \text{Tr}_{\sigma, \eta} \delta G_{ii}(x, x); \quad (6.47)$$

$$\delta S_n(x) = \frac{1}{4} \text{Tr}_{\sigma, \eta} (\delta G_{ii}(x, x) \sigma_n), \quad (6.48)$$

where the trace  $\text{Tr}_{\sigma,\eta}$  is made over spin and wire bases, and the index  $i$  labels the component of  $\delta G(x, x)$  in Nambu space :  $i = 1$  corresponds to the LDOS of electrons, whereas  $i = 2$  corresponds to hole LDOS. The spatially dependent part of the Green's function,  $\delta G(x, x)$ , is given by the second term of Eq. (6.42) :

$$\delta G(x, x) = G_0(x) \vec{h} \cdot \vec{\sigma} \frac{\mathbb{1}_\eta + \eta_z}{2} \left[ \mathbb{1} - G_0(0) \vec{h} \cdot \vec{\sigma} \frac{\mathbb{1}_\eta + \eta_z}{2} \right]^{-1} G_0(-x) , \quad (6.49)$$

To compute the Green's functions  $G_0(\pm x)$  appearing in  $\delta G(x, x)$ , it is worth noting that  $G_0(p)$  can be written as a sum of even and odd components in  $\xi$ , namely  $G_0(p) = G_{\text{even}}(\xi) + G_{\text{odd}}(\xi)$ , such that

$$G_{\text{even}}(\xi) = - \frac{(i\omega_n - \Delta \tau_x) (\omega_n^2 + \Delta^2 + \xi^2 + t^2) + t (\omega_n^2 + \Delta^2 - \xi^2 + t^2) \tau_z \eta_x}{t^4 + 2t^2 (\omega_n^2 + \Delta^2 - \xi^2) + (\omega_n^2 + \Delta^2 + \xi^2)^2} ; \quad (6.50)$$

$$G_{\text{odd}}(\xi) = \xi \frac{2t (i\omega_n - \Delta \tau_x) \eta_x - (\omega_n^2 + \Delta^2 + \xi^2 - t^2) \tau_z}{t^4 + 2t^2 (\omega_n^2 + \Delta^2 - \xi^2) + (\omega_n^2 + \Delta^2 + \xi^2)^2} . \quad (6.51)$$

The Green's function  $G_0(\pm x)$  can thus be calculated using Eq. (6.18), which gives :

$$G_0(\pm x) = -N_F e^{-|x|/\zeta} \left[ \left( \frac{i\omega_n - \Delta \tau_x}{\sqrt{\omega_n^2 + \Delta^2}} \cos(p_F |x|) - \tau_z \sin(p_F |x|) \right) \cos\left(\frac{t}{v_F} |x|\right) + \left( \tau_z \cos(p_F |x|) + \frac{i\omega_n - \Delta \tau_x}{\sqrt{\omega_n^2 + \Delta^2}} \sin(p_F |x|) \right) \eta_x \sin\left(\frac{t}{v_F} |x|\right) \right] , \quad (6.52)$$

where  $N_F = 1/v_F$  is the density of states at the Fermi energy and  $\zeta = v_F/\sqrt{\omega_n^2 + \Delta^2}$ .

Finally, after replacing Eqs. (6.52) and (6.44) into the Green's function Eq. (6.49), the LDOS at positive energy  $\varepsilon_s = +\Delta(1 - J^2)/(1 + J^2)$  are derived from Eqs. (6.53) and (6.54) :

$$\delta\nu(x) = \frac{N_F}{2} e^{-2|x|/\zeta_s} \frac{\varepsilon_s}{\varepsilon^2 - \varepsilon_s^2} \Delta \left[ 1 + \frac{\varepsilon_s}{\Delta} \cos(2p_F |x| \mp \theta) \cos\left(2t \frac{|x|}{v_F}\right) \right] \frac{J}{1 + J^2} ; \quad (6.53)$$

$$\delta S_n(x) = -\frac{N_F}{2} e^{-2|x|/\zeta_s} \frac{\varepsilon_s}{\varepsilon^2 - \varepsilon_s^2} \Delta \left[ 1 + \frac{\varepsilon_s}{\Delta} \cos(2p_F |x| \mp \theta) \cos\left(2t \frac{|x|}{v_F}\right) \right] \frac{J_n}{1 + J^2} , \quad (6.54)$$

where  $\theta$  is defined in Eq. (6.23) and  $\zeta_s = v_F(1 + J^2)/2J\Delta$  is the characteristic length describing the spatial decay of the Shiba LDOS.

Our main result is the presence of a double spatial oscillation of the LDOS Eqs. (6.53) and (6.54), illustrated in Fig. 6.8. The frequencies of these oscillations correspond respectively to the sum and difference of the Fermi momentum of each wire,  $p_F \pm t/v_F$ . Moreover, we recover the phase shift of  $2\theta$  between electron and hole LDOS, which only occurs for the oscillation of frequency  $2p_F$ .

Therefore we have demonstrated through effective models that the necessary condition to observe a double spatial oscillation of the LDOS at Shiba energy may be the presence of two non helical bands, participating both in the superconductivity.

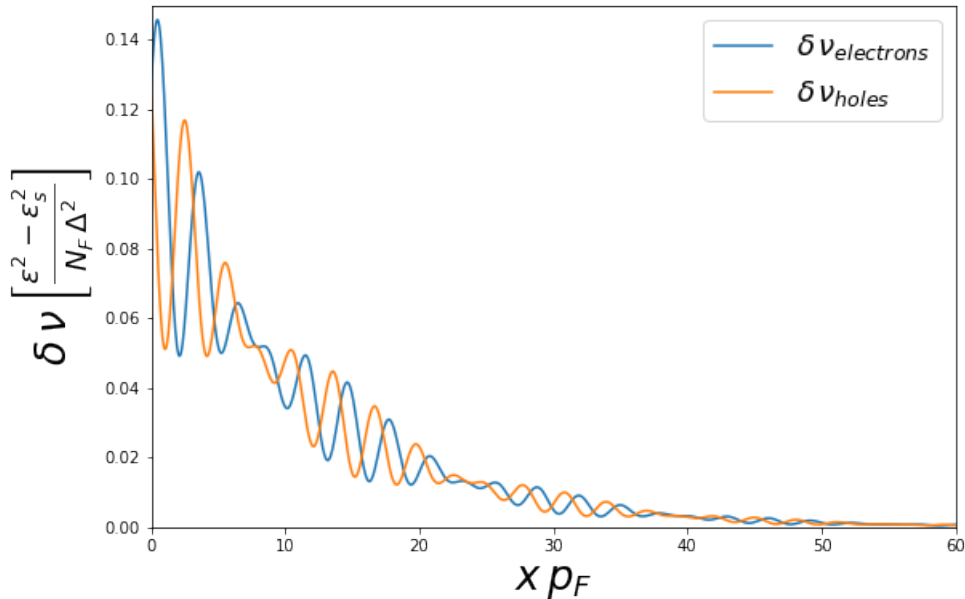


FIGURE 6.8 – Spatial dependence of the Shiba bound states with positive energy, highlighting the phase shift between electron and hole states. A double period spatial oscillation with frequencies  $2p_F$  and  $2t/v_F$  can be observed. The parameters used for this figure are  $J = 0.6$ ,  $\Delta/\mu = 0.1$  and  $t/\mu = 0.2$ .

## 6.5 Conclusion

In this chapter, we investigated the appearance of Yu-Shiba-Rusinov bound states in superconductors coupled to a magnetic impurity. Our work was motivated by experiments recently realized by J. Zaldívar and J. I. Pascual on  $\beta$ -Bi<sub>2</sub>Pd crystal superconductors in the presence of Vanadium impurities. STM measurements showed three Shiba states in the superconducting gap, originating from the three spin-polarized d-orbitals of Vanadium. Surprisingly, they have found that each Shiba state was characterized by a double period spatial oscillation of the LDOS, whereas in the normal state, QPI displayed five oscillations of the LDOS.

Specifically, we focused on explaining the double oscillation of the LDOS. To this purpose, we considered different effective models. In a first case, we studied a single superconducting wire with helical dispersion in order to reproduce the spin-polarization of the spectrum of  $\beta$ -Bi<sub>2</sub>Pd. In the presence of a magnetic impurity, we demonstrated that Shiba states appear in the superconducting gap, but are characterized by the absence of spatial oscillations of the non-polarized LDOS. Therefore, the spatial dependence of YSR state cannot be explained by purely chiral bands. Notice that the spin-polarized LDOS of the helical wire shows a spatial oscillation, which could in principle be detected experimentally by STM with magnetic tips in real materials.

Then, we studied a second model made of two superconducting wires with quadratic dispersion, connected via a hopping term (see Fig. 6.7). We coupled the upper wire to a magnetic impurity and investigated the appearance of YSR bound states. As expected, we found that Shiba states were localized in the upper wire, and that their energy is not affected by the presence of the second wire. We showed that both the non-polarized and spin-polarized LDOS display a double spatial oscillation with frequencies corresponding to the sum and the difference of the Fermi momenta of each wire.

Therefore, the necessary condition to obtain a double spatial oscillation of the

Shiba states seems to be the presence of two electronic bands, participating both in the superconductivity. Moreover, a helical dispersion of at least one of the bands would kill the double oscillation of the LDOS. It is thus necessary to consider other types of dispersions, for example a quadratic dispersion as we did in Sec.6.4, or at least a non-perfectly helical dispersion.

Finally, we outline that the effective models developed in this chapter could be easily generalized to describe the spectrum of multiband superconductors in the presence of magnetic impurities. The next step is to understand the mismatch between Shiba and QPI oscillations of the LDOS in  $\beta$ -Bi<sub>2</sub>Pd, namely to explain why Shiba states present a double spatial oscillation, whereas in the normal state QPI display five oscillations of the LDOS. A possible explanation is that the magnetic impurity is coupled to only two bands of the energy spectrum, which are thus the only bands involved in the appearance of YSR states.



# Chapter 7

## General conclusion

**I**N THIS THESIS, we investigated the interplay between low-dimensional superconductivity and spin-dependent fields, namely Zeeman and Rashba spin-orbit fields. This work allows a better understanding of several effects which can arise, in particular the enhancement of the critical magnetic field related to the helical phase which emerges in the presence of Zeeman and Rashba interactions, the magnetoelectric effects stemming from the combination of both interactions, and the appearance of Yu-Shiba-Rusinov states originating from a paramagnetic impurity coupled to the superconductor.

In Chapter 4, we considered two distinct systems : a superconducting wire in which Zeeman and spin-orbit interactions coexist, and a two wire setup in which superconducting pairing and spin-dependent fields are spatially separated. We first showed that it is possible to predict the form of the anomalous charge current in terms of the Zeeman and spin-orbit fields from the  $SU(2)$  covariant formalism. We further confirmed this result by computing the anomalous currents within the framework of Gor'kov Green's function formalism for both systems, in the limit of small spin-orbit interaction  $\alpha p_F \ll T_c$ . Then, we determined the self-consistent order parameter, and showed that the combination of both Zeeman and spin-orbit fields may lead to the appearance of a superconducting inhomogeneous phase for each temperature  $T < T_{c0}$ . Moreover, we proved that the ground state of each setup is in fact a zero-current state in which the anomalous charge current is compensated by the current stemming from the wave-vector of the superconducting order parameter. Finally, we investigated the limit of large spin-orbit interaction  $\alpha p_F \gg T_c$  for the one wire system, and still using the self-consistency relation, we obtained the field-temperature phase diagram for different orientations of the Zeeman field and several values of the spin-orbit coupling constant. As expected from the small spin-orbit limit, when the Zeeman field is purely parallel to the SO field, we obtain the well-known FFLO phase diagram.

Several perspectives result from this work. First, we emphasize that in principle such systems could be achieved experimentally, for example using organic superconductors for the first setup, and a semiconducting double wire system in which one of the wires is superconducting with a small section (smaller than the coherence length) for the two wire setup. However, to really describe these realistic cases, it would be necessary to take into account the proximity effects present in both experimental setups, which become rather complicated. Moreover, we have outlined that the systems presented in this chapter could be used as weak links between two identical superconductors to create anomalous  $\varphi_0$ -Josephson junctions [14, 148], similarly as [149]. In such systems, the superconducting wave vector would play the role of the phase difference needed to

generate a current in the junction, which would open new possibilities of application of these  $\varphi_0$ -junctions in memory devices [150].

In Chapter 5, we studied the possible emergence of a vortex in a type-II superconductor proximity coupled to a Néel skyrmion, in the absence of external magnetic fields. Due to the interplay between Zeeman and spin-orbit interactions, the skyrmion induces a spin polarization in the superconducting layer, which may lead to the appearance of supercurrents at the interface, and a spontaneous magnetic field which can in turn nucleate a vortex in the superconductor. From the minimization of the free energy, we derived the condition on the spin-orbit coupling constant for the vortex emergence, and thus have shown that it is even possible for the vortex to carry more than one quantum of flux for a sufficiently strong spin-orbit interaction.

We can provide some outlooks to this work. Even if the Rashba coupling threshold condition for the vortex emergence is not reached, it is possible to nucleate vortices in the superconducting layer simply by applying an external magnetic field larger than  $H_{c1}$ . In this case, our free energy calculations have demonstrated an attractive coupling which will pin vortices to the skyrmion for one orientation of the magnetic field. For the opposite orientation, the vortices should be pushed away by the skyrmion [137]. Such decoration/antidecoration of the skyrmion by vortices can be, in principle, detected experimentally. The inverse effect, namely the nucleation of a skyrmion via the proximity of a superconducting vortex is also suggested by our results, and could in principle be observed experimentally via magnetic force microscopy or topological Hall effect in systems like Nb/Co/Pt [151]. It has been recently demonstrated that such skyrmion/vortex pair should support Majorana bound states [17], opening new perspectives for Majorana spatial control.

Finally, in Chapter 6, we investigated the spatial dependence of Yu-Shiba-Rusinov states induced by the presence of paramagnetic impurities in superconductors. In order to understand qualitatively the coupling between the magnetic impurity and superconductivity in non-conventional multiband superconductors, we studied simplified quasi 1D models in which 1D electronic bands are modeled by wires. More specifically, we built two effective 1D models : a superconducting wire with a helical dispersion, and a two wire system with a quadratic dispersion in which the impurity is coupled to only one of the wires. Two results emerged from these models : a helical band does not lead to spatial oscillations of the Shiba states, and the minimal condition to describe a double period spatial oscillation of YSR states is the presence of at least two non helical bands, participating both in the superconductivity.

This work was motivated by recent experiments from J. Zaldívar and J. I. Pascual on  $\beta$ -Bi<sub>2</sub>Pd crystal superconductors in the presence of Vanadium impurities, in which a double period oscillation of the Shiba states was found. In this manuscript, we have chosen to reduce the problem to a 1D system to provide a first fundamental understanding of the mechanisms at the origin of the spatial dependence of Shiba states. However, to give a quantitative explanation of the experimental results, our effective models must be complemented by more accurate models, as for example tight-binding simulations taking into account the 2D and 3D character of the bands of  $\beta$ -Bi<sub>2</sub>Pd, which is the object of our on-going collaboration with M. Alvarado Herrero and A. Levy Yeyati.

# Annexe A

## One wire system : Linear-in- $q$ term of the self-consistency equation

Let us consider the system represented in Fig. 4.1, made of an infinite superconducting wire along the  $x$ -direction, in the presence of a two component Zeeman field  $\vec{h} = (h_x, 0, h_z)$  and Rashba spin-orbit interaction  $\alpha p \sigma_z$ . The Zeeman field implies spatial oscillations of the superconducting order parameter  $\Delta(x) = \Delta e^{iqx}$ .

In this appendix, we explain how we obtained the linear term in  $q$  in the self-consistency equation Eq. (4.14) in the limit of small fields with respect to the critical temperature  $T_c$ . Specifically, we first expand the self-consistency equation in  $h_x, h_z, q$  and  $\alpha$ , keeping only the term proportional to  $h_x^2 h_z \alpha q$ . Then we perform the integration over  $p$  and show that this term does not contribute to the expansion of the self-consistency equation.

### A.1 Self-consistency equation

Let us recall the self-consistency equation Eq. (4.14) :

$$\ln \left( \frac{T_c}{T_{c0}} \right) = 2 T_c \sum_{\omega_n \geq 0} \left[ \frac{v_F}{2} \int_{-\infty}^{+\infty} \text{Re}(F) dp - \frac{\pi}{\omega_n} \right], \quad (\text{A.1})$$

where  $F = \frac{1}{4} \text{Tr} \left( \frac{G}{\Delta} \tau_x \right)$  and the expression of the Green's function  $G$  is obtained from Eqs. (4.11 - 4.13). Specifically, after doing the change  $p \rightarrow p + q/2$  which does not modify the integral,  $F$  reads :

$$F = -\frac{1}{2} \frac{(i\omega + \xi_p - \alpha p + h_z) (i\omega - \xi_{p+q} + \alpha(p+q) + h_z) + h_x^2}{(i\omega - \xi_{p+q} - \alpha(p+q) - h_z) (i\omega - \xi_{p+q} + \alpha(p+q) + h_z) - h_x^2} \times \frac{1}{(i\omega + \xi_p + \alpha p - h_z) (i\omega + \xi_p - \alpha p + h_z) - h_x^2} + (\alpha \rightarrow -\alpha, h_z \rightarrow -h_z), \quad (\text{A.2})$$

where  $\xi_p = \frac{p^2}{2m} - \mu$ ,  $\mu$  being the chemical potential, and  $\xi_{p+q} = \xi_p + \frac{qp}{m} + \frac{q^2}{2m}$ . To simplify, we will only study the first term, and add the term where  $\alpha \rightarrow -\alpha$  and  $h_z \rightarrow -h_z$  at the end.

To integrate this function analytically, we need to simplify it. Therefore, we will assume that several parameters are small with respect to the critical temperature  $T_c$  :

The Zeeman field components  $h_x$  and  $h_z$ , the spin-orbit energy  $\alpha p_F$  and the energy associated to the superconducting wave-vector  $q v_F$ , where  $p_F$  ( $v_F$ ) is the Fermi momentum (velocity). Moreover, we consider that the chemical potential is the largest energy involved in this system :  $\mu \gg T_c$ .

## A.2 Expansion in $h_x$ and $h_z$

First, we consider that the Zeeman field component  $h_x$  is small :  $h_x \ll T_c$ . Therefore, we expand the anomalous Green's function Eq. (A.2) at second order in  $h_x$  :

$$\begin{aligned}
 F \approx & -\frac{1}{(i\omega + \xi_p + \alpha p - h_z)(i\omega - \xi_{p+q} - \alpha p - \alpha q - h_z)} \\
 & -\frac{h_x^2}{2} \left[ \frac{1}{(i\omega + \xi_p + \alpha p - h_z)(i\omega + \xi_p - \alpha p + h_z)(i\omega - \xi_{p+q} - \alpha p - \alpha q - h_z)(i\omega - \xi_{p+q} + \alpha p + \alpha q + h_z)} \right. \\
 & + \frac{1}{(i\omega + \xi_p + \alpha p - h_z)^2 (i\omega + \xi_p - \alpha p + h_z)(i\omega - \xi_{p+q} - \alpha p - \alpha q - h_z)} \\
 & \left. + \frac{1}{(i\omega + \xi_p + \alpha p - h_z)(i\omega - \xi_{p+q} - \alpha p - \alpha q - h_z)^2 (i\omega - \xi_{p+q} + \alpha p + \alpha q + h_z)} \right]. \tag{A.3}
 \end{aligned}$$

We only keep the second order term in  $h_x$  in Eq. (A.3), that we call  $F_{h_x^2}$ , and expand it at first order in  $h_z$  by considering that  $h_z \ll T_c$ . Then the linear term in  $h_z$  reads :

$$\begin{aligned}
 F_{h_x^2 h_z} \approx & -\frac{h_x^2 h_z}{2} \left[ \frac{1}{(i\omega + \xi_p + \alpha p)^2 (i\omega + \xi_p - \alpha p)(i\omega - \xi_{p+q} - \alpha p - \alpha q)(i\omega - \xi_{p+q} + \alpha p + \alpha q)} \right. \\
 & - \frac{1}{(i\omega + \xi_p + \alpha p)(i\omega + \xi_p - \alpha p)^2 (i\omega - \xi_{p+q} - \alpha p - \alpha q)(i\omega - \xi_{p+q} + \alpha p + \alpha q)} \\
 & + \frac{1}{(i\omega + \xi_p + \alpha p)(i\omega + \xi_p - \alpha p)(i\omega - \xi_{p+q} - \alpha p - \alpha q)^2 (i\omega - \xi_{p+q} + \alpha p + \alpha q)} \\
 & - \frac{1}{(i\omega + \xi_p + \alpha p)(i\omega + \xi_p - \alpha p)(i\omega - \xi_{p+q} - \alpha p - \alpha q)(i\omega - \xi_{p+q} + \alpha p + \alpha q)^2} \\
 & + \frac{1}{(i\omega + \xi_p + \alpha p)^3 (i\omega + \xi_p - \alpha p)(i\omega - \xi_{p+q} - \alpha p - \alpha q)} \\
 & - \frac{1}{(i\omega + \xi_p + \alpha p)^2 (i\omega + \xi_p - \alpha p)^2 (i\omega - \xi_{p+q} - \alpha p - \alpha q)} \\
 & + \frac{1}{(i\omega + \xi_p + \alpha p)^2 (i\omega + \xi_p - \alpha p)(i\omega - \xi_{p+q} - \alpha p - \alpha q)^2} \\
 & + \frac{1}{(i\omega + \xi_p + \alpha p)^2 (i\omega - \xi_{p+q} - \alpha p - \alpha q)^2 (i\omega - \xi_{p+q} + \alpha p + \alpha q)} \\
 & + \frac{1}{(i\omega + \xi_p + \alpha p)(i\omega - \xi_{p+q} - \alpha p - \alpha q)^3 (i\omega - \xi_{p+q} + \alpha p + \alpha q)} \\
 & \left. - \frac{1}{(i\omega + \xi_p + \alpha p)(i\omega - \xi_{p+q} - \alpha p - \alpha q)^2 (i\omega - \xi_{p+q} + \alpha p + \alpha q)^2} \right]. \tag{A.4}
 \end{aligned}$$

## A.3 Linear term in $q$

Since we are interested in the emergence of the modulated phase, one can consider that the wave vector of the superconducting order parameter is small :  $q v_F \ll T_c$ . The terms containing  $q$  have the form :  $\frac{q}{m}(p \pm m\alpha)$ . The spin-orbit energy  $E_{so} = \frac{1}{2} m \alpha^2$  being small with respect to the chemical potential, which is equivalent to  $\alpha \ll v_F$ , the

total term  $\frac{q}{m}(p \pm m\alpha)$  is small with respect to  $T_c$ , so we can expand Eq. (A.4) in  $q$ . Moreover, we are only interested in the linear-in- $q$  term :

$$\begin{aligned}
 F_{h_x^2 h_z q} \approx & -h_x^2 h_z \frac{q}{2m} \left[ \frac{p+m\alpha}{(\mathrm{i}\omega + \xi_p + \alpha p)^2 (\mathrm{i}\omega + \xi_p - \alpha p) (\mathrm{i}\omega - \xi_p - \alpha p)^2 (\mathrm{i}\omega - \xi_p + \alpha p)} \right. \\
 & + \frac{p-m\alpha}{(\mathrm{i}\omega + \xi_p + \alpha p)^2 (\mathrm{i}\omega + \xi_p - \alpha p) (\mathrm{i}\omega - \xi_p - \alpha p) (\mathrm{i}\omega - \xi_p + \alpha p)^2} \\
 & - \frac{p+m\alpha}{(\mathrm{i}\omega + \xi_p + \alpha p) (\mathrm{i}\omega + \xi_p - \alpha p)^2 (\mathrm{i}\omega - \xi_p - \alpha p)^2 (\mathrm{i}\omega - \xi_p + \alpha p)} \\
 & - \frac{p-m\alpha}{(\mathrm{i}\omega + \xi_p + \alpha p) (\mathrm{i}\omega + \xi_p - \alpha p)^2 (\mathrm{i}\omega - \xi_p - \alpha p) (\mathrm{i}\omega - \xi_p + \alpha p)^2} \\
 & + \frac{2(p+m\alpha)}{(\mathrm{i}\omega + \xi_p + \alpha p) (\mathrm{i}\omega + \xi_p - \alpha p) (\mathrm{i}\omega - \xi_p - \alpha p)^3 (\mathrm{i}\omega - \xi_p + \alpha p)} \\
 & + \frac{p-m\alpha}{(\mathrm{i}\omega + \xi_p + \alpha p) (\mathrm{i}\omega + \xi_p - \alpha p) (\mathrm{i}\omega - \xi_p - \alpha p)^2 (\mathrm{i}\omega - \xi_p + \alpha p)^2} \\
 & - \frac{p+m\alpha}{(\mathrm{i}\omega + \xi_p + \alpha p) (\mathrm{i}\omega + \xi_p - \alpha p) (\mathrm{i}\omega - \xi_p - \alpha p)^2 (\mathrm{i}\omega - \xi_p + \alpha p)^2} \\
 & - \frac{2(p-m\alpha)}{(\mathrm{i}\omega + \xi_p + \alpha p) (\mathrm{i}\omega + \xi_p - \alpha p) (\mathrm{i}\omega - \xi_p - \alpha p) (\mathrm{i}\omega - \xi_p + \alpha p)^3} \\
 & + \frac{2(p+m\alpha)}{(\mathrm{i}\omega + \xi_p + \alpha p)^3 (\mathrm{i}\omega + \xi_p - \alpha p) (\mathrm{i}\omega - \xi_p - \alpha p)^2} \\
 & - \frac{p+m\alpha}{(\mathrm{i}\omega + \xi_p + \alpha p)^2 (\mathrm{i}\omega + \xi_p - \alpha p)^2 (\mathrm{i}\omega - \xi_p - \alpha p)^2} \\
 & + \frac{2(p+m\alpha)}{(\mathrm{i}\omega + \xi_p + \alpha p)^2 (\mathrm{i}\omega + \xi_p - \alpha p) (\mathrm{i}\omega - \xi_p - \alpha p)^3} \\
 & + \frac{2(p+m\alpha)}{(\mathrm{i}\omega + \xi_p + \alpha p)^2 (\mathrm{i}\omega - \xi_p - \alpha p)^3 (\mathrm{i}\omega - \xi_p + \alpha p)} \\
 & + \frac{p-m\alpha}{(\mathrm{i}\omega + \xi_p + \alpha p)^2 (\mathrm{i}\omega - \xi_p - \alpha p)^2 (\mathrm{i}\omega - \xi_p + \alpha p)^2} \\
 & + \frac{6(p+m\alpha)}{(\mathrm{i}\omega + \xi_p + \alpha p) (\mathrm{i}\omega - \xi_p - \alpha p)^4 (\mathrm{i}\omega - \xi_p + \alpha p)} \\
 & + \frac{2(p-m\alpha)}{(\mathrm{i}\omega + \xi_p + \alpha p) (\mathrm{i}\omega - \xi_p - \alpha p)^3 (\mathrm{i}\omega - \xi_p + \alpha p)^2} \\
 & - \frac{2(p+m\alpha)}{(\mathrm{i}\omega + \xi_p + \alpha p) (\mathrm{i}\omega - \xi_p - \alpha p)^3 (\mathrm{i}\omega - \xi_p + \alpha p)^2} \\
 & \left. - \frac{2(p-m\alpha)}{(\mathrm{i}\omega + \xi_p + \alpha p) (\mathrm{i}\omega - \xi_p - \alpha p)^2 (\mathrm{i}\omega - \xi_p + \alpha p)^3} \right]. \tag{A.5}
 \end{aligned}$$

## A.4 Expansion in $\alpha$

Finally, assuming that  $\alpha p_F \ll T_c$ , we expand the linear-in- $q$  term Eq. (A.5) at first order in  $\alpha$ . The linear term in  $\alpha$  is thus :

$$\begin{aligned}
 F_{h_x^2 h_z q \alpha} \approx & -\alpha h_x^2 h_z \frac{q}{2m} \left[ 4p^2 \left( \frac{5}{(i\omega_n + \xi)(i\omega - \xi)^6} + \frac{2}{(i\omega + \xi)^2(i\omega - \xi)^5} \right. \right. \\
 & \left. \left. - \frac{1}{(i\omega + \xi)^4(i\omega - \xi)^3} - \frac{1}{(i\omega + \xi)^5(i\omega - \xi)^2} \right) \right. \\
 & + m \left( \frac{4}{(i\omega + \xi)(i\omega - \xi)^5} + \frac{3}{(i\omega + \xi)^2(i\omega - \xi)^4} \right. \\
 & \left. \left. + \frac{2}{(i\omega + \xi)^3(i\omega - \xi)^3} + \frac{1}{(i\omega + \xi)^4(i\omega - \xi)^2} \right) \right]. \quad (\text{A.6})
 \end{aligned}$$

We will now integrate this term with respect to  $p$ .

## A.5 Integration over $p$

Since the linear term of the anomalous Green's function only depends on  $\xi$  and  $p^2$ , we will transform the integral over  $p$  into an integral over  $\xi$  using Eq. (4.16) :

$$\int_{-\infty}^{+\infty} \frac{p^2}{m} f(\xi) dp \approx \frac{2}{v_F} \int_{-\infty}^{+\infty} \xi f(\xi) d\xi + \frac{4\mu}{v_F} \int_{-\infty}^{+\infty} f(\xi) d\xi. \quad (\text{A.7})$$

Using this transformation, we can then integrate Eq. (A.6) by the residue method. The term proportional to  $m$  in Eq. (A.6) gives  $\frac{2\pi\alpha h_x^2 h_z q}{v_F \omega^5}$ , whereas the  $p^2$  term gives  $-\frac{2\pi\alpha h_x^2 h_z q}{v_F \omega^5}$ . Therefore the linear term in  $\alpha$  does not contribute to the linear-in- $q$  term in the self-consistency equation, and we have to go to the order 3 in  $\alpha$  to have a finite contribution, provided in Eq. (4.17).

# Annexe B

## Two wire system : Linear-in- $q$ term of the self-consistency equation

Let us consider the system illustrated in Fig. 4.2. It is made of two infinite wires along the  $x$ -direction, spatially separated but connected via a hopping term  $t$ . The first wire is a normal wire with Rashba spin-orbit interaction  $\alpha p \sigma_z$  and a Zeeman field  $h_z$  parallel to the spin-orbit field. The second one is a superconductor, whose order parameter can oscillate due to the presence of the Zeeman field :  $\Delta(x) = \Delta e^{iqx}$ .

In this appendix, we explain how we obtained the linear term in  $q$  of the self-consistency equation Eq. (4.27) in the limit of small fields with respect to the critical temperature  $T_c$ . Specifically, we first expand the self-consistency equation in  $t$ ,  $h_z$ ,  $q$  and  $\alpha p_F$ , keeping only the term proportional to  $t^2 h_z \alpha q$ . Then, we perform the integration over  $p$ , and show that this term gives a finite contribution to the self-consistency equation.

### B.1 Self-consistency equation

Let us recall the self-consistency equation Eq. (4.26) :

$$\ln \left( \frac{T_c}{T_{c0}} \right) = 2 T_c \sum_{\omega_n \geq 0} \left[ \frac{v_F}{2} \int_{-\infty}^{+\infty} \text{Re}(F) dp - \frac{\pi}{\omega_n} \right], \quad (\text{B.1})$$

where  $F = \frac{1}{4} \text{Tr} \left( \frac{G}{\Delta} \tau_x \frac{\eta_0 - \eta_z}{2} \right)$  and the expression of the Green's function  $G$  is obtained from Eqs. (4.11), (4.24) and (4.25). Specifically, after doing the change  $p \rightarrow p + q/2$  which does not modify the integral,  $F$  reads :

$$2F = - \frac{i\omega_n - \xi_{p+q} - \alpha p - \alpha q - h_z}{(i\omega_n - \xi_{p+q})(i\omega_n - \xi_{p+q} - \alpha p - \alpha q - h_z) - t^2} \times \frac{i\omega_n + \xi_p + \alpha p - h_z}{(i\omega_n + \xi_p)(i\omega_n + \xi_p + \alpha p - h_z) - t^2} - \frac{i\omega_n - \xi_{p+q} + \alpha p + \alpha q + h_z}{(i\omega_n - \xi_{p+q})(i\omega_n - \xi_{p+q} + \alpha p + \alpha q + h_z) - t^2} \times \frac{i\omega_n + \xi_p - \alpha p + h_z}{(i\omega_n + \xi_p)(i\omega_n + \xi_p - \alpha p + h_z) - t^2}, \quad (\text{B.2})$$

where  $\xi_p = \frac{p^2}{2m} - \mu$ ,  $\mu$  being the chemical potential, and  $\xi_{p+q} = \xi_p + \frac{qp}{m} + \frac{q^2}{2m}$ .

To integrate this function analytically, we need to simplify it. Therefore, we will assume that several parameters are small with respect to the critical temperature  $T_c$  : The hopping term  $t$ , the Zeeman field component  $h_z$ , the spin-orbit energy  $\alpha p_F$  and the energy associated to the superconducting wave-vector  $q v_F$ , where  $p_F$  ( $v_F$ ) is the

Fermi momentum (velocity). Moreover, we consider that the chemical potential is the largest energy involved in this system :  $\mu \gg T_c$ .

## B.2 Expansion in $t$

First, let us consider that the hopping term  $t$  is small with respect to the critical temperature :  $t \ll T_c$ . Therefore, we expand the anomalous Green's function Eq. (B.2) at second order in  $t$ , it reads :

$$\begin{aligned}
 F \approx & -\frac{1}{(i\omega_n + \xi_p)(i\omega_n - \xi_{p+q})} \\
 & -\frac{t^2}{2} \left[ \frac{1}{(i\omega_n + \xi_p)(i\omega_n - \xi_{p+q})^2(i\omega_n - \xi_{p+q} - \alpha p - \alpha q - h_z)} \right. \\
 & + \frac{1}{(i\omega_n + \xi_p)^2(i\omega_n - \xi_{p+q})(i\omega_n + \xi_p + \alpha p - h_z)} \\
 & + \frac{1}{(i\omega_n + \xi_p)(i\omega_n - \xi_{p+q})^2(i\omega_n - \xi_{p+q} + \alpha p + \alpha q + h_z)} \\
 & \left. + \frac{1}{(i\omega_n + \xi_p)^2(i\omega_n - \xi_{p+q})(i\omega_n + \xi_p - \alpha p + h_z)} \right]. \tag{B.3}
 \end{aligned}$$

The zeroth order term of Eq. (B.3) corresponds to the anomalous Green's function of an isolated superconducting wire. Therefore, this term will not contribute to the linear-in- $q$  term of the self-consistency equation. In what follows, we keep only the second order term in  $t$ , that we call  $F_{t^2}$ .

## B.3 Expansion in $h_z$

Then we expand the anomalous Green's function Eq. (B.3) at first order in  $h_z$  by considering that  $h_z \ll T_c$  and keep only the linear term in  $h_z$ ,  $F_{t^2 h_z}$  :

$$\begin{aligned}
 F_{t^2 h_z} \approx & -\frac{t^2 h_z}{2} \left[ \frac{1}{(i\omega_n + \xi_p)(i\omega_n - \xi_{p+q})^2(i\omega_n - \xi_{p+q} - \alpha p - \alpha q)^2} \right. \\
 & + \frac{1}{(i\omega_n + \xi_p)^2(i\omega_n - \xi_{p+q})(i\omega_n + \xi_p + \alpha p)^2} \\
 & - \frac{1}{(i\omega_n + \xi_p)(i\omega_n - \xi_{p+q})^2(i\omega_n - \xi_{p+q} + \alpha p + \alpha q)^2} \\
 & \left. - \frac{1}{(i\omega_n + \xi_p)^2(i\omega_n - \xi_{p+q})(i\omega_n + \xi_p - \alpha p)^2} \right]. \tag{B.4}
 \end{aligned}$$

In the following, we will expand Eq. (B.4) over  $q$ . To simplify the expression, one can make the change  $p \rightarrow p - q$  in the first and third terms of Eq. (B.4), which will not

change the integral in the self-consistency equation Eq. (B.1). We obtain :

$$F_{t^2 h_z} \rightarrow -\frac{t^2 h_z}{2} \left[ \frac{1}{(i\omega_n + \xi_{p-q})(i\omega_n - \xi_p)^2 (i\omega_n - \xi_p - \alpha p)^2} + \frac{1}{(i\omega_n + \xi_p)^2 (i\omega_n - \xi_{p+q})(i\omega_n + \xi_p + \alpha p)^2} - \frac{1}{(i\omega_n + \xi_{p-q})(i\omega_n - \xi_p)^2 (i\omega_n - \xi_p + \alpha p)^2} - \frac{1}{(i\omega_n + \xi_p)^2 (i\omega_n - \xi_{p+q})(i\omega_n + \xi_p - \alpha p)^2} \right]. \quad (\text{B.5})$$

## B.4 Linear term in $q$

Since we are interested in the emergence of the modulated phase, one can consider that the wave vector of the superconducting order parameter is small :  $q v_F \ll T_c$ . We are only interested in the linear-in- $q$  term of the self-consistency equation :

$$F_{t^2 h_z q} \approx -t^2 h_z \frac{qp}{2m} \left[ \frac{1}{(i\omega_n + \xi)^2 (i\omega_n - \xi)^2 (i\omega_n - \xi - \alpha p)^2} + \frac{1}{(i\omega_n + \xi)^2 (i\omega_n - \xi)^2 (i\omega_n + \xi + \alpha p)^2} - \frac{1}{(i\omega_n + \xi)^2 (i\omega_n - \xi)^2 (i\omega_n - \xi + \alpha p)^2} - \frac{1}{(i\omega_n + \xi)^2 (i\omega_n - \xi)^2 (i\omega_n + \xi - \alpha p)^2} \right], \quad (\text{B.6})$$

where we have written  $\xi$  instead of  $\xi_p$  for more simplicity.

## B.5 Expansion in $\alpha$

Finally, assuming that  $\alpha p_F \ll T_c$ , we will expand the linear-in- $q$  term Eq. (B.6) at first order in  $\alpha$ . The linear term in  $\alpha$  is thus :

$$F_{t^2 h_z q \alpha} \approx 2 t^2 h_z \alpha q \frac{p^2}{m} \left[ \frac{1}{(i\omega_n + \xi)^5 (i\omega_n - \xi)^2} - \frac{1}{(i\omega_n + \xi)^2 (i\omega_n - \xi)^5} \right]. \quad (\text{B.7})$$

We can now analytically integrate this term with respect to  $p$ .

## B.6 Integration over $p$

Since the linear term of the anomalous Green's function only depends on  $\xi$  and  $p^2$ , we will transform the integral over  $p$  to an integral over  $\xi$  using :

$$\int_{-\infty}^{+\infty} \frac{p^2}{m} f(\xi) dp \approx \frac{2}{v_F} \int_{-\infty}^{+\infty} \xi f(\xi) d\xi + \frac{4\mu}{v_F} \int_{-\infty}^{+\infty} f(\xi) d\xi. \quad (\text{B.8})$$

Using this transformation, it is then straightforward to integrate Eq. (B.7) :

$$\int_{-\infty}^{+\infty} F_{t^2 h_z q \alpha} dp \approx \frac{4 t^2 h_z \alpha q}{v_F} \left[ \int_{-\infty}^{+\infty} \frac{\xi}{(i\omega_n + \xi)^5 (i\omega_n - \xi)^2} d\xi + 2\mu \int_{-\infty}^{+\infty} \frac{d\xi}{(i\omega_n + \xi)^5 (i\omega_n - \xi)^2} - \int_{-\infty}^{+\infty} \frac{\xi}{(i\omega_n + \xi)^2 (i\omega_n - \xi)^5} d\xi - 2\mu \int_{-\infty}^{+\infty} \frac{d\xi}{(i\omega_n + \xi)^2 (i\omega_n - \xi)^5} \right]. \quad (\text{B.9})$$

Using the residue technique to integrate over  $\xi$ , we obtain :

$$\int_{-\infty}^{+\infty} F_{t^2 h_z q \alpha} dp \approx -\frac{3\pi}{4 v_F \omega^5} t^2 h_z \alpha q. \quad (\text{B.10})$$

Then, the linear-in- $q$  term of the self-consistency equation Eq. (B.1), that we call  $B$ , reads :

$$B = -2\pi T_c \sum_{\omega > 0} \frac{3}{8\omega^5} t^2 h_z \alpha q. \quad (\text{B.11})$$

Contrary to the one wire system, the Zeeman component  $h_x$ , which is normal to the spin-orbit field, is not needed to generate the linear-in- $q$  term in the self-consistency relation.

# Annexe C

## Free energy of the S/F bilayer in the presence of a Néel skyrmion

### C.1 Derivation of the magnetoelectric energy $F_L$

In this appendix, we derive the expression of the coupling energy between the superconductor and magnetic order induced by the skyrmion, the so-called Lifshitz invariant  $F_L$  (Eq. 5.23). We start from the Ginzburg-Landau free energy (see Chapter 2, Eq. 2.1) :

$$F^{\text{GL}} = F_0^{\text{GL}} + \int \frac{1}{4m} \left| \hat{D}\Psi \right|^2 d^3\vec{r} + F_L^{\text{GL}}, \quad (\text{C.1})$$

where  $F_0^{\text{GL}}$  contains all the terms without derivative of  $\Psi$  and  $\hat{D} = \left( -i\hbar\vec{\nabla} + 2e\vec{A} \right)$  is the gauge-invariant momentum operator. Because of the interplay between the exchange field  $h_{\text{ex}}$  and the Rashba spin-orbit interaction in the ferromagnetic layer proximity coupled to the superconducting thin film, the order parameter may be spatially modulated (see Chapter 3) :  $\Psi = \Psi_0 e^{i\vec{q}\cdot\vec{r}}$ , where  $\Psi_0$  is a constant.

Within the Ginzburg-Landau formalism, the Lifshitz invariant  $F_L^{\text{GL}}$  reads [5, 71, 139] :

$$F_L^{\text{GL}} = \varepsilon \int \left( \vec{e}_z \times \vec{S} \right) \cdot \left[ \Psi^* \hat{D}\Psi + \text{h.c.} \right] d^3\vec{r}, \quad (\text{C.2})$$

where  $\varepsilon$  is a constant proportional to the Rashba spin-orbit coupling constant  $\alpha_R$ . In the following, we focus on deriving an estimate of  $\varepsilon$ .

From the minimization of the free energy  $F^{\text{GL}}$  with respect to  $\vec{q}$  for  $\vec{A} = \vec{0}$ , it is possible to obtain the expression of the wave-vector  $\vec{q}$  as a function of  $\varepsilon$  :

$$q = -\frac{4m}{\hbar}\varepsilon. \quad (\text{C.3})$$

Moreover, from Ref. [6] we have an estimate of  $q$  :

$$q \approx \frac{\alpha_R h_{\text{ex}}}{\hbar v_F^2}. \quad (\text{C.4})$$

Thus, by comparing both expressions for  $q$ , Eqs. (C.3) and (C.4), we get the following estimate of  $\varepsilon$  :

$$\varepsilon \approx -\frac{\alpha_R h_{\text{ex}}}{4m v_F^2}. \quad (\text{C.5})$$

Contrary to the Ginzburg-Landau formalism, in which temperatures must be close to the critical temperature  $T_c$ , the London approach is valid for  $T \ll T_c$ . However, it is possible to rewrite the Ginzburg-Landau free energy (Eqs. C.1-C.2) in the London approach by taking  $\Psi = \Psi_0 e^{i\varphi}$ , where  $\Psi_0$  is constant such that  $\Psi_0^2 = n_s/2$ , and  $n_s$  is the density of superconducting electrons. Thus, the free energy becomes :

$$F = F_0 + F_{\text{mag}} + \frac{e^2 n_s}{2m} \int (\vec{\phi} - \vec{A})^2 d^3\vec{r} + e n_s \frac{\alpha_R h_{\text{ex}}}{4m v_F^2} \int (\vec{e}_z \times \vec{S}) \cdot (\vec{\phi} - \vec{A}) d^3\vec{r}, \quad (\text{C.6})$$

where  $F_0$  is the free energy in the absence of superconductivity and magnetic field,  $F_{\text{mag}}$  corresponds to the energy of the magnetic field, defined in Eq. (5.7), and  $\vec{\phi}$  is the gradient of the local superconducting phase, given in Eq. (5.6).

For the thin superconducting film of thickness  $d_S \ll \lambda$ , the quantity  $\vec{\phi} - \vec{A}$  is almost constant over  $d_S$ . We emphasize that the spin-orbit interaction and the exchange field penetrate the superconducting layer over a distance  $a$ , corresponding to the atomic thickness. We also assume that the magnetization in the ferromagnetic layer is weak, thus the Zeeman field is negligible compared to the exchange field. Then we can compute the integrals of Eq. (C.6) over the direction normal to the layer,  $z$  :

$$F = F_{\text{mag}} + \frac{d_S}{2\mu_0 \lambda^2} \int (\vec{\phi} - \vec{A})^2 d^2\vec{r} + \frac{\alpha_R h_{\text{ex}} a}{4\mu_0 e \lambda^2 v_F^2} \int (\vec{e}_z \times \vec{S}) \cdot (\vec{\phi} - \vec{A}) d^2\vec{r}, \quad (\text{C.7})$$

where  $\lambda$  is the London penetration length, derived in Chapter 2 (Eq. 2.13). Finally, introducing the effective screening length  $\lambda_{\text{eff}} = d_S/\lambda^2$ , we obtain the final expression of the free energy of the F/S bilayer :

$$F = F_0 + F_{\text{mag}} + \frac{1}{2\mu_0 \lambda_{\text{eff}}} \int (\vec{\phi} - \vec{A})^2 d^2\vec{r} + \alpha_0 \int (\vec{e}_z \times \vec{S}) \cdot (\vec{\phi} - \vec{A}) d^2\vec{r}, \quad (\text{C.8})$$

where  $\alpha_0$  is defined by :

$$\alpha_0 = \frac{1}{4\mu_0 e \lambda_{\text{eff}}} \frac{a}{d_S} \frac{\alpha_R h_{\text{ex}}}{v_F^2}. \quad (\text{C.9})$$

The third term of the free energy (C.8) is the superconducting current energy  $F_{\text{sc}}$  (Eq. 5.5), whereas the last term corresponds to the magnetoelectric energy  $F_L$  (Eq. 5.23).

## C.2 Final expression of the free energy F

Here, we explain how we reworked the above free energy Eq. (C.8) to obtain the expression defined in Eq. (5.31).

Each term of the free energy  $F$  (in which we omit the term  $F_0$ ) can be written in terms of the Fourier transforms  $\vec{A}_{kl}$ ,  $\vec{A}_k$ ,  $\vec{\phi}_k$  and  $\vec{\alpha}_k$  (Eqs. 5.10, 5.11, 5.12 and 5.26) :

$$F_{\text{sc}} = \frac{1}{(2\pi)^2} \frac{1}{2\mu_0 \lambda_{\text{eff}}} \int |\vec{\phi}_k - \vec{A}_k|^2 d^2\vec{k}; \quad (\text{C.10})$$

$$F_L = \frac{1}{(2\pi)^2} \int \vec{\alpha}_k^* \cdot (\vec{\phi}_k - \vec{A}_k) d^2\vec{k}; \quad (\text{C.11})$$

$$F_{\text{mag}} = \frac{1}{(2\pi)^3} \int \frac{|\vec{B}_{kl}|^2}{2\mu_0} d^2\vec{k} dl, \quad (\text{C.12})$$

where  $\vec{B}_{kl}$  is the Fourier transform of  $\vec{B}$ , which may be obtained from Eq. (5.19) :

$$\left| \vec{B}_{kl} \right|^2 = (k^2 + l^2) \left| \vec{A}_{kl} \right|^2 = \frac{4k^2}{k^2 + l^2} \frac{1}{(1 + 2k\lambda_{\text{eff}})^2} \left( \frac{\Phi_0}{k} + \mu_0 \lambda_{\text{eff}} \alpha_k \right)^2, \quad (\text{C.13})$$

where the expression of  $\vec{A}_{kl}$  is given by (Eq. 5.27). After replacing  $\vec{A}_k$  by its expression Eq. (5.28) in Eqs. (C.10) and (C.11) and performing the  $l$  integration in Eq. (C.12), we get the following :

$$F_{\text{sc}} = \frac{\lambda_{\text{eff}}}{4\pi\mu_0} \int \frac{k}{(1 + 2k\lambda_{\text{eff}})^2} (2\Phi_0 - \mu_0 \alpha_k)^2 dk; \quad (\text{C.14})$$

$$F_L = \frac{1}{2\pi} \int \frac{\lambda_{\text{eff}} k}{1 + 2k\lambda_{\text{eff}}} (2\Phi_0 - \mu_0 \alpha_k) \alpha_k dk; \quad (\text{C.15})$$

$$F_{\text{mag}} = \frac{1}{2\pi\mu_0} \int \frac{(\Phi_0 + \mu_0 \lambda_{\text{eff}} k \alpha_k)^2}{(1 + 2k\lambda_{\text{eff}})^2} dk. \quad (\text{C.16})$$

Finally, the free energy  $F = F_{\text{sc}} + F_L + F_{\text{mag}}$  can be ordered with respect to  $\Phi_0$  and  $\alpha_k$  :

$$F = \frac{\Phi_0^2}{2\pi\mu_0} \int \frac{dk}{1 + 2k\lambda_{\text{eff}}} - \frac{\mu_0 e^2}{4\pi} \int \frac{k\lambda_{\text{eff}}}{1 + 2k\lambda_{\text{eff}}} \alpha_k^2 dk - \frac{\Phi_0 e}{\pi} \int \frac{k\lambda_{\text{eff}}}{1 + 2k\lambda_{\text{eff}}} \alpha_k dk. \quad (\text{C.17})$$

The first term of Eq. (C.17), proportional to  $\Phi_0^2$ , is the self-energy of the vortex,  $F_v$ . The second one is proportional to  $\alpha_k^2$ , and corresponds to the current energy induced by the skyrmion,  $F_s$ , whereas the third term, depending on the product  $\Phi_0 \alpha_k$ , is the energy resulting from the interaction between the vortex and the skyrmion, called  $F_{\text{int}}$ .



# Bibliography

- [1] P. Fulde and R. A. Ferrell, “Superconductivity in a strong spin-exchange field,” *Physical Review*, vol. 135, no. 3A, p. A550, 1964. [1](#), [15](#), [16](#), [18](#)
- [2] A. I. Larkin and Y. N. Ovchinnikov, “Nonuniform state of superconductors,” *Zh. Eksp. Teor. Fiz.*, vol. 47, pp. 1136–1146, 1964. [Sov. Phys. JETP 20, 762 (1965)]. [1](#), [15](#), [16](#), [20](#)
- [3] C. C. Agosta, L. Bishop-Van Horn, and M. Newman, “The Signature of Inhomogeneous Superconductivity,” *Journal of Low Temperature Physics*, vol. 185, pp. 220–229, Nov. 2016. [1](#)
- [4] V. Barzykin and L. P. Gor’kov, “Inhomogeneous Stripe Phase Revisited for Surface Superconductivity,” *Physical Review Letters*, vol. 89, p. 227002, Nov. 2002. [1](#), [15](#), [24](#), [27](#)
- [5] K. V. Samokhin, “Magnetic properties of superconductors with strong spin-orbit coupling,” *Physical Review B*, vol. 70, p. 104521, Sept. 2004. [1](#), [15](#), [27](#), [52](#), [87](#)
- [6] O. Dimitrova and M. V. Feigel’man, “Theory of 2d superconductor with broken inversion symmetry,” *Physical Review B*, vol. 76, p. 014522, July 2007. [1](#), [24](#), [31](#), [34](#), [87](#)
- [7] D. F. Agterberg and R. P. Kaur, “Magnetic-field-induced helical and stripe phases in Rashba superconductors,” *Physical Review B*, vol. 75, p. 064511, Feb. 2007. [1](#), [24](#)
- [8] M. Houzet and J. S. Meyer, “Quasiclassical theory of disordered Rashba superconductors,” *Physical Review B*, vol. 92, p. 014509, July 2015. [1](#)
- [9] G. Zwicknagl, S. Jahns, and P. Fulde, “Critical magnetic field of ultrathin superconducting films and interfaces,” *Journal of the Physical Society of Japan*, vol. 86, p. 083701, Aug. 2017. [1](#), [44](#)
- [10] D. F. Agterberg, “Magnetoelectric Effects, Helical Phases, and FFLO Phases,” in *Non-Centrosymmetric Superconductors : Introduction and Overview* (E. Bauer and M. Sigrist, eds.), pp. 155–170, Berlin, Heidelberg : Springer Berlin Heidelberg, 2012. [1](#), [24](#), [29](#)
- [11] T. Ojanen, “Magnetoelectric Effects in Superconducting Nanowires with Rashba Spin-Orbit Coupling,” *Physical Review Letters*, vol. 109, p. 226804, Nov. 2012. [1](#), [15](#), [27](#), [30](#), [34](#), [44](#), [45](#)
- [12] F. Konschelle, I. V. Tokatly, and F. S. Bergeret, “Theory of the spin-galvanic effect and the anomalous phase shift  $\varphi_0$  in superconductors and Josephson junctions with intrinsic spin-orbit coupling,” *Physical Review B*, vol. 92, no. 125443, p. 125443, 2015. [1](#), [15](#), [27](#), [28](#), [45](#)
- [13] F. S. Bergeret and I. V. Tokatly, “Manifestation of extrinsic spin Hall effect in superconducting structures : Nondissipative magnetoelectric effects,” *Physical Review B*, vol. 94, p. 180502, Nov. 2016. [1](#)

- 
- [14] A. Buzdin, “Direct Coupling Between Magnetism and Superconducting Current in the Josephson  $\phi_0$  Junction,” *Physical Review Letters*, vol. 101, p. 107005, Sept. 2008. [1](#), [15](#), [27](#), [28](#), [45](#), [77](#)
- [15] J. Baumard, J. Cayssol, F. S. Bergeret, and A. Buzdin, “Generation of a superconducting vortex via Néel skyrmions,” *Physical Review B*, vol. 99, no. 014511, p. 7, 2019. [2](#), [28](#)
- [16] A. A. Abrikosov, “On the Magnetic Properties of Superconductors of the Second Group,” *Sov. Phys. JETP*, vol. 5, p. 1174, 1957. [2](#), [9](#), [47](#)
- [17] S. Rex, I. V. Gornyi, and A. D. Mirlin, “Majorana bound states in magnetic skyrmions imposed onto a superconductor,” *Physical Review B*, vol. 100, p. 064504, 2019. [2](#), [78](#)
- [18] S. Nadj-Perge, I. K. Drozdov, B. A. Bernevig, and A. Yazdani, “Proposal for realizing Majorana fermions in chains of magnetic atoms on a superconductor,” *Physical Review B*, vol. 88, p. 020407, July 2013. [2](#), [59](#), [65](#)
- [19] F. Pientka, L. I. Glazman, and F. von Oppen, “Topological superconducting phase in helical Shiba chains,” *Physical Review B*, vol. 88, p. 155420, Oct. 2013. [2](#), [59](#), [65](#)
- [20] B. Braunecker and P. Simon, “Interplay between Classical Magnetic Moments and Superconductivity in Quantum One-Dimensional Conductors : Toward a Self-Sustained Topological Majorana Phase,” *Phys. Rev. Lett.*, vol. 111, p. 147202, Oct. 2013. [2](#), [59](#), [65](#)
- [21] S. Nadj-Perge, I. K. Drozdov, J. Li, H. Chen, S. Jeon, J. Seo, A. H. MacDonald, B. A. Bernevig, and A. Yazdani, “Observation of Majorana fermions in ferromagnetic atomic chains on a superconductor,” *Science*, vol. 346, pp. 602–607, Oct. 2014. [2](#), [59](#), [65](#)
- [22] J. Li, H. Chen, I. K. Drozdov, A. Yazdani, B. A. Bernevig, and A. H. MacDonald, “Topological superconductivity induced by ferromagnetic metal chains,” *Physical Review B*, vol. 90, p. 235433, Dec. 2014. [2](#), [59](#), [65](#)
- [23] F. Pientka, L. I. Glazman, and F. von Oppen, “Unconventional topological phase transitions in helical Shiba chains,” *Physical Review B*, vol. 89, p. 180505, May 2014. [2](#), [59](#), [65](#)
- [24] K. Pöyhönen, A. Westström, J. Röntynen, and T. Ojanen, “Majorana states in helical Shiba chains and ladders,” *Physical Review B*, vol. 89, p. 115109, Mar. 2014. [2](#), [59](#), [65](#)
- [25] B. Braunecker and P. Simon, “Self-stabilizing temperature-driven crossover between topological and nontopological ordered phases in one-dimensional conductors,” *Phys. Rev. B*, vol. 92, p. 241410, Dec. 2015. [2](#), [59](#), [65](#)
- [26] F. Pientka, Y. Peng, L. Glazman, and F. v. Oppen, “Topological superconducting phase and Majorana bound states in Shiba chains,” *Physica Scripta*, vol. T164, p. 014008, Dec. 2015. [2](#), [59](#), [65](#)
- [27] L. Yu, “Bound state in superconductors with paramagnetic impurities,” *Acta Physica Sinica*, vol. 21, no. 1, p. 75, 1965. [2](#), [59](#), [60](#)
- [28] H. Shiba, “Classical Spins in Superconductors,” *Progress of Theoretical Physics*, vol. 40, pp. 435–451, Sept. 1968. [2](#), [59](#), [60](#)
- [29] A. Rusinov, “Superconductivity near a paramagnetic impurity,” *Zh. Eksp. Teor. Fiz. Pisma Red.*, vol. 9, p. 146, 1969. [2](#), [59](#), [60](#)

- [30] A. I. Rusinov, “On the theory of gapless superconductivity in alloys containing paramagnetic impurities,” *Zh. Eksp. Teor. Fiz.*, vol. 56, p. 2047, 1969. [Sov. Phys. JETP 29, 1101 (1969)]. [2](#), [59](#), [60](#)
- [31] A. Yazdani, B. A. Jones, C. P. Lutz, M. F. Crommie, and D. M. Eigler, “Probing the Local Effects of Magnetic Impurities on Superconductivity,” *Science*, vol. 275, pp. 1767–1770, Mar. 1997. [2](#), [59](#), [60](#), [64](#)
- [32] V. Kaladzhyan, C. Bena, and P. Simon, “Asymptotic behavior of impurity-induced bound states in low-dimensional topological superconductors,” *Journal of Physics : Condensed Matter*, vol. 28, p. 485701, Dec. 2016. [2](#), [64](#), [66](#)
- [33] H. K. Onnes, “The resistance of pure mercury at helium temperatures,” *Commun. Phys. Lab. Univ. Leiden*, vol. 12, p. 120, 1911. [5](#)
- [34] F. London and H. London, “The electromagnetic equations of the supraconductor,” *Proceedings of the Royal Society London A*, vol. 149, p. 71, 1935. [5](#)
- [35] A. B. Pippard, “An Experimental and Theoretical Study of the Relation between Magnetic Field and Current in a Superconductor,” *Proceedings of the Royal Society London A*, vol. 216, p. 547, 1953. [5](#)
- [36] V. L. Ginzburg and L. D. Landau, “On the theory of Superconductivity,” *Zh. Eksp. Teor. Fiz.*, vol. 20, 1950. [5](#)
- [37] J. Bardeen, L. N. Cooper, and J. R. Schrieffer, “Theory of Superconductivity,” *Physical Review*, vol. 108, pp. 1175–1204, Dec. 1957. [5](#), [10](#)
- [38] L. N. Cooper, “Bound Electron Pairs in a Degenerate Fermi Gas,” *Physical Review*, vol. 104, pp. 1189–1190, Nov. 1956. [5](#), [10](#)
- [39] P. G. D. Gennes, *Superconductivity of Metals and Alloys*. Benjamin, 1966. [5](#), [47](#), [48](#), [52](#)
- [40] L. P. Gor’Kov, “On the energy spectrum of superconductors,” *Sov. Phys. JETP*, vol. 34, p. 735, 1958. [5](#), [10](#), [11](#)
- [41] L. P. Gor’Kov, “Microscopic derivation of the Ginzburg-Landau equations in the theory of superconductivity,” *Zh. Eksp. Teor. Fiz.*, vol. 36, p. 1918, 1959. [Sov. Phys. JETP 9, 1364 (1959)]. [5](#)
- [42] M. Tinkham, *Introduction to superconductivity, Second Edition*. Dover Publications, 2004. [6](#), [10](#)
- [43] A. Fetter and J. Walecka, *Quantum Theory of Many-particle Systems*. Dover Books on Physics, Dover Publications, 2003. [6](#), [10](#)
- [44] L. D. Landau, “Theory of phase transformations. I,” *Zh. Eksp. Teor. Fiz.*, vol. 7, p. 19, 1937. [Phys. Z. Sowjetunion 11, 26 (1937)]. [6](#)
- [45] L. D. Landau, “Theory of phase transformations. II,” *Zh. Eksp. Teor. Fiz.*, vol. 7, p. 627, 1937. [Phys. Z. Sowjetunion 11, 545 (1937)]. [6](#)
- [46] V. M. Edelstein, “Characteristics of the Cooper pairing in two-dimensional non-centrosymmetric electron systems,” *Zh. Eksp. Teor. Fiz.*, vol. 95, p. 2151, 1989. [Sov. Phys. JETP 78, 401 (1989)]. [15](#)
- [47] S. H. Jacobsen, J. A. Ouassou, and J. Linder, “Critical temperature and tunneling spectroscopy of superconductor-ferromagnet hybrids with intrinsic Rashba-Dresselhaus spin-orbit coupling,” *Physical Review B*, vol. 92, p. 024510, July 2015. [15](#), [27](#)

- [48] K. N. Nesterov, M. Houzet, and J. S. Meyer, “Anomalous Josephson effect in semiconducting nanowires as a signature of the topologically nontrivial phase,” *Physical Review B*, vol. 93, p. 174502, May 2016. [15](#), [27](#), [30](#), [34](#), [44](#)
- [49] S. V. Mironov and A. I. Buzdin, “Spontaneous currents in superconducting systems with strong spin-orbit coupling,” *Physical Review Letters*, vol. 118, p. 077001, Feb. 2017. [15](#), [27](#), [45](#), [52](#)
- [50] I. V. Bobkova, A. M. Bobkov, and M. A. Silaev, “Gauge theory of the long-range proximity effect and spontaneous currents in superconducting heterostructures with strong ferromagnets,” *Physical Review B*, vol. 96, p. 094506, Sept. 2017. [15](#), [27](#)
- [51] F. S. Bergeret and I. V. Tokatly, “Singlet-Triplet Conversion and the Long-Range Proximity Effect in Superconductor-Ferromagnet Structures with Generic Spin Dependent Fields,” *Physical Review Letters*, vol. 110, p. 117003, Mar. 2013. [15](#), [27](#)
- [52] F. S. Bergeret and I. V. Tokatly, “Spin-orbit coupling as a source of long-range triplet proximity effect in superconductor-ferromagnet hybrid structures,” *Physical Review B*, vol. 89, p. 134517, Apr. 2014. [15](#), [27](#), [30](#), [45](#)
- [53] B. S. Chandrasekhar, “A note on the maximum critical field of high-field superconductors,” *Applied Physics Letters*, vol. 1, pp. 7–8, Sept. 1962. [17](#)
- [54] A. M. Clogston, “Upper Limit for the Critical Field in Hard Superconductors,” *Physical Review Letters*, vol. 9, pp. 266–267, Sept. 1962. [17](#)
- [55] D. Saint-James, G. Sarma, and E. J. Thomas, *Type II Superconductivity [by] D. Saint-James, and G. Sarma, [and] E.J. Thomas*. International series of monographs in natural philosophy, v. 17, Pergamon Press, 1969. [17](#)
- [56] M. Strongin and O. F. Kammerer, “Effect of Electron-Spin Paramagnetism on the Critical Field of Thin Al Films,” *Physical Review Letters*, vol. 16, pp. 456–460, Mar. 1966. [17](#)
- [57] A. I. Buzdin and S. V. Polonskii, “Nonuniform state in quasi-1d superconductors,” *Sov. Phys. JETP*, vol. 66, no. 422, p. 8, 1987. [18](#), [19](#), [20](#)
- [58] T. M. Rice, “Superconductivity in One and Two Dimensions,” *Physical Review*, vol. 140, pp. A1889–A1891, Dec. 1965. [19](#)
- [59] A. I. Buzdin and L. N. Bulaevskii, “Organic superconductors,” *Soviet Physics Uspekhi*, vol. 27, pp. 830–844, Nov. 1984. [19](#)
- [60] M. D. Croitoru and A. I. Buzdin, “Peculiarities of the orbital effect in the Fulde-Ferrell-Larkin-Ovchinnikov state in quasi-one-dimensional superconductors,” *Phys. Rev. B*, vol. 89, p. 224506, June 2014. [19](#)
- [61] T. Tsuzuki, “On the long-range order in superconducting intercalated layer compounds,” *Journal of Low Temperature Physics*, vol. 9, pp. 525–538, Dec. 1972. [19](#)
- [62] C. C. Agosta, N. A. Fortune, S. T. Hannahs, S. Gu, L. Liang, J.-H. Park, and J. A. Schleuter, “Calorimetric Measurements of Magnetic-Field-Induced Inhomogeneous Superconductivity Above the Paramagnetic Limit,” *Physical Review Letters*, vol. 118, p. 267001, June 2017. [22](#), [23](#)
- [63] L. G. Azlamazov, “Influence of impurities on the existence of an inhomogeneous state in a ferromagnet superconductor,” *Soviet Physics JETP*, vol. 28, pp. 773–775, Apr. 1969. [22](#)

- [64] Y. Matsuda and H. Shimahara, “Fulde-Ferrell-Larkin-Ovchinnikov State in Heavy Fermion Superconductors,” *Journal of the Physical Society of Japan*, vol. 76, p. 051005, May 2007. [22](#)
- [65] A. Bianchi, R. Movshovich, C. Capan, P. G. Pagliuso, and J. L. Sarrao, “Possible Fulde-Ferrell-Larkin-Ovchinnikov Superconducting State in  $\text{CeCoIn}_5$ ,” *Physical Review Letters*, vol. 91, p. 187004, Oct. 2003. [22](#)
- [66] B.-L. Young, R. R. Urbano, N. J. Curro, J. D. Thompson, J. L. Sarrao, A. B. Vorontsov, and M. J. Graf, “Microscopic Evidence for Field-Induced Magnetism in  $\text{CeCoIn}_5$ ,” *Physical Review Letters*, vol. 98, p. 036402, Jan. 2007. [22](#)
- [67] J. A. Wright, E. Green, P. Kuhns, A. Reyes, J. Brooks, J. Schlueter, R. Kato, H. Yamamoto, M. Kobayashi, and S. E. Brown, “Zeeman-Driven Phase Transition within the Superconducting State of  $\kappa$ -(BEDT-TTF) $_2$  Cu(NCS) $_2$ ,” *Physical Review Letters*, vol. 107, p. 087002, Aug. 2011. [22](#), [23](#)
- [68] H. Mayaffre, S. Krämer, M. Horvatić, C. Berthier, K. Miyagawa, K. Kanoda, and V. F. Mitrović, “Evidence of Andreev bound states as a hallmark of the FFLO phase in  $\kappa$ -(BEDT-TTF) $_2$  Cu(NCS) $_2$ ,” *Nature Physics*, vol. 10, pp. 928–932, Dec. 2014. [22](#), [23](#)
- [69] C. C. Agosta, J. Jin, W. A. Coniglio, B. E. Smith, K. Cho, I. Stroe, C. Martin, S. W. Tozer, T. P. Murphy, E. C. Palm, J. A. Schlueter, and M. Kurmoo, “Experimental and semiempirical method to determine the Pauli-limiting field in quasi-two-dimensional superconductors as applied to  $\kappa$ -(BEDT-TTF) $_2$  Cu(NCS) $_2$  : Strong evidence of a FFLO state,” *Physical Review B*, vol. 85, p. 214514, June 2012. [22](#), [23](#)
- [70] R. Lortz, Y. Wang, A. Demuer, P. H. M. Böttger, B. Bergk, G. Zwicky, Y. Nakazawa, and J. Wosnitza, “Calorimetric Evidence for a Fulde-Ferrell-Larkin-Ovchinnikov Superconducting State in the Layered Organic Superconductor  $\kappa$ -(BEDT-TTF) $_2$  Cu(NCS) $_2$ ,” *Physical Review Letters*, vol. 99, p. 187002, Oct. 2007. [22](#), [23](#)
- [71] V. M. Edelstein, “The Ginzburg - Landau equation for superconductors of polar symmetry,” *Journal of Physics : Condensed Matter*, vol. 8, pp. 339–349, Jan. 1996. [24](#), [29](#), [52](#), [87](#)
- [72] V. M. Edelstein, “Magnetoelectric Effect in Polar Superconductors,” *Physical Review Letters*, vol. 75, pp. 2004–2007, Sept. 1995. [24](#), [28](#), [52](#)
- [73] O. V. Dimitrova and M. V. Feigel’man, “Phase diagram of a surface superconductor in parallel magnetic field,” *Journal of Experimental and Theoretical Physics Letters*, vol. 78, pp. 637–641, Nov. 2003. [Pis’ma v ZhETF 78, 1132 (2003)]. [24](#)
- [74] K. V. Samokhin, “Upper critical field in noncentrosymmetric superconductors,” *Physical Review B*, vol. 78, p. 224520, Dec. 2008. [24](#)
- [75] N. Hiasa, T. Saiki, and R. Ikeda, “Vortex lattice structure dependent on pairing symmetry in Rashba superconductors,” *Physical Review B*, vol. 80, p. 014501, July 2009. [24](#)
- [76] L. Santos, T. Neupert, C. Chamon, and C. Mudry, “Superconductivity on the surface of topological insulators and in two-dimensional noncentrosymmetric materials,” *Physical Review B*, vol. 81, p. 184502, May 2010. [24](#)
- [77] R. M. Lutchyn, J. D. Sau, and S. Das Sarma, “Majorana Fermions and a Topological Phase Transition in Semiconductor-Superconductor Heterostructures,” *Physical Review Letters*, vol. 105, p. 077001, Aug. 2010. [27](#), [45](#)

- [78] Y. Oreg, G. Refael, and F. von Oppen, “Helical Liquids and Majorana Bound States in Quantum Wires,” *Physical Review Letters*, vol. 105, p. 177002, Oct. 2010. [27](#), [45](#)
- [79] J. Alicea, “New directions in the pursuit of Majorana fermions in solid state systems,” *Reports on Progress in Physics*, vol. 75, p. 076501, July 2012. [27](#), [45](#)
- [80] C. W. J. Beenakker, “Search for Majorana fermions in superconductors,” *Annual Review of Condensed Matter Physics*, vol. 4, pp. 113–136, Apr. 2013. [27](#)
- [81] G.-Q. Zha, L. Covaci, F. M. Peeters, and S.-P. Zhou, “Majorana zero-energy modes and spin current evolution in mesoscopic superconducting loop systems with spin-orbit interaction,” *Physical Review B*, vol. 92, p. 094516, Sept. 2015. [27](#)
- [82] C. Reeg and D. L. Maslov, “Transport signatures of topological superconductivity in a proximity-coupled nanowire,” *Physical Review B*, vol. 95, p. 205439, May 2017. [27](#)
- [83] O. M. Auslaender, H. Steinberg, A. Yacoby, Y. Tserkovnyak, B. I. Halperin, K. W. Baldwin, L. N. Pfeiffer, and K. W. West, “Spin-Charge Separation and Localization in One Dimension,” *Science*, vol. 308, no. 5718, pp. 88–92, 2005. [27](#), [34](#)
- [84] O. M. Auslaender, A. Yacoby, R. de Piccioto, K. W. Baldwin, L. N. Pfeiffer, and K. W. West, “Tunneling Spectroscopy of the Elementary Excitations in a One-Dimensional Wire,” *Science*, vol. 295, pp. 825–828, Feb. 2002. [27](#), [34](#)
- [85] H. Steinberg, G. Barak, A. Yacoby, L. N. Pfeiffer, K. W. West, B. I. Halperin, and K. Le Hur, “Charge fractionalization in quantum wires,” *Nature Physics*, vol. 4, pp. 116–119, Feb. 2008. [27](#), [34](#)
- [86] C. Scheller, T.-M. Liu, G. Barak, A. Yacoby, L. Pfeiffer, K. West, and D. Zumbühl, “Possible Evidence for Helical Nuclear Spin Order in GaAs Quantum Wires,” *Physical Review Letters*, vol. 112, p. 066801, Feb. 2014. [27](#), [34](#)
- [87] M. I. D’Yakonov and V. I. Perel’, “Possibility of Orienting Electron Spins with Current,” *Journal of Experimental and Theoretical Physics Letters*, vol. 13, p. 467, 1971. [28](#)
- [88] M. I. D’Yakonov and V. I. Perel’, “Current-induced spin orientation of electrons in semiconductors,” *Physics Letters A*, vol. 35, p. 459, 1971. [28](#)
- [89] A. G. Aronov and Y. Lyanda-Geller, “Nuclear electric resonance and orientation of carrier spins by an electric field,” *Journal of Experimental and Theoretical Physics Letters*, vol. 50, p. 431, 1989. [28](#)
- [90] V. M. Edelstein, “Spin polarization of conduction electrons induced by electric current in two-dimensional asymmetric electron systems,” *Solid State Communications*, vol. 73, no. 3, pp. 233 – 235, 1990. [28](#)
- [91] Y. K. Kato, R. C. Myers, A. C. Gossard, and D. D. Awschalom, “Current-Induced Spin Polarization in Strained Semiconductors,” *Physical Review Letters*, vol. 93, p. 176601, Oct. 2004. [28](#)
- [92] A. Y. Silov, P. A. Blajnov, J. H. Wolter, R. Hey, K. H. Ploog, and N. S. Averkiev, “Current-induced spin polarization at a single heterojunction,” *Applied Physics Letters*, vol. 85, p. 5929, 2004. [28](#)

- [93] J. C. Rojas Sánchez, L. Vila, G. Desfonds, S. Gambarelli, J. P. Attané, J. M. De Teresa, C. Magén, and A. Fert, “Spin-to-charge conversion using Rashba coupling at the interface between non-magnetic materials,” *Nature Communications*, vol. 4, p. 2944, Dec. 2013. [28](#)
- [94] Q. Shao, G. Yu, Y.-W. Lan, Y. Shi, M.-Y. Li, C. Zheng, X. Zhu, L.-J. Li, P. K. Amiri, and K. L. Wang, “Strong Rashba-Edelstein Effect-Induced Spin-Orbit Torques in Monolayer Transition Metal Dichalcogenide/Ferromagnet Bilayers,” *Nano Letters*, vol. 16, pp. 7514–7520, Dec. 2016. [28](#)
- [95] Q. Song, H. Zhang, T. Su, W. Yuan, Y. Chen, W. Xing, J. Shi, J. Sun, and W. Han, “Observation of inverse Edelstein effect in Rashba-split 2deg between Sr-TiO<sub>3</sub> and LaAlO<sub>3</sub> at room temperature,” *Science Advances*, vol. 3, p. e1602312, Mar. 2017. [28](#)
- [96] S. K. Yip, “Two-dimensional superconductivity with strong spin-orbit interaction,” *Physical Review B*, vol. 65, p. 144508, Mar. 2002. [28](#)
- [97] F. S. Bergeret and I. V. Tokatly, “Theory of diffusive  $\varphi_0$  Josephson junctions in the presence of spin-orbit coupling,” *EPL (Europhysics Letters)*, vol. 110, p. 57005, June 2015. [28](#), [29](#), [45](#)
- [98] D. S. Rabinovich, I. V. Bobkova, A. M. Bobkov, and M. A. Silaev, “Magnetoelectric effects in superconductor/ferromagnet bilayers,” *Physical Review B*, vol. 99, p. 214501, June 2019. [28](#)
- [99] I. V. Tokatly, “Equilibrium Spin Currents : Non-Abelian Gauge Invariance and Color Diamagnetism in Condensed Matter,” *Physical Review Letters*, vol. 101, p. 106601, Sept. 2008. [28](#), [29](#)
- [100] C. Gorini, P. Schwab, R. Raimondi, and A. L. Shelankov, “Non-Abelian gauge fields in the gradient expansion : Generalized Boltzmann and Eilenberger equations,” *Physical Review B*, vol. 82, p. 195316, Nov. 2010. [28](#)
- [101] F. Konschelle, I. V. Tokatly, and F. S. Bergeret, “Ballistic Josephson junctions in the presence of generic spin dependent fields,” *Physical Review B*, vol. 94, p. 014515, July 2016. [28](#), [45](#)
- [102] D. F. Agterberg, E. Babaev, and J. Garaud, “Microscopic prediction of skyrmion lattice state in clean interface superconductors,” *Physical Review B*, vol. 90, p. 064509, Aug. 2014. [29](#)
- [103] O. V. Dimitrova and M. V. Feigel’man, “Two-dimensional S-N-S junction with Rashba spin-orbit coupling,” *Journal of Experimental and Theoretical Physics*, vol. 102, pp. 652–660, Apr. 2006. [40](#)
- [104] A. I. Buzdin, “Proximity effects in superconductor-ferromagnet heterostructures,” *Reviews of Modern Physics*, vol. 77, pp. 935–976, Sept. 2005. [45](#)
- [105] F. S. Bergeret, A. F. Volkov, and K. B. Efetov, “Odd triplet superconductivity and related phenomena in superconductor-ferromagnet structures,” *Reviews of Modern Physics*, vol. 77, pp. 1321–1373, Nov. 2005. [45](#)
- [106] J. Linder and J. W. A. Robinson, “Superconducting spintronics,” *Nature Physics*, vol. 11, pp. 307–315, Apr. 2015. [45](#)
- [107] M. G. Blamire and J. W. A. Robinson, “The interface between superconductivity and magnetism : understanding and device prospects,” *Journal of Physics : Condensed Matter*, vol. 26, p. 453201, Nov. 2014. [45](#)

- 
- [108] A. Y. Kitaev, “Unpaired Majorana fermions in quantum wires,” *Physics-Uspekhi*, vol. 44, pp. 131–136, Oct. 2001. [45](#)
- [109] C. Nayak, S. H. Simon, A. Stern, M. Freedman, and S. Das Sarma, “Non-Abelian anyons and topological quantum computation,” *Reviews of Modern Physics*, vol. 80, pp. 1083–1159, Sept. 2008. [45](#)
- [110] C.-T. Wu, B. M. Anderson, W.-H. Hsiao, and K. Levin, “Majorana zero modes in spintronics devices,” *Physical Review B*, vol. 95, p. 014519, Jan. 2017. [45](#)
- [111] A. M. Black-Schaffer and J. Linder, “Majorana fermions in spin-orbit-coupled ferromagnetic Josephson junctions,” *Physical Review B*, vol. 84, p. 180509, Nov. 2011. [45](#)
- [112] M. Garnier, A. Mesaros, and P. Simon, “Topological superconductivity with deformable magnetic skyrmions,” *Communications Physics*, vol. 2, p. 126, Oct. 2019. [45](#)
- [113] F. Konschelle and A. Buzdin, “Magnetic Moment Manipulation by a Josephson Current,” *Physical Review Letters*, vol. 102, p. 017001, Jan. 2009. [45](#)
- [114] S. S. Pershoguba, K. Björnson, A. M. Black-Schaffer, and A. V. Balatsky, “Currents Induced by Magnetic Impurities in Superconductors with Spin-Orbit Coupling,” *Physical Review Letters*, vol. 115, p. 116602, Sept. 2015. [45](#)
- [115] E. M. Chudnovsky, “Manipulating magnetic moments by superconducting currents,” *Physical Review B*, vol. 95, p. 100503, Mar. 2017. [45](#)
- [116] Y. V. Fominov, A. F. Volkov, and K. B. Efetov, “Josephson effect due to the long-range odd-frequency triplet superconductivity in S F S junctions with Néel domain walls,” *Physical Review B*, vol. 75, p. 104509, Mar. 2007. [45](#)
- [117] I. Kulagina and J. Linder, “Spin supercurrent, magnetization dynamics, and  $\varphi$ -state in spin-textured Josephson junctions,” *Physical Review B*, vol. 90, p. 054504, Aug. 2014. [45](#)
- [118] K. Halterman, O. T. Valls, and P. H. Barsic, “Induced triplet pairing in clean s-wave superconductor/ferromagnet layered structures,” *Physical Review B*, vol. 77, p. 174511, May 2008. [45](#)
- [119] V. Braude and Y. V. Nazarov, “Fully Developed Triplet Proximity Effect,” *Physical Review Letters*, vol. 98, p. 077003, Feb. 2007. [45](#)
- [120] M. A. Silaev, I. V. Tokatly, and F. S. Bergeret, “Anomalous current in diffusive ferromagnetic Josephson junctions,” *Physical Review B*, vol. 95, p. 184508, May 2017. [45](#)
- [121] J. W. A. Robinson, J. D. S. Witt, and M. G. Blamire, “Controlled Injection of Spin-Triplet Supercurrents into a Strong Ferromagnet,” *Science*, vol. 329, p. 59, July 2010. [45](#)
- [122] A. S. Mel’nikov, A. V. Samokhvalov, S. M. Kuznetsova, and A. I. Buzdin, “Interference Phenomena and Long-Range Proximity Effect in Clean Superconductor-Ferromagnet Systems,” *Physical Review Letters*, vol. 109, p. 237006, Dec. 2012. [45](#)
- [123] T. Skyrme, “A non-linear field theory,” *Proceedings of the Royal Society London A*, vol. 260, no. 127, p. 12, 1961. [46](#)
- [124] F. Jonietz, S. Mühlbauer, C. Pfleiderer, A. Neubauer, W. Münzer, A. Bauer, T. Adams, R. Georgii, P. Böni, R. A. Duine, K. Everschor, M. Garst, and

- A. Rosch, “Spin Transfer Torques in MnSi at Ultralow Current Densities,” *Science*, vol. 330, p. 1648, 2010. [46](#)
- [125] N. S. Kiselev, A. N. Bogdanov, R. Schäfer, and U. K. Rößler, “Chiral skyrmions in thin magnetic films : new objects for magnetic storage technologies?,” *J. Phys. D : Appl. Phys.*, vol. 44, p. 392001, 2011. [46](#)
- [126] X. Yu, N. Kanazawa, W. Zhang, T. Nagai, T. Hara, K. Kimoto, Y. Matsui, Y. Onose, and Y. Tokura, “Skyrmion flow near room temperature in an ultralow current density,” *Nature Communications*, vol. 3, p. 988, 2012. [46](#)
- [127] J. Iwasaki, M. Mochizuki, and N. Nagaosa, “Current-induced skyrmion dynamics in constricted geometries,” *Nature Nanotechnology*, vol. 8, pp. 742–747, Oct. 2013. [46](#)
- [128] A. Hrabec, J. Sampaio, M. Belmeguenai, I. Gross, R. Weil, S. M. Chérif, A. Stashkevich, V. Jacques, A. Thiaville, and S. Rohart, “Current-induced skyrmion generation and dynamics in symmetric bilayers,” *Nature Communications*, vol. 8, p. 15765, June 2017. [46](#)
- [129] A. A. Fraerman, I. R. Karetnikova, I. M. Nefedov, I. A. Shereshevskii, and M. A. Silaev, “Magnetization reversal of a nanoscale ferromagnetic disk placed above a superconductor,” *Physical Review B*, vol. 71, p. 094416, Mar. 2005. [46](#)
- [130] V. L. Vadimov, M. V. Sapozhnikov, and A. S. Mel’nikov, “Magnetic skyrmions in ferromagnet-superconductor (F/S) heterostructures,” *Applied Physics Letters*, vol. 113, p. 032402, July 2018. [46](#)
- [131] D. S. Rabinovich, I. V. Bobkova, A. M. Bobkov, and M. A. Silaev, “Chirality selective spin interactions mediated by the moving superconducting condensate,” *Physical Review B*, vol. 98, p. 184511, Nov. 2018. [46](#)
- [132] G. Yang, P. Stano, J. Klinovaja, and D. Loss, “Majorana bound states in magnetic skyrmions,” *Physical Review B*, vol. 93, p. 224505, June 2016. [46](#)
- [133] U. GÜNGÖRDÜ, S. Sandhoefner, and A. A. Kovalev, “Stabilization and control of Majorana bound states with elongated skyrmions,” *Physical Review B*, vol. 97, p. 115136, Mar. 2018. [46](#)
- [134] R. Takashima and S. Fujimoto, “Supercurrent-induced skyrmion dynamics and tunable Weyl points in chiral magnet with superconductivity,” *Physical Review B*, vol. 94, p. 235117, Dec. 2016. [46](#)
- [135] S. S. Pershoguba, S. Nakosai, and A. V. Balatsky, “Skyrmion-induced bound states in a superconductor,” *Physical Review B*, vol. 94, p. 064513, Aug. 2016. [46](#)
- [136] N. Nagaosa and Y. Tokura, “Topological properties and dynamics of magnetic skyrmions,” *Nature Nanotechnology*, vol. 8, pp. 899–911, Dec. 2013. [46](#)
- [137] K. M. Hals, M. Schechter, and M. S. Rudner, “Composite Topological Excitations in Ferromagnet-Superconductor Heterostructures,” *Physical Review Letters*, vol. 117, p. 017001, June 2016. [50](#), [78](#)
- [138] I. F. Lyuksyutov and V. L. Pokrovsky, “Ferromagnet superconductor hybrids,” *Advances in Physics*, vol. 54, pp. 67–136, Jan. 2005. [52](#)
- [139] R. P. Kaur, D. F. Agterberg, and M. Sigrist, “Helical Vortex Phase in the Non-centrosymmetric CePt<sub>3</sub>Si,” *Physical Review Letters*, vol. 94, p. 137002, Apr. 2005. [52](#), [87](#)

- 
- [140] M. Sakano, K. Okawa, M. Kanou, H. Sanjo, T. Okuda, T. Sasagawa, and K. Ishizaka, “Topologically protected surface states in a centrosymmetric superconductor  $\beta$ -PdBi<sub>2</sub>,” *Nature Communications*, vol. 6, Dec. 2015. [59](#), [65](#)
- [141] K. Iwaya, Y. Kohsaka, K. Okawa, T. Machida, M. S. Bahramy, T. Hanaguri, and T. Sasagawa, “Full-gap superconductivity in spin-polarised surface states of topological semimetal  $\beta$ -PdBi<sub>2</sub>,” *Nature Communications*, vol. 8, Dec. 2017. [59](#), [65](#)
- [142] V. Kaladzhyan, *Spin polarisation and topological properties of Yu-Shiba-Rusinov states*. PhD thesis, Université Sorbonne Paris Cité, 2017. [60](#)
- [143] G. C. Ménard, *2D superconductors perturbed by local magnetism : from Yu-Shiba-Rusinov bound states to Majorana quasiparticles*. PhD thesis, Université Pierre et Marie Curie-Paris VI, 2016. [60](#)
- [144] G. C. Ménard, S. Guissart, C. Brun, S. Pons, V. S. Stolyarov, F. Debontridder, M. V. Leclerc, E. Janod, L. Cario, D. Roditchev, P. Simon, and T. Cren, “Coherent long-range magnetic bound states in a superconductor,” *Nature Physics*, vol. 11, pp. 1013–1016, Dec. 2015. [60](#), [66](#)
- [145] A. V. Balatsky, I. Vekhter, and J.-X. Zhu, “Impurity-induced states in conventional and unconventional superconductors,” *Reviews of Modern Physics*, vol. 78, pp. 373–433, May 2006. [62](#), [64](#)
- [146] R. Wiesendanger, “Spin mapping at the nanoscale and atomic scale,” *Reviews of Modern Physics*, vol. 81, pp. 1495–1550, Nov. 2009. [65](#)
- [147] B. W. Heinrich, J. I. Pascual, and K. J. Franke, “Single magnetic adsorbates on s-wave superconductors,” *Progress in Surface Science*, vol. 93, pp. 1–19, Feb. 2018. [66](#)
- [148] I. V. Krive, A. M. Kadigrobov, R. I. Shekhter, and M. Jonson, “Influence of the Rashba effect on the Josephson current through a superconductor/Luttinger liquid/superconductor tunnel junction,” *Physical Review B*, vol. 71, p. 214516, June 2005. [77](#)
- [149] D. B. Szombati, S. Nadj-Perge, D. Car, S. R. Plissard, E. P. A. M. Bakkers, and L. P. Kouwenhoven, “Josephson  $\phi_0$ -junction in nanowire quantum dots,” *Nature Physics*, vol. 12, pp. 568–572, May 2016. [77](#)
- [150] C. Padurariu and Y. V. Nazarov, “Theoretical proposal for superconducting spin qubits,” *Physical Review B*, vol. 81, p. 144519, Apr. 2010. [78](#)
- [151] A. Hrabec, N. A. Porter, A. Wells, M. J. Benitez, G. Burnell, S. McVitie, D. McGrouther, T. A. Moore, and C. H. Marrows, “Measuring and tailoring the Dzyaloshinskii-Moriya interaction in perpendicularly magnetized thin films,” *Physical Review B*, vol. 90, p. 020402, July 2014. [78](#)



## Transport and spectral properties of low-dimensional superconductors in the presence of spin-dependent fields

The interplay between superconductivity and spin-dependent fields is known to lead to striking phenomena, like critical field enhancement, magnetoelectric effects and the appearance of Yu-Shiba-Rusinov bound states at magnetic impurities. In this thesis, we investigate these effects in low dimensional systems.

We first demonstrate that the combination of both spin-orbit and Zeeman fields in superconducting one-dimensional systems leads to the appearance of an inhomogeneous phase at low magnetic field and high critical temperature. We show that the ground state corresponds to a zero-current state where the current stemming from spin-orbit coupling, called anomalous charge current, is exactly compensated by the current coming from the wave-vector of the superconducting order parameter. We also discuss how it is possible to predict the appearance of the anomalous current from symmetry arguments based on the  $SU(2)$ -covariant formalism.

In a second part, we consider a type-II superconducting thin film in contact with a Néel skyrmion. The skyrmion induces spontaneous currents in the superconducting layer, which under the right condition generate a superconducting vortex in the absence of external magnetic fields. We compute the magnetic field and current distributions in the superconducting layer in the presence of the Néel skyrmion.

In the last part of this thesis, we focus on the appearance of Yu-Shiba-Rusinov states in the superconducting crystal  $\beta$ - $Bi_2Pd$ . We propose effective models in order to explain recent experimental results showing a double spatial oscillation of the local density of states at Shiba energy. We demonstrate that the minimal condition to reproduce this double oscillation is the presence of two superconducting channels connected via a hopping term or via a magnetic impurity. These effective models can be easily generalized to describe the spectrum of multiband superconductors with magnetic impurities.

**Keywords :** superconductivity, spin-dependent fields, superconducting inhomogeneous phase, anomalous current, Néel skyrmion, Yu-Shiba-Rusinov states.

## Propriétés spectrales et de transport de supraconducteurs à basse dimension en présence de champs dépendant du spin

Lorsqu'un supraconducteur est soumis à des champs dépendant du spin, on observe l'émergence de nouveaux phénomènes comme l'augmentation du champ magnétique critique, des effets magnétoélectriques ou encore l'apparition d'états de bord de Yu-Shiba-Rusinov autour d'impuretés magnétiques. Dans cette thèse, on s'intéresse à ces effets dans des systèmes de basse dimension.

Tout d'abord, on démontre que la combinaison d'un champ Zeeman avec un couplage spin-orbite dans des systèmes supraconducteurs unidimensionnels induit une phase inhomogène à faible champ magnétique et haute température critiques. On montre que l'état fondamental correspond à un état de courant nul, où le courant induit par le couplage spin-orbite, nommé courant de charges anomal, est exactement compensé par le courant venant du vecteur d'onde du paramètre d'ordre supraconducteur. On discute également la possibilité de prédire l'apparition du courant anomal à partir d'arguments de symétrie basés sur le formalisme covariant  $SU(2)$ .

Dans un second temps, on considère une couche mince supraconductrice de type II en contact avec un skyrmion de Néel. Ce dernier induit des courants spontanés dans la couche supraconductrice, pouvant conduire à l'émergence d'un vortex supraconducteur en l'absence de champ magnétique extérieur. Les distributions de champ magnétique et de courant sont calculées dans le supraconducteur en présence du skyrmion de Néel.

La dernière partie de cette thèse est consacrée à l'étude de l'apparition d'états de Yu-Shiba-Rusinov dans le cristal  $\beta$ - $Bi_2Pd$ . On propose des modèles effectifs pour expliquer les récents résultats expérimentaux montrant une double oscillation spatiale de la densité d'états locale à l'énergie de Shiba. On démontre que la condition minimale pour reproduire cette double oscillation correspond à la présence de deux canaux supraconducteurs connectés via un terme de saut ou via une impureté magnétique. Ces modèles effectifs peuvent facilement être généralisés pour décrire le spectre de supraconducteurs multi-bandes en présence d'impuretés magnétiques.

**Mots-clés :** Supraconductivité, champs dépendant du spin, phase supraconductrice inhomogène, courant anomal, skyrmion de Néel, états de Yu-Shiba-Rusinov.